Title:

Development of Multifunctional Silk fibroin/PCL Based Electrospun Nanofiber for Skin Tissue Regeneration

A thesis submitted towards partial fulfillment of the requirements for the award of degree of

MASTERS OF ENGINEERING

IN

BIOMEDICAL ENGINEERING

Submitted by

DEBOLINA SAHA

Examination Roll No: **M2BMD22005**

Class Roll No: **002130201008**

Registration No: **160468**

Under the Supervision of

Dr Subhadip Bodhak

Principal Scientist

Bio-Ceramics and Coating Division

CSIR-Central Glass and Ceramic

Research Institute,

Kolkata 700032

Dr Piyali Basak

Director and Associate Professor

School of Bioscience and Engineering

Jadavpur University

Kolkata 700032

Course affiliated to

Faculty of Engineering and Technology

Jadavpur University

Koikata 700032

India

2021-2023

M.E. (Biomedical Engineering) course affiliated to

Faculty of Engineering and Technology

Jadavpur University

Kolkata, West Bengal, India - 700032

2021-2023

CERTIFICATE OF RECOMMENDATION

This is certified to that the thesis entitled **"Development of Multifunctional Silk fibroin/PCL Based Electrospun Nanofiber for Skin Tissue Regeneration"** is a genuine work carried out by DEBOLINA SAHA under our supervision and guidance for partial fulfilment of the requirement for the Post Graduate Degree of Master of Engineering in Biomedical Engineering during the academic session 2021-2023.

डॉ शुभदीप बोधक / DR. SUBHADIP BODHAK
प्रमुख वैज्ञानिक / Principal Scientist
बायोसिरामिक्स एवं कोटिंग विभाग / Bio-Ceramics & Coating Division
सिएसआईआर-केन्द्रीय कांच एवं सिरामिक अनुसंधान संस्थान
CSIR-Central Glass & Ceramic Research Institute
कोलकाता / Kolkata-700032, भारत / India

12/06/2023

Thesis Co-Advisor

Dr. Subhadip Bodhak

Principal Scientist

Bio-ceramics and Coating Division

CSIR- Central Glass and Ceramic Research Institute

Kolkata 700032

Piyali Basak
12th June 2023

Thesis Advisor

Dr. Piyali Basak

Associate Professor

Director of School of Bioscience and Engineering,

Jadavpur University,

Kolkata 700032

DR. PIYALI BASAK
ASSOCIATE PROFESSOR
SCHOOL OF BIOSCIENCE & ENGG.
JADAVPUR UNIVERSITY
KOLKATA - 700032

Piyali Basak
12th June 2023

DIRECTOR

School of Bioscience and Engineering,

Jadavpur University,

Kolkata 700032

Dr. Piyali Basak
Director
School of Bioscience & Engineering
Jadavpur University
Kolkata-700 032

12/6/2023

DEAN

Faculty Council of Interdisciplinary Studies, Law and Management

Jadavpur University,

Kolkata 700032

Dean
Faculty of Interdisciplinary Studies
Law & Management
Jadavpur University, Kolkata-700032

E. (Biomedical Engineering) course affiliated to

culty of Engineering and Technology

davpur University

lkata, West Bengal, India - 700032

21-2023

CERTIFICATE OF APPROVAL

This foregoing thesis is hereby approved as a creditable study of an Engineering subject carried out and presented in a manner satisfactory to warrant its acceptance as a perquisite to the degree for which it has been submitted. It is understood that by this approval the undersigned do not necessarily endorse or approve any statement made, opinion expressed or conclusion drawn therein but approve the thesis only for the purpose for which it has been submitted.

डॉ सुभादीप बोधक / DR. SUBHADIP BODHAK
प्रमुख वैज्ञानिक / Principal Scientist
जैवसिरामिक एवं कोटिंग विभाग / Bio-ceramics & Coating Division
सिरामिक प्रौद्योगिकी केन्द्रीय काँच एवं सिरामिक अनुसंधान संस्थान
CSIR-Central Glass & Ceramic Research Institute
कोलकाता / Kolkata-700032, भारत / India

12/06/2023

Thesis Co-Advisor

Dr. Subhadip Bodhak

Principal Scientist of

Bio-ceramics and Coating Division

CSIR- Central Glass and Ceramic Research Institute

Kolkata 700032

Thesis Advisor

Dr. Piyali Basak

Associate Professor

Director of School of Bioscience and Engineering,

Jadavpur University,

Kolkata 700032

SIGNATURE OF THE EXAMINER

M.E. (Biomedical Engineering) course affiliated to

Faculty of Engineering and Technology

Jadavpur University

Kolkata, West Bengal, India - 700032

2021-2023

CERTIFICATE OF APPROVAL

This foregoing thesis is hereby approved as a creditable study of an Engineering subject carried out and presented in a manner satisfactory to warrant its acceptance as a perquisite to the degree for which it has been submitted. It is understood that by this approval the undersigned do not necessarily endorse or approve any statement made, opinion expressed or conclusion drawn therein but approve the thesis only for the purpose for which it has been submitted.

डॉ शुभदीप बोधक / DR. SUBHADIP BODHAK
प्रमुख वैज्ञानिक / Principal Scientist
बायोसिरामिक्स एवं कोटिंग विभाग / Bio-ceramics & Coating Division
सिएसआईआर-केन्द्रीय काच एवं सिरामिक अनुसंधान संस्थान
CSIR-Central Glass & Ceramic Research Institute
कोलकाता / Kolkata-700032, भारत / India
12/06/2023

Thesis Co-Advisor

Dr. Subhadip Bodhak

Principal Scientist of

Bio-ceramics and Coating Division

CSIR- Central Glass and Ceramic Research Institute

Kolkata 700032

Thesis Advisor

Dr. Piyali Basak

Associate Professor

Director of School of Bioscience and Engineering,

Jadavpur University,

Kolkata 700032

SIGNATURE OF THE EXAMINER

DECLARATION OF ORIGINALITY AND COMPLIANCE OF ACADEMIC ETHICS

I hereby declare that this thesis contains literature survey and original research work by the undersigned candidate, as part of his Master of Engineering in Biomedical Engineering studies during academic session 2021-2023.

All information in this document has been obtained and presented in accordance with academic rules and ethical conduct.

I also declare that, as required by these rules and conduct I have fully cited and referred all materials and results that are not original to this work.

NAME: DEBOLINA SAHA

CLASS ROLL NO: 002130201008

EXAMINATION ROLL NO: M2BMD22005

REGISTRATION NO: 160468

THESIS TITLE: Development of Multifunctional Silk fibroin/PCL Based Electrospun Nanofiber for Tissue Regeneration

Debolina Saha
Signature:

12/6/23
Date:

ACKNOWLEDGEMENT

I would like to take this opportunity to express my sincere appreciation and indebtedness to persons whose help, supports and wishes have been a source of inspiration and strength personally and professionally during the entire thesis work.

I would like to express my deepest gratitude to Dr. Suman K. Mishra, Director of CSIR-Central Glass and Ceramic Research Institute for giving me this opportunity to carry out this wok in this central research and development institute.

I would like to express my deepest appreciation to the Director Dr. Piyali Basak, Associate professor School of Bioscience and Engineering of Jadavpur University for being my thesis advisor and her guidance, support and encouragement through out the two years of M.E. course journey to complete my course work as well as thesis work. This endeavour would not have been possible without the guidance of Dr. Subhadip Bodhak, Principal Scientist, Associate Professor, Faculty of Engineering Sciences, AcSIR, Bioceramics and Coating Division (BCCD), CSIR-Central Glass and Ceramic Research Institute, 196 Raja SC Mullick Road, Kolkata 700032. Throughout this M.E. journey they shared their research experience and their research work helped me to gain different research work experiences and knowledge. They allow me to think new concept and supported me to process this and develop that work successfully. I would like to express my deepest appreciation to Dr. Vamsi Krisna Balla, Head, BCCD, CSIR-CGCRI for allow me for doing this dissertation thesis work in his division and access me all laboratory opportunities through out this M.E. thesis work.

I would like to extend my sincere thanks to the Pratik Das, Tathagata Adhikary and Moumita Shee, research team members of Dr. Piyali Basak, Biomaterials and Cell culture Labarotory, School of Bioscience and Engineering, Jadavpur University for their immense help and support during my thesis work. I extend my special thanks to Pratik Das who helped me to acquire knowledge in nanomaterial green synthesis and data interpretation of XRD, UV, FTIR, RAMAN, Hemolysis study and Tathagata Adhikary for share his knowledge about different ways of antibacterial and antioxidant studies.

I am also grateful to Hasanur Rahaman sharing his molecular biology knowledge and help me to gain confidence of hand on research experience in mammalian tissue culture and Rathina Vel for sharing his polymer synthesis knowledge and data interpretation as well as different

software knowledge. Special thanks to Sutanu Dutta for sharing his instrument knowledge and Moumita Debroy for her guidance in very early days about ceramic materials which helped me to complete my thesis work.

Finally, I'd like to mention my family members, classmates and my B.Pharm professors and my school teachers for their support and help in my personal and professional life. Last but not least, I express all my gratitude towards God for providing me mentally and physically strength to carry out this work.

.

CONTENT

LIST OF FIGURES

Development of Multifunctional Silk fibroin - polycaprolactone Based Electrospun Nanofiber for Tissue Regeneration

1. Abstract:

Bombyx mori silk cocoon derived Silk fibroin (SF) is a natural polymer which have good quality of mechanical and elasticity properties with several therapeutic efficacy such as tissue regeneration, wound healing, antibacterial etc. In this present era, SF is broadly used in novel drug delivery system (NDDS) due to its easy purification, good biocompatibility, low immunogenicity and less reaction with loaded drugs. Since last few years, electrospun nanofiber is an emerging scaffold development technique in biomedical application due to its following properties, such as high surface area, less use of chemical cross-linking agent, high processability to incorporate different therapeutic agents to modify their functional properties. Here, in this study, green synthesized reduced graphene oxide (RGO), silver nanoparticles (AgNPs) and Calendula officinalis mother tincture have incorporated in the water in oil (W/O) emulsion of biodegradable aliphatic polyester polycaprolactone (PCL) and SF to fabricate nanofiber by electrospinning technique. In this study, incorporated RGO nanosheet has prepared by one pot green synthesis method with the help of C. officinalis mother tincture extract from graphene oxide (GO) which has confirmed by the obtained FTIR, XRD and RAMAN peak and morphological image of SEM and TEM. This green synthesized RGO has also shown a promising biocompatible, antibacterial and cell proliferation properties as a therapeutic agent. ATR-FTIR, XRD, SEM, UTM, contact angle analysis, swelling index, in vitro biodegradability studies of nanofibers have shown good physiochemical and mechanical properties. Antibacterial (E. coli and B. subtilis) and cell proliferation properties (L929, mouse fibroblast cells) have compared among RGO, C. officinalis mother tincture and AgNPs doped nanofibers where 1% AgNPs doped SF- PCL based NF has shown a promising result.

Key words: Silk fibroin, green synthesis, Reduced graphene oxide, PCL, tissue engineering

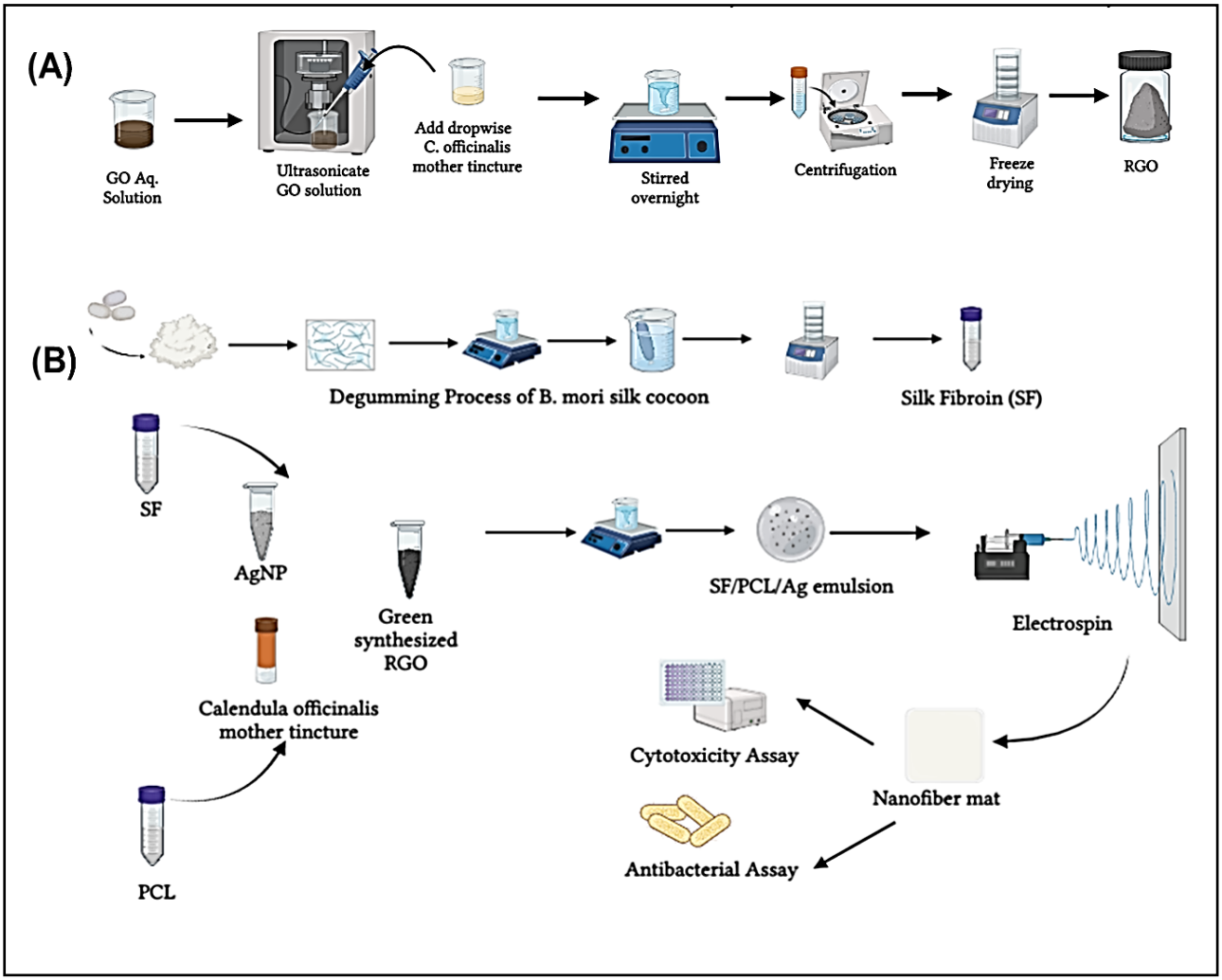

Graphical abstract (A) One pot green synthesis of RGO (B) Green synthesized RGO, AgNPs and C. officinalis mother tincture doped SF-PCL Based Electrospun Nanofiber

2. AIMS & OBJECTIVES

Aim:

One pot green synthesis of RGO from GO with Calendula officinalis mother tincture and Fabrication of Multifunctional Silk fibroin - polycaprolactone Based Electrospun Nanofiber for Tissue Regeneration with doping one pot green synthesized Reduced graphene oxide (RGO), Silver nanoparticles (AgNPs) and Calendula officinalis mother tincture

Objectives:

- One pot green synthesis of Reduced graphene oxide from graphene oxide (GO) by using C. officinalis mother tincture as green reducing agent and evaluation its physiochemical characterization, antibacterial assessment against E. coli and B. subtilis bacterial and invitro biocompatibility evaluation of green synthesized RGO to L929 mouse fibroblast cell.
- Isolation of silk fibroin protein from Bombyx mori silkworm cocoon and determination its molecular weight and physiochemical characterization.
- Fabrication of Silk fibroin- PCL based electrospun nanofiber.
- Comparative antibacterial assessment against E. coli and B. subtilis bacteria and in vitro cytocompatibility study of green synthesized Reduced graphene oxide (RGO), Silver nanoparticles (AgNPs) and Calendula officinalis mother tincture doped SF-PCL based electrospun nanofiber along their physiochemical characterization.

3. Emergence of use of B. mori silk cocoon derived silk fibroin to prepare scaffold

To fabricate the bone grafts and other scaffolds can benefit from a number of potential uses for B. mori silkworm cocoon derived silk fibroin. In terms of biological and physical characteristics, such as biocompatibility, biodegradability, and mechanical flexibility, SF is a desirable material to employ for bone grafts. Several research on this application have been done, and the outcomes are encouraging. Studies have revealed that using silk fibroin as a scaffold helped diverse cell types adhere to one another, proliferate, and differentiate. According to one study, for instance, enhanced new bone formation was observed six weeks after silk fibroin was used as a scaffold material for bone regeneration. Furthermore, a study contrasting autografts and silk-based bone grafts discovered that the silk-based NF has greater osteogenic activity and tissue regeneration.

4. Statement of the Problem

In biomedical application fabrication of antibacterial therapeutic agent loaded silk fibroin- PCL nanofiber is a process that involves the production of extremely small fibers composed of silk fibroin and polycaprolactone (PCL) polymers using nanofabrication techniques. These nanofibers can be used in various biomedical applications, such as tissue engineering, drug delivery, wound healing, and skin grafts. They possess superior antibacterial properties due to the presence of both silk and PCL, which make them highly desirable for such applications. The fabrication process involves the use of a variety of methods, including electrospun nanofibers, atomic layer deposition (ALD), and surface modification with functional groups, which can be used to customize the properties of the nanofibers to suit specific biomedical purposes. The high degree of control over the structure and composition of the nanofibers makes them ideal for use in biomedical applications where precision, accuracy and reproducibility are essential.

Here, one another aim was to synthesis RGO in green synthesis method. Green synthesis of graphene-based materials, such as reduced graphene oxide (RGO), is becoming increasingly popular due to its low cost, scalability, and environmental friendliness. Green synthesis methods are typically based on the conversion of biomass by-products such as plant materials or food waste into high-performance nanomaterials. RGO has various potential applications in areas such as energy storage, environmental protection, biomedical applications, catalysis, and electronic devices. Green synthesis methods can offer improved yields and superior control over charge transfer properties compared to traditional chemical-based production methods. Additionally, green synthesis can be conducted under mild reaction conditions, reducing energy expenditure and the risk of environmental contamination.

5. Delimitations of the Terms Used of the Study

One pot Green Synthesis of RGO

- Green synthesis of RGO requires a limited range of biodegradable precursors, which makes the process limited in terms of chemical composition and structure.
- Green synthesis cannot achieve nanoribbon-scale thickness and is limited to the production of relatively thick graphene samples.
- The lack of precise control over reaction parameters can result in defects and impurities in the graphene samples, as well as an unpredictable rate of defect formation.
- The green synthesis route is limited in terms of scalability, making it difficult to produce large quantities of graphene.

Fabrication of SF-PCL Based Electrospun Nanofiber

- Electrospun SF-PCL based nanofibers have limited production scalability and are therefore suited only to small-scale applications.
- The manufacturing process for electrospun SF-PCL based nanofibers is expensive and time consuming.
- Electrospun SF-PCL based nanofibers are sensitive to environmental changes, such as humidity, temperature, and pH, which may affect their structure and properties.
- The morphology, size, and composition of the nanofibers cannot be easily controlled.
- There is limited data available on the toxicity of electrospun SF-PCL based nanofibers.

Use of Antibacterial Dopants Loaded SF-PCL Based Nanofiber

- Antibacterial dopant may reduce the fiber diameters of electrospun nanofiber, making them difficult to use in certain applications.
- The high cost of antibacterial dopant might limit its use in some projects.
- The current market availability of antibacterial dopants is limited, meaning they may not be suitable for large-scale production processes.
- The effectiveness of antibacterial dopant on silk fibroin PCL based electrospun nanofiber is not yet fully established or understood, and further research is required.
- There is a risk that the presence of antibacterial dopant could have unintentional effects on the properties of the nanofiber.

6. Hypothesis of the Study

- One pot green synthesis of RGO can be achieved by using various eco-friendly reactants and solvents combined with an effective reaction condition that maximizes the formation of graphene oxide sheets. This process can be used to reduce or replace traditional chemical methods for the synthesis of graphene oxide, thereby reducing environmental impacts and cost.
- The fabrication of silk fibroin PCL based electrospun nanofiber will result in a strong and durable material with properties suitable for various biomedical applications. Our hypothesis is that an electrospun nanofiber material composed of silk fibroin and polycaprolactone (PCL) will demonstrate enhanced antibacterial efficacy when compared with the individual components of silk fibroin and PCL.
- Incorporation of an antibacterial dopant in silk fibroin PCL-based electrospun nanofibers will show a significant reduction in the growth of bacterial colonies on treated samples compared to non-treated controls.

7. Introduction:

In this 21st century, as a novel drug delivery system (NDDS) use of nanofiber is an emerging trend in biomedical and pharmaceutical research. The diameter of nanofiber is responsible for physiochemical, mechanical and biological properties, such as cell adhesion, cell attachment, cell migration on the nanofiber mat (Narayanan et al., 2015). Due to large surface area, it has broad applications in biomedical research, such as wound healing, tissue engineering (Chen and Lin, 2020).

In tissue engineering, biomaterials are broadly used to regenerate tissues of skin, blood vessels, internal organs, bone and cartilages due to their structural, biocompatible, mechanical and therapeutic properties. (Mollaghadimi, 2022) Natural biopolymers, such as silk fibroin, elastic fiber, gelatine, collagen fiber, hyaluronic acid is widely used to prepare extracellular matrix ss(ECM) for their good biocompatibility, mechanical properties and controlled drug release properties. (Shiroud Heidari et al., 2023) Among those, Bombyx mori silkworm cocoon derived silk fibroin (SF) protein also used to prepare nanofiber for its biocompatible, physiochemical, mechanical, cell adhesion, proliferation of fibroblast cells, (Cai et al., 2002), mesenchymal cells, osteoblast cell (Luo et al., 2022). There is glycine (46%), serine (12 %), alanine (30%) is present in silk fibroin heavy chain which act as reactive functional groups (Qi et al., 2017a) and leucine, isoleucine, valine are present in light chain (Shimura, 1983). Both of these heavy chains (390KDa) and light chain (26 kDa) are linked together with disulphide bond.

Through degumming method, SF (M.W. 10-250 kDa) can be regenerated by removing coated hydrophilic protein sericin (20-310 kDa).

To overcome the low flexibility due to presence of high amount of β sheet of regenerated silk fibroin electrospun nanofiber (NF) and increase hydrophilicity, synthetic degradable polymers are blended with silk fibroin solution to fabricate nanofiber (Chutipakdeevong et al., 2015).

Here, in this study SF-PCL based electrospun has fabricated where as a dopant green synthesized RGO, silver nanoparticles (AgNPs) and C. officinalis mother tincture were used and cell proliferation and antibacterial properties of those fabricated nanofibers has studied.

As a copolymer with silk fibroin biodegradable aliphatic polymer PCL has used. PCL nanofibers have been used in biomedical applications due to their properties such as biocompatibility, electro spinnability and non-toxicity. Possible uses include wound healing dressings, drug delivery systems, and scaffolds for regenerative medicine. PCL nanofibers are

also used as a substrate for cell culture, as they provide support for cells and proteins, allowing for better attachment and growth. Additionally, PCL nanofibers can be combined with other materials to create composite nanofiber scaffolds for tissue engineering. Furthermore, PCL nanofibers have been used in a variety of textile applications such as protective apparel, active sportswear, medical textiles and air filtration media. In addition, they are also used in the semiconductor industry for a variety of applications including photonic devices and insulation components. It has the potential to provide a moist healing environment while promoting tissue growth. PCL shows good antimicrobial and cell-friendly properties as well as a high levels of biodegradability and biocompatibility. Research has shown that using PCL as a wound dressing can stimulate faster tissue regeneration, reduce scarring, and promote faster healing.

Graphene is a 2-dimensional, honeycomb-like sp2 bonded carbon-based nanomaterial (Perreault et al., 2015) (Bharech and Kumar, 2015). The expanding use of nanomaterials in the fields of biomedical research, graphene and graphene-based derivatives like graphene oxide (GO), reduced graphene oxide (RGO) is one of the emerging topics of research due to their properties (Mbayachi et al., 2021).These biocompatible nanomaterials have taken top priority based on their sustainability and extensive applications in several fields like biomedical science (Guo et al., 2011), mechanical, electrochemical, pharmacological and environmental fields. Due to highly demand of graphene derivatives GO and RGO, global industry is focusing on the requirement of cost effective and eco-friendly synthesis methods from commercial graphite. In tissue engineering, RGO has broad applications, such as biosensor to check Acetylcholinesterase (AchE) level which cause different neurodegenerative disorders. (Yan et al., 2021)

Graphene derivatives can be synthesized since several years by the following procedures such as electrochemical methos, chemical vapour deposition, hydrothermal method, mechanical exfoliation, tour method. Due to drawbacks of these methods included instrument constraints, high energy prerequisite, use of lots of synthetic chemicals and low yield researchers are trying to establish a cost effective, eco-friendly method for the synthesis of RGO. Reduced graphene oxide (RGO) has emerged as a promising material in various applications due to its remarkable optical, electrical, and mechanical properties. In chemical methods, lithium aluminium hydride, sodium borohydride and hydrazine monohydrate have been used as reducing agents to synthesis RGO from GO (Ambrosi et al., 2012). So, this green synthesis method is an emerging eco-friendly and facile alternative method for chemical reduction to overcome the above-mentioned limitations. The green synthesis of rGO is considered to be a

better alternative over traditional chemical and physical methods which involves the use of strong reducing agents and large amounts of energy. Several green routes have been explored for the production of rGO such as electrochemical exfoliation, hydrothermal reduction, carbonization of plant biomass, microwave-assisted exfoliation, sonication-assisted reduction, biological reduction using microbes, etc. For instance, the combination of microwaves and ultrasound has been used to reduce graphene oxide (GO) to rGO under mild conditions. Different green agents have reported to reduce the GO into RGO include aloe vera, lemon peel (Zhang et al., 2010) , neem leaves, bougainvillea flower, mango, epigallocatechin-3-*O*-gallate (EGCG) (Kang et al., 2023), calendula flower as well leaves, Capparis spinosa fruit extract (Zarei et al., 2021). For example, Vitamin C was used as green reducing agent for the 1st time to produce graphene which shows all desired physiochemical properties (Gao et al., 2010). Wang et al. reported that the chemical interaction between GO and polyphenol group of green tea is able to synthesis of reduced graphene oxide bio composite (Wang et al., 2011).

There are different medicinal plants which have pharmacological uses. From the ancient times, human is used traditional medicine. As example, Calendula officinalis has been used as wound healing agent. In European country, C. officinalis leaves extract has been used as expectorant and diaphoretic where the flower extract used as antispasmodic and stimulant. Decoction of C. officinalis petal extract is used to reduce menstrual flow, menstrual irregularities (Muley et al., 2009) and to treat constipation, haemorrhoids, peptic ulcers, internal organ (oral and pharyngeal) inflammation (Arora et al., 2013).

Among different green reducing agents in this study, *Calendula officinalis* mother tincture has selected as green reducing agent due to its biocompatibility, antibacterial, coagulative, wound healing properties. In this study Calendula officinalis L. (Family: Asteraceae) 41 % (v/v) mother tincture has been used for one pot green synthesis of RGO. In this study, Physiochemical properties, antibacterial, cytotoxicity study has been performed of this green synthesized RGO. The phenotype morphological characteristics have also been studied with live-dead assay, FITC-DAPI staining to evaluate its non-cytotoxic characteristic as a therapeutic agent in tissue engineering.

In recent years, researchers have studied the potential of combining silver nanoparticles with silk fibroin PCL nanofiber to create a material with antibacterial properties. Studies have shown that the combination of these two materials can be effective at inhibiting the growth of various bacteria, such as Escherichia coli and Staphylococcus aureus, Bacillus subtilis. Furthermore,

the silver nanoparticles also provide a sustained release of silver ions which can prolong the antimicrobial effects of the material. The material can also be tailored to release different concentrations of silver ions depending on the application, allowing for greater flexibility in its use. This combination of materials could prove to be a powerful tool in the fight against bacterial infections.

Silver nanoparticles incorporated in silk fibroin/polycaprolactone (PCL) nanofibers have been found to possess pro-proliferative properties as confirmed by various studies. These nanofibers have shown potential for use in tissue engineering applications as they can provide a 3D microenvironment for biomaterials and cells. Studies have demonstrated that silver nanoparticles incorporated into silk fibroin/PCL nanofibers can modulate the cell adhesion, proliferation, and morphology. Furthermore, these nanofibers can also reduce cytotoxicity of silver nanoparticles, thereby promoting cell growth. The capability of silver nanoparticles to promote cell proliferation may be attributed to their ability to prevent bacterial infections and to release silver ions, which can accelerate cell metabolism. Additionally, silver nanoparticles incorporated into the silk fibroin/PCL nanofibers can also interact with the cell receptors present on the cell membrane, thus promoting cell proliferation.

Green synthesized RGO from GO with help of Calendula officinalis mother tincture was confirmed by characterization of peak provided of FTIR, XRD, RAMAN and morphological study of SEM and TEM image. It also shown hemocompatibility, non-cytotoxic to mouse fibroblast cell L929 which was more evaluated by FITC-DAPI staining study and Live-Dead assay.

From the SEM image of fabricated nanofibers' diameter, it was seen all diameters are below 1000 nm which indicates a good nanofiber profile. ATR-FTIR study, XRD study, contact angle measurement, in vivo biodegradation study, swelling index study confirmed about the physiochemical properties. UTM study shown a good mechanical property of these fabricated nanofibers through its ultimate strain, young modulus.

From the comparison study among green synthesized RGO, Silver nanoparticles (AgNPs), C. officinalis mother tincture and both of RGO-Ag doped SF-PCL based nanofibers group SF-PCL-1Ag nanofiber shown a good antibacterial against gm negative bacteria E. coli and gm positive bacteria B. subtilis and in vitro cell proliferation properties on L929 cell.

As future study, cell morphological study, wound healing efficacy and in vivo studies can be done.

8. Literature Review

8.1 Emerging Use of Bombyx mori Silkworm Cocoon Derived Silk Fibroin Protein for Nanofiber Fabrication

Biomaterials take an emerging role in biomedical and pharmaceutical research for their therapeutic efficacy in tissue engineering, regenerative medicine, and wound healing. Desirable biocompatible, physiochemical, biological, mechanical properties, and therapeutic efficacy has increased their demand in biomedical research as wound dressing materials, bioactive scaffolds, composites, and matrix. Artificial skin graft to replace or regenerate injured tissue, novel drug delivery system (NDDS)(Lutolf and Hubbell, 2005) . The silk fiber is a protein biopolymer that derived from natural sources like variant species like silkworms, native spiders, scorpions, and mites that create variations in composition as well as amino acid sequences, primary structure, and biological, physiochemical properties also(Gh et al., 2003) . Bombyx mori (B. mori) silkworm family is the domestic variety of mulberry silk which cocoon emanated silk fiber is the mostly used for biomedical research purposes (Gupta et al., 2021). Silk cocoon is the shelter of silk worm during metamorphism period of their life cycle developed by silkworm by spinning the silk fibres(Kundu et al., 2012).

Due to biocompatible physiochemical and self-wound healing and tissue regeneration properties, B. mori derived silk fibroin (SF) has broad applications as a protein biopolymer in tissue engineering. Degradation time is one of the most essential perquisite characteristics for a tissue regenerating and wound healing material. Metabolism and excretion are safe of the SF scaffold for human (Kundu et al., 2013).

Degumming method is used to remove sericin protein from the raw B. mori silk worm cocoon to extract pure SF. Sericin is a group of soluble glycoproteins secreted from the middle silk gland of B. mori which cover the core protein SF in the cocoon, like a filament and take 30 % weight of silk worm cocoon(Craig and Riekel, 2002) . After removing this adhesive sericin protein, SF can easily dissolve in aqueous solution for further use. In this 21st century silk sericin and SF both are used in wound healing and tissue regeneration applications for their chemical composition with highly biocompatible physiochemical, mechanical, biological properties (Rockwood et al., 2011a). The molecular weight of silk fibroin depends on following parameters, such as temperature, chemical and time used for degumming. Due to biocompatible, bioresorbable, non-immunogenic silk fiber has been used in wound healing

applications as dressing material and tissue engineering since ancient times (Vepari and Kaplan, 2007). Inherent properties of SF show wound healing efficacy by cell migration and proliferation (Park et al., 2018). Skin is the largest organ of our body which acts like a barrier of internal organs by giving protection from external environment and harmful pathogens. Disruption of the structure and function of healthy skin tissue is responsible for wound where wound healing and tissue regeneration is needed (Clark et al., 2007) . Though skin has self-healing property, but several wounds like diabetic wound, burn injuries, deep wounds and a large portion of wound need to depend on bioactive wound dressing material, bioartificial grafts for healing treatment. In this 21st century, several studies have proved that silk is good choice for development of bioartificial skin graft (Chouhan et al., 2017a). Use of different antibiotics, bioactive ceramic materials, glass, different growth factors and phytocompounds show synergistic effect in wound healing and tissue regeneration treatment.

Wound healing mechanism is a complicated mechanism of action which is followed by interaction with different cells, matrices, overlapping inflammation phases, tissue regeneration and remodelling. In the first phase of wound healing, immune system prevents the blood loss by activating inflammatory pathway, coagulation cascade. Neutrophils and macrophages prevent infection by removing the pathogen through phagocytosis and producing different growth factors and cytokines (Midwood et al., 2004) . The second phase follow through the angiogenesis, re-epithelization, tissue configuration, matrix -collagen deposition and wound contraction (Gurtner et al., 2008). Remodelling of the phase can extent from few weeks to a year or more than that(Stadelmann et al., 1998) .

For tissue engineering and wound healing purposes, different bioactive scaffolds such as films, nanofilms, hydrogel, nanoparticles, mats, foams are prepared with silk fibroin (Rockwood et al., 2011b) . Inclusion of nanoparticles of inorganic salts, metal ions, ceramic materials and other therapeutic agents show synergistic efficacy of silk fibroin scaffold by improving the cell adhesiveness, tissue remodelling, antimicrobial effect, anti-cytotoxic effect, immunomodulation and biostability (Kim et al., 2012) . Advantages of the use of silk fibroin to prepare tissue regeneration scaffold for its standard mechanical properties including strength, tenacity (Ahmadi et al., 2022) . The phase interaction between silk fibroins and other materials depends on week Vander walls forces, electrostatic attractions and hydrogen bonds also which shows effects on mechanical performances, physiochemical properties and following biological properties also biocompatibility, host response modulation and tissue

regeneration. Sometimes strong interactions such as ionic and covalent bonds are also seen between silk fibroin and other phases (Park et al., 2020) .

In 2019, solubilized SF scaffold Silk Voice of Sofregen Medical, Inc. Medford company, got the U.S. Food and Drug Administration (FDA) approval as commercial use ("Sofregen Receives 510(k) Clearance for Silk Voice® - The First and Only Natural Silk Protein Injectable Product for Tissue Bulking," 2019) . SF-hydroxyapatite (SF-HA) injectable filters, a NDDS is used for vocal cord augmentation (Brown et al., 2019) . SERI, a surgical SF based scaffold also got the 510(k) clearance by the US-FDA as a promising resorbable bioengineered material for use in reconstructive surgery (Kijanska et al., 2016) .

Here, the research works of B. mori silk worm cocoon derived silk fibroin-based bio artificial grafts such as scaffold, nanofilm, composite, films, matrix, hydrogel and other devices for wound healing and tissue regeneration purposes have been discussed. In this review preparation process, physiochemical, mechanical, biological properties, synergistic effects of incorporation of other bioactive materials such as ceramic, synthetic and natural therapeutic agents, nano particles of metal ions, targeted cells and mechanism of action for wound healing and tissue regeneration have been described. In this review, clinical studies of silk fibroin based bioartificial grafts with their performances and future aspects for tissue engineering and wound healing properties have been discussed.

8.2. B. mori silkworm derived Biopolymers Sources, Structures and Properties

8.2.1 Sources of Silk:

As a biopolymer silk has taken an emerging role in this 21st century for its own tissue regeneration properties. There are more than 200000 different arthropods exist in nature who [provides silk by biosynthesis of their epithelial cells (He et al., 2013). Different natural sources such as silk worms, spiders, bees, mats derived silk biopolymer are used for the preparation of wound dressing material and tissue regenerations scaffolds. Different sources of silk create variations in their molecular weight, chemical constituents, primary sequences, amino acid sequences and structural properties also.

According to the shelter and feeding habits of silkworms, there are two classes such as mulberry and non-mulberry silkworms. (Song et al., 2021) Those silkworms feed mulberry silk; they

are called mulberry silk. Mulberry silk is generally produced by domestic silkworm family B mori. Others families like Tussar (Antheraea mylitta), Eri (Philosamia ricini/Samia ricini), Muga (Anthrraea asana/assamensis) are belong in non-mulberry silk or wild variety of silkworms. (Naskar et al., 2014)

In non-mulberry silk, the abundant Arg-Gly-Asp motif acts as a ligand for integrins and provides a good cell adhesion and proliferation mechanism. (Zuluaga-Vélez et al., 2021) Silk fibroin derived from non-mulberry silk is also highly hydrophobic than mulberry silk that is responsible for an excellent mechanical stability as a biopolymer. (Chouhan et al., 2017b) There are 75–83.3% SF and 16.7–25% of sericin are present in B. mori silkworm cocoon. (Sun et al., 2021) Semicrystalline proteins with self-healing and tissue regeneration characteristics include silk fibroin. It is utilised to prepare bioartificial skin grafts and scaffolds as well since it has the appropriate physiochemical, mechanical, and therapeutic properties. (Vidya and Rajagopal, 2021a) Sericin is amorphous glycoprotein biopolymer which acts as gumming agent to hold the fibroin fiber to form cocoon. (Kunz et al., 2016) Sericin has a slight inflammatory effect, consequently degumming is employed to eliminate it in order to boost its biocompatibility in tissue regeneration and wound healing. (Das et al., 2021) Sericin has a slight inflammatory effect, consequently degumming is employed to eliminate it in order to boost its biocompatibility in tissue regeneration and wound healing. (Biswal et al., 2022)

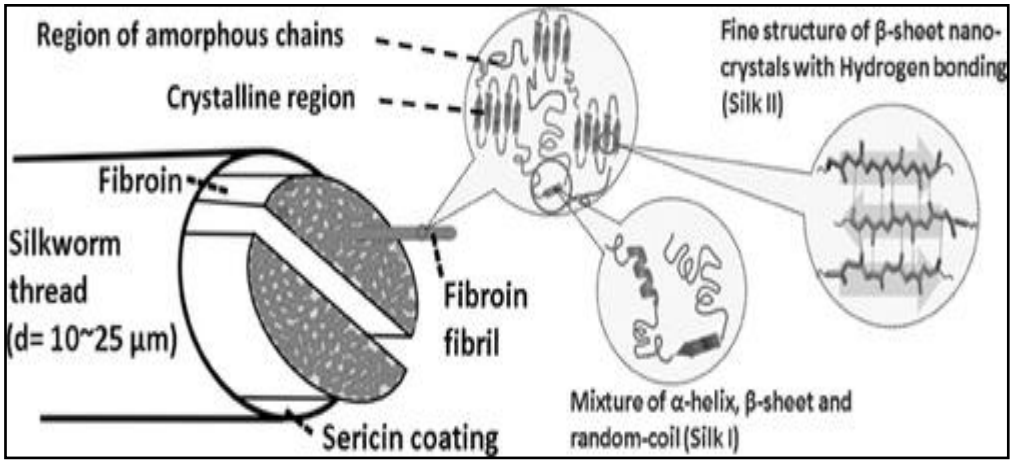

Fig 1: Schematic representation of the degummed SF structure. (Volkov et al., 2015)

To obtain qualitative SF, researchers focus on the using chemicals and temperature parameters during this process. To obtain pure SF, 0.02 M sodium carbonate (Na_2CO_3) is used to boil the cocoon and this boiling solution should be changed in each 30 min. After degumming, the dried

SF dissolved in 9.3 M, LiBr solution or AJISAWA solution of calcium chloride, water and ethanol (molar ratio 1:8:2) and dialysis to remove extra salts as well as get pure SF solution. (Rastogi and Kandasubramanian, 2020)

8.2.2. Structural Properties of Silk Fibroin:

In B. mori silkworm cocoon SF (75-83% (w/w)), sericin (16.7-25 % (w/w)), fat/wax (0.8-1% (w/w)) and colour/ash (1-1.4% (w/w)) are present. Silk fibroin is secreted from posterior gland of B. mori silkworm where sericin is produced from B. mori silkworm's middle and anterior glands (Belhaj Khalifa et al., 2012) .

The US Food and Drug Administration (FDA) has granted approval for SF as a highly adaptive, slow disintegration biopolymer with the ability for self-healing wounds and regenerate tissue. The spinning process brings about the cocoon. Sericin, a glycoprotein released from the middle and front exocrine glands, acts as a gumming agent to hold the two extremely thin (10 μm diameter) fibroin double strands together while the larvae are spinning. The protein fibres created structure becomes more durable and strong in the presence of air. (Scheibel, 2005) A single silk fibre was created when two silk fibroin filaments were bound together with sericin. From earlier studies, it can be concluded that SF filaments are composed of 3.5 nm diameter nanofibers, which are the basic components of silk fibre. Strong interactions between nanofibrils lead to the formation of microfibrils (20–200 nm in diameter) of silk fibroin. (Kwak et al., 2017) Silk fibre has a parallel arrangement of microfibrils. Due to the variance that exists for each of the components of the degumming process, SF is the major structural protein, ranging in size from 20 KDa to 350 KDa. (Singh et al., 2021)

The heavy chain polypeptide and light chain polypeptide that make up the primary structure of SF are connected by a single di-sulfide bond at the heavy chain's C-terminus. (Vidya and Rajagopal, 2021b) The overall integrity of the fibroin is maintained by glycoprotein P25, which contains Asn-linked oligosaccharide chains and is hydrophobically attached to the H-L complex. In H Chains, glycine (46%), alanine (30%), and serine (12%) are most frequently present. (Qi et al., 2017b) In L-chains, leucin, isoleucine, valine and others amino acids are present. (Shimura, 1983)

8.3 Poly(e-caprolactone) (PCL)

According to (Albertsson and Varma, 2003) the mechanical and elasticity characteristics of poly(e-caprolactone), an aliphatic polyester, depend on its molecular weight. It is employed as

a co-polymer of biomedical scaffolds and graft preparation, such as sutures, cartilage, bone, and other 2D or 3D bioprinting applications, due to its superior mechanical and biocompatible properties. (Mo et al., 2004) Its hydrophobic surface, which limits cell adherence to PCL scaffold due to the long alkaline chain present in its structure, is a barrier to its usage as a polymer for scaffold creation in biomedical applications. Clinical reports indicate that over two years or longer, the PCL-based scaffold does not entirely disintegrate in bodily fluid. (2006) Sun et al. Occasionally, PCL is the cause of skin irritation. Because PCL releases acidic byproducts as it degrades, it occasionally delays healing and is responsible for a few topical inflammations. (Sung et al., 2004) PCL is employed as a co-polymer of graft and scaffold creation due to its cell proliferation, high biocompatibility, and mechanical qualities.

In this study, poly(e-caprolactone) (PCL) was combined with sericin removed degummed regenerate SF solution to prepare an imitation for fabricating core shell electrospun nanofiber, which demonstrates good biodegradability, mechanical, and drug release properties as wound dressing material. (Sultan et al., 2018)

8.4 Use of Silver as antibacterial dopant in SF-PCL based Electrospun Nanofiber:

Due to their excellent efficiency as a drug delivery mechanism, silver nanoparticles (AgNPs) are being used progressively in biomedical research in tissue regeneration applications. Due of its antibacterial capabilities, silver Nanoparticles (AgNPs) are employed through various carriers. (Behravan et al., 2019) Due to its tiny size and homogeneous dispersion characteristics in polymeric emulsion, AgNPs are used as a therapeutic agent in polymeric nanofiber. (Behravan et al. 2019)

8.5 Use of C. officinalis Mother Tincture as Antibacterial Dopant in SF-PCL Based Electrospun Nanofiber:

Homoeopathic medicine termed calendula officinalis mother tincture is available as an oral drug or for external application as a topical application. Nanofibers, made composed of minuscule fibres with an average diameter of less than 1000 nanometres, can be employed as a drug delivery mechanism. There is no information to support the use of calendula officinalis mother tincture in nanofibers, but it would be conceivable to embed the tincture into the fibres and have it released systematically over time as the fibres disintegrate down. The effectiveness of this approach would need to be evaluated further. According to studies, the mother tincture of calendula officinalis may be used to treat cancer because of its ability to have

antiproliferative and cell-cytotoxic properties. (Jyotisree et al., 2020) According to studies, Calendula officinalis mother tincture can slow down the growth of many different kinds of cancer cells while simultaneously causing them to die through apoptosis. (Jiménez-Medina et al., 2006) It has also been discovered that it possesses antiviral and antifungal characteristics, which could be beneficial in inhibiting the spread of tumour-causing cells.

8.6. Role of One Pot Green Synthesized RGO from GO in Biomedical Applications:

Reduced graphene oxide (RGO) is a derivative of graphene, which is composed of numerous layers of carbon atoms arranged in a single hexagonal lattice. It is composed of carbon atoms linked together by oxygen atoms in the form of a two-dimensional sheet. RGO is an ideal material to be used for a variety of applications, including electrical and thermal conductivity, chemical sensing, water filtration, and bioelectronic applications. The unique properties of RGO have been studied extensively and found to be beneficial for numerous applications.

The use of green-synthesised Reduced graphene oxide (RGO) in biomedical applications is an emerging research field with great potential to revolutionise medical treatments. RGO has been explored for use in drug delivery, biosensing, electric stimulation, magnetic resonance imaging (MRI), tissue engineering, artificial organs, gene transfection, and in vitro cell culture. The unique combination of physical, chemical, and electrical properties of RGO makes it well-suited for biomedical uses due to its accessibility, influence on cell adhesion, compatibility with bio-macromolecules, and biocompatibility. In addition, the small size, large surface area, and superb mechanical strength of RGO makes it highly advantageous in biomedical applications where a maximum amount of loading capacity combined with uncommon physical durability is needed. The green-synthesis of RGO also offers the possibility of creating safer and more sustainable materials for biomedical applications, as compared to traditional techniques involving the use of harsher chemicals and higher temperatures.

The wound healing properties of reduced graphene oxide (RGO) have been studied extensively. Studies have shown that RGO can be used to promote faster wound healing in several ways: by increasing the cell proliferation and migration of fibroblasts, decreasing inflammation, and helping to reduce scarring. Additionally, due to its high conductivity, electrical stimulation has been explored as a potential application of RGO in wound healing, as electric fields can increase cell proliferation and migration. Not only as a wound healing therapeutic agent in tissue engineering, RGO has been found to have antimicrobial and antibacterial properties due

to its intrinsic antibacterial nature and ability to inactivate bacterial cells. Its antibacterial activity has been observed against Gram-positive, Gram-negative, and fungal infections

8.6.1. Advantages of Green Synthesis method to Prepare RGO

The potential uses of nanomaterials in areas like energy, medicine, and electronics have led to a surge in the usage of green nanomaterial manufacturing in recent years. Green synthesis methods reduce waste, energy use, and environmental effect while providing an appealing alternative to conventional methods for the manufacture of nanomaterials. Comparing the green synthesis method to traditional methods could possibly be more advantageous economically. Examples of ecologically conscious techniques for creating nanomaterials consist of using natural components like microorganisms and extracts from plants as well as water in place of organic solvents. Ultrasound and microwave synthesis constitute further new green synthesis techniques for nanomaterials that show possibilities.

8.6.2. Use of C. officinalis mother tincture as Green Reducing Agent:

Calendula officinalis, popularly known as pot marigold, is a popular herbal treatment used to cure minor cuts and wounds and reduce inflammation. (Doustar et al., 2010) By removing the need for extreme synthetic chemicals, the use of calendula mother tincture as a green reducing agent may assist with minimising environmental damage. It is possible to either directly apply calendula mother tincture to a wound or mix it with water and spray it on the desired location. The effectiveness of Calendula officinalis mother tincture as a green reducing agent was validated by this research.

8.7. Use of Green Synthesized RGO as antibacterial dopant in SF-PCL based Electrospun Nanofiber:

A comprehensive study has been done on the antibacterial properties of silver nanoparticles for many different kinds of biomedical applications. Gram-positive and Gram-negative bacteria, as well as some fungi, all have been shown to be sensitive to silver nanoparticle treatment. According to hypothesis, silver nanoparticles destroy bacteria by rupturing the cell membrane, producing reactive oxygen species that penetrate the cell walls, and suppressing crucial proteins and enzymes. (Yin et al., 2020) Furthermore, it has been demonstrated that silver nanoparticles prevent a number of bacteria from forming biofilms, which limits their capacity to form colonies and disseminate infection. Overall, because of their broad range of activities and their

focus on specific targets, silver nanoparticles offer a significant potential for application in antibacterial treatments.

8.8 Use of Formic Acid to as a Solvent to Dissolve SF:

In this study, silk fibroin was dissolved in formic acid to generate silk-based biomaterials for use in medical applications. Formic acid, an organic acid that is rather benign, has been used to dissolve silk fibroin since the 1920s. It is often used to dissolve silk fibroin for a variety of reasons and has garnered extensive research. Examples include the extraction of silk fibroin and its use in the production of films and other products as well as in the delivery of medications. Formic acid can also be used to preserve the original properties of silk, such as its structural conformation, thermal stability, performance, and biocompatibility. (Ming et al., 2014) Formic acid can also be used with other organic acids, including acetic acid, to improve the dissolving of silk fibroin. Numerous investigations have shown that formic acid is an effective, safe, and adaptable solvent for removing silk fibroin. The benefit of formic acid is that silk's fibroins can be broken down without affecting its fundamental properties, such as its mechanical strength and biocompatibility. As a result, it can be utilised to create silk-based biomaterials for uses in regenerative medicine, drug delivery, tissue engineering, and wound healing.

8.9. Use of Acetic Acid as a Solvent to Dissolve PCL:

Polycaprolactone (PCL) can be dissolved in an acetic acid solution. Depending on the desired outcomes, the concentration of acetic acid in this solution should range from 20 to 50%. Acetic acid aids in the dissolution of PCL into a solution and the formation of new polymeric structures by breaking down the polyester chains. The polycaprolactone can be degraded, therefore it's crucial to use the right concentration and watch that the solution is not too acidic. Furthermore, it's crucial to make sure that the solution's temperature stays below 50°C because higher temperatures can speed up the breakdown of polymer chains, leading to a lower-quality end product. Acetic acid has received a lot of attention as a PCL nanofiber manufacturing technique. Because it is inexpensive and is prepared under gentle processing conditions, acetic acid has come to be used for this purpose. It has been shown that acetic acid, depending on the quantity of acetic acid molecules utilised and the concentration of the fluid used for spinning, can be used to generate uniform and homogeneous PCL nanofibers in a variety of forms, sizes, and shapes. (Kim et al., 2009) Additionally, it has been shown that the addition of acetic vinegar can give PCL nanofibers a variety of mechanical and thermal properties, enabling applications in tissue engineering, drug administration, and wound healing. (Mahdieh et al.,

2020) In conclusion, the usage of acetic acid for the creation of PCL nanofibers is well documented, and numerous research have shown the benefits of doing so. It creates PCL nanofibers that are consistent and homogenous and have a variety of various properties, making it appropriate for a wide range of applications. (Lanzalaco and Armelin, 2017)

8.10 Use of Chloroform as a Solvent to Dissolve PCL:

Polycaprolactone (PCL) can be dissolved in chloroform to create a solution. Due to its hydrophobicity, PCL, a kind of thermoplastic polymer, can dissolve in chloroform. (Armeda, 2018) Chloroform can be used as a PCL solvent and in a variety of industrial settings, including the manufacturing of medical devices, medication delivery systems, and other products. In order to dissolve PCL in chloroform, the necessary volume of chloroform must be heated and evaporated before the PCL particles are added. The mixture is then heated a bit further until it completely dissolves.

8.11. Biomedical Applications of Silk Fibroin Nanofiber:

8.10.1. SF Nanofiber as Cardiovascular Graft

Recent studies have demonstrated the usefulness of using Bombyx mori silkworm cocoon-derived silk fibroin (SF) nanofibers as vascular grafts. Since SF has the requisite strength and flexibility in its nanofibers to endure physiological pressures without inducing a significant immunological response, it is highly suited for tissue engineering applications. In order to encourage cell attachment and proliferation, the structure of SF also enables it to be functionalized with different cell adhesion molecules. SF nanofiber scaffolds have been shown in studies to support endothelial cells in vitro and exhibit increased angiogenic activity in vivo, suggesting that they may be appropriate for vascular graft applications. (Pan et al., 2023) Their restricted permeability, inability to function as vascular grafts, and other issues could be disadvantages. These studies have concentrated on the application of B. mori silk fibroin nanofibers as a platform for the generation of adherent vascular endothelial progenitor cells, stem cell transport, and cardiac tissue engineering. The usage of these nanofibers in combination with different other biomaterials or growth factors has proved useful in enhancing cellular adhesion, survival, and/or proliferation, according to research. Additionally, numerous studies have shown that it is feasible to deliver medications or other substances utilising these nanofibers straight to the damaged heart tissue. (Li et al., 2013)

8.10.2. Silk fibroin nanofibers for antibiotic delivery:

A very interesting and cutting-edge area of inquiry is the use of silk fibroin nanofibers for antibiotic delivery. To improve the solubility, stability, and release profile of antibiotics, research is now being done on the use of silk fibroin nanofibers as a drug delivery system. The direct encapsulation of antibiotics in silk fibroin nanofibers, the incorporation of antibiotics into the hydrogel-like fibroin matrix, the electrospinning of antibiotic-loaded silk fibroin nanofibers, and the conjugation of antibiotics onto the nanofibers are a few of the methods that have been studied. (Farokhi et al., 2020) Due to their biocompatibility and biodegradability, research to far suggests that silk fibroin nanofibers have a significant potential for use in targeted delivery applications. Additionally, it has been demonstrated that silk fibroin nanofibers efficiently enable the regulated release of a variety of medications, including antibiotics.

The current focus of study is on improving the effectiveness of antibiotics being encapsulated in silk fibroin nanofibers and further investigating the possibilities of these promising materials for antibiotic delivery. The nanofiber scaffolds are intended to gradually release a sustained dose of antibiotics over time, improving patient safety and comfort while also providing better control over drug levels in the body. Due to its capacity to precisely administer medicines at therapeutic levels, the approach may potentially help fight antibiotic resistance.

Silk fibroin-PCL nanofibers that have been loaded with antibiotics are a promising medication delivery technology for antibiotics. With the help of this delivery mechanism, the antibiotic can be released over a longer period of time with little adverse effects on the body while yet being highly concentrated when it reaches the site of action. High surface area, homogeneous medication distribution, and superior mechanical qualities like flexibility and tear resistance are all provided by Silk-PCL nanofibers. (Wang et al., 2022) These qualities make the nanofibers perfect for applications involving medication administration. These nanofibers can also be simply altered to accommodate various antibiotics and their controlled release profiles. Additionally, adding targeting molecules to the nanofibers can increase antibiotic delivery's overall effectiveness and specificity.

8.10.3. Electrospun silk fibroin nanofibers for antioxidant delivery

In tissue engineering, antioxidants are essential. By scavenging free radicals, defending cell membranes from lipid peroxidation, and stabilising proteins from oxidation that might result

in cellular damage and death, they shield designed tissues from oxidative damage. (Sakai et al., 2020) Additionally, antioxidants have the power to enhance cell signalling, control cell division, angiogenesis, and wound healing. They might also lessen ischemia and reperfusion destruction and regulate the inflammatory response. Antioxidants can also improve how well tissue engineering scaffolds encourage cell adhesion, proliferation, and the growth of new tissues.

The creation of an antioxidant made from silk fibroin nanofibers is the main goal of this study. The antioxidant substance that will be included into the nanofibers will be used to counteract oxidative stress in cells and tissues. To do this, an electrospinning technique will be used, in which the antioxidant component and silk fibroin solution are combined to create the nanofiber scaffolds. The effectiveness of the loading, the mechanical characteristics, and the biocompatibility of the antioxidant-loaded nanofibers will subsequently be evaluated. The antioxidant effectiveness of the nanofibers will then be assessed using in vitro studies. It can be used to deliver antioxidants, allowing for a steady and controlled release of these substances. Applications like promoting wound healing and reducing food oxidation could all benefit from this.

8.10.4 Electrospun silk fibroin nanofibers for vitamin delivery

Vitamins sustain the health of cells and tissue structures, which is vital for tissue engineering. Vitamins can offer vital nutrients for the development, maintenance, and repair of cells and tissue structures. They can also assist in defending cells against oxidative stress, which over time can harm tissues and cells. Vitamins can support effective tissue engineering efforts and maintain cell health by giving vital nutrients and defending cells from oxidative stress. Due to their special characteristics, electrospun silk fibroin nanofibers have been investigated as a potential vitamin delivery mechanism. The controlled release of vitamins may be enhanced by using nanofibers with homogeneous sizes and shapes, which can be produced by the electrospinning method. The controlled release of vitamins may be enhanced by using nanofibers with homogeneous sizes and shapes, which can be produced by the electrospinning method. Additionally, silk fibroin nanofibers have properties that make them biocompatible, making them suited for use in the transport of drugs and vitamins. Studies have demonstrated that a variety of vitamins, including Vitamin E, Vitamin C, and other water-soluble vitamins, can be delivered using electrospun silk fibroin nanofibers. These nanofibers can also be functionalized with a variety of elements to enhance vitamin delivery. Vit D-loaded silk fibroin

nanofiber has produced really encouraging tissue engineering results. (Mostafavi and Naeimi, 2022)

8.10.5. Electrospun silk fibroin nanofibers for ion delivery

Releasing ions with electrospun silk fibroin nanofibers. to look into the possibility of controlling ion delivery with electrospun silk fibroin nanofibers. This work created electrospun silk fibroin nanofibers with various ion concentrations and assessed their potential to deliver ions to the target region. To assess the biological reactions to the ion-loaded nanofibers, an in vitro cell culture model was developed. To evaluate the electrospun nanofibers' capacity for absorbing and delivering ions selectively to the cell surface, uptake assays were also carried out. (Farokhi et al., 2020)

The outcomes demonstrated that the electrospun silk fibroin nanofibers enabled effective ion delivery, and the rate of delivery could be modified by varying the nanofiber diameter. When compared to fibre that weren't ion loaded, the nanofibers shown improved cell adhesion and proliferation. The outcomes also showed that ions may be precisely captured and delivered to cell surfaces using electrospun silk fibroin nanofibers. According to the study results, electrospun silk fibroin nanofibers have the potential to serve as a powerful platform for accurate delivery of ions.

8.10.6. Electrospun silk fibroin nanofibers for wound dressing

Due to its capacity to operate as a physical barrier against bacteria and other pathogens, absorb wound exudate, and hasten skin healing, electrospun silk fibroin nanofibers have demonstrated potential as a material for wound dressings. To adhere to the contour of the wound and produce a seal that can hold while healing, the nanofibers can be mixed into a variety of materials. Electrospun silk fibroin nanofibers are a potential material for wound dressing applications because they are biocompatible and biodegradable as well. (Chen et al., 2022)

Because of its great biocompatibility, low inflammatory response, and high-water vapour permeability, silk fibroin is a desirable biomaterial for wound treatment. It has a number of medical uses, including tissue engineering, medication administration, and wound healing. Strong adhesive characteristics in silk fibroin allow it to remain attached to the wound successfully and speed up healing. Silk fibroin is also extremely elastic and is simple to shape to fit into the contours of the wound. The immune system's ability to inhibit infection aids in

lowering inflammation and managing wound fluids. Additionally helpful in stimulating wound contraction and able to lessen scarring is silk fibroin.

9. Materials and Methodology

9.1 Materials

9.1.1. Materials for One Pot Green Synthesis of RGO from GO

Graphene oxide powder (Tata steel), Calendula officinalis 41% (v/v) mother tincture (Dr. Willmar Schwabe India Pvt. Ltd.), Streptomycin Sulphate (STM) (SRL), FITC staining solution (Himedia), DAPI staining solution (Himedia), Triton^{TM} X-100 (Sigma), Deionized water (DIW), Nutrient broth (HiMedia), Agar powder (bacteriological grade) (Himedia), Phosphate Buffered Solution-10X (Himedia), DMEM media (Gibco)

9.1.2. Materials for Fabrication of SF-PCL Based Nano Fiber

Bombyx mori silkworm cocoon, LiBr (SRL), Formic Acid (SRL), Calcium chloride (Emplura), Silver nanopowder (SRL), Dialysis bag, Nutrient broth (HiMedia), Agar powder (bacteriological grade) (Himedia), Phosphate Buffered Solution-10X (Himedia), DMEM media (Gibco), Tris HCl (P^H 6.8), SDS powder, β- Mercaptoethanol (BME), Tris Base, Glycine, SDS powder, Acrylamide-bis acrylamide solution, Tris HCl (P^H 8.8), Ammonium persulfate (APS), N, N, N', N'-tetramethyl ethylene diamine (TEMED), Brilliant blue R-250, Methanol, Acetic acid, distilled water

9.2 Method:

9.2.1 One Pot Green Synthesis of RGO from GO by Using C. officinalis mother tincture

9.2.1.1. Green Synthesis of RGO

RGO has prepared by one pot green synthesis method by using 41% (v/v) C. officinalis mother tincture with some modification. At first, 1 mg/ml GO powder was mixed in 20 ml DIW and sonicated the mixture to complete dissolve the GO powder by a probe sonicator (LabMan Scientific Instruments) at a pulse of 2 s and pulse off 2 s. During the sonication 4 ml of Calendula officinalis 41% (v/v) mother tincture was added dropwise during sonication. After the sonication homogenously stirred the mixture for the next 15-20 hours at 60 ℃ on the magnetic stirrer. To remove the extra calendula extract from the sample, centrifuge the sample several times at 10000 rpm for 10 min and washed with deionized water until obtained the clear supernatant. The final product was dried in a lyophilizer at -50 ℃ until obtained the dry powder of RGO prepared by Calendula officinalis mother tincture.

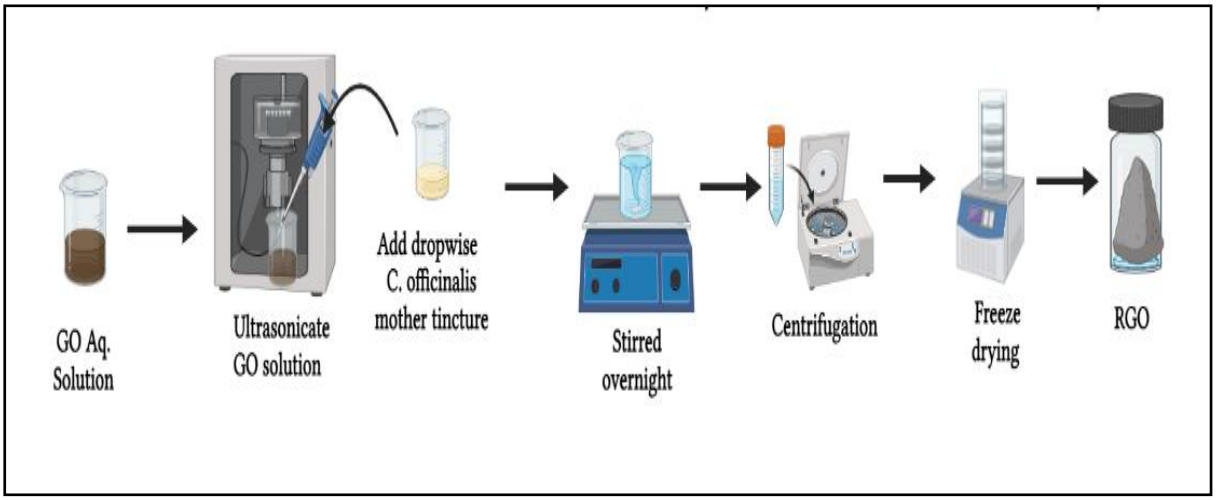

Fig 2: Schematic representation of green synthesis of RGO with Calendula officinalis mother tincture

9.2.1.2 Characterization:

Green synthesized RGO with Calendula officinalis mother tincture has characterized via Fourier Transformed Infrared Spectroscopy, Raman spectroscopy, X-ray Diffraction, SEM, and TEM in order to confirm the reduction.

9.2.1.2.1. Fourier Transformed Infrared Spectroscopy (FTIR) Study of Green Synthesized RGO

FTIR spectrophotometer (Frontier IRL 1280119; Waltham, MA, USA) was used for analysing RGO powder samples. The mixture of synthesized RGO powder and KBr (Sigma Aldrich, uvasol) with a weight ratio of 1:100 was pelletized using a hydraulic press and the pellets were used for obtaining spectra in the transmission mode within 500 to 4000 cm-1 range.

9.2.1.2.2. X-ray Diffraction (XRD) Study of Green Synthesized RGO

Synthesised RGO powder was investigated using an X-ray Diffractometer (Ultima IV, Rigaku) equipped with Ni-filtered Cu Kα radiation having a wavelength of 1.5418 Å. Samples were scanned within a range of 10-60° with a 0.02° step size and 6 steps/second scan rate.

9.2.1.2.3. RAMAN Spectroscopy Study of Green Synthesized RGO

Prepared RGO powder by using C. officinalis mother tincture investigated by the means of Raman spectroscopy (Horiba Scientific, LabRAM HR Evolution) for extracting structural information. Spectra were recorded within the 200-1600 cm-1 range using a 488 nm laser source and 20 s acquisition time.

9.2.1.2.4. Scanning Electron Microscopy (SEM) of Green Synthesized RGO

Morphology of the RGO was observed by SEM To capture the image, the samples were gold coated with a thin layer of gold alloy after mounting on a double-sided carbon tape.

9.2.1.2.5. Transmission Electron Microscopy (TEM) of Green Synthesized RGO

To evaluate the morphology, size and shape of the RGO nanopowder, TEM was done. For testing TEM grid was prepared by placing a drop of the diluted RGO aqueous solution on a carbon-coated copper grid and later drying it.

9.2.1.3. Hemocompatibility assay

Hemocompatibility assay has done to check the hemocompatibility as well as biocompatibility of the green synthesized RGO by C. officinalis mother tincture. To perform this hemocompatibility assay fresh blood sample was collected from a healthy volunteer in a sterile EDTA vial and finally it was further diluted in saline water to prepare blood (RBC) suspension. This blood suspension was added to the different concentration of samples (Fig 9) and incubated all samples at 37 ℃ for half an hour. After this incubation keep the samples at static conditions for 4 h at 37℃. Then, centrifuged at 5000 rpm in cooling centrifuge at 4 ℃ and supernatant were transferred to a 96-well plate. The haemolytic activity was determined by measuring the absorbance at 570 nm Control samples of 0% lysis (negative control) and 100% lysis (positive control) were employed in the experiment (Escudero et al., 2019). Here, all samples were prepared in triplicate. The concentrations (µg/ml) of samples were are GO 100 µg/ml, RGO 10 µg/ml, 50 µg/ml and 100 µg/ml.

Formula:

Hemolysis (%) = $\{OD_{sample}-OD_{NC}/OD_{PC}-OD_{NC}\} * 100$

NC: Negative control

PC: Positive control

9.2.1.4. Antimicrobial Assay

The broth dilution method and determination of minimum inhibitory concentration (MIC) value were utilized for the assessment of the antibacterial properties of GO and green synthesized RGO-Calendula nanocomposite samples at different concentrations. The Luria-Bertani (LB) broth containing a single colony of an Escherichia coli and *Bacillus subtilis* strain were cultured overnight at 37°C and was further diluted with LB broth to obtain the bacterial suspension. Here, as positive control standard marketed antibiotic Streptomycin has been used. The primary culture has diluted into 0.1 optical density (OD) concentrated bacterial culture in autoclaved test tube and prepare different concentration of GO and RGO samples and Streptomycin (200µg/ml) solution as positive control and as negative control only 0.1 OD

bacterial culture was used which also incubated for next 18 hrs and measure the optical density of the secondary cultures in 96 well plate. For this secondary culture, each sample solution was added into 0.1 OD concentrated primary bacterial culture in 1:10 ratio. From this OD bacterial viability has count.

9.2.1.5. In-vitro cytotoxicity assay

In vitro cell proliferation assay of the green synthesized RGO nanopowder was assessed by MTT assay. L929, mouse fibroblast cells were cultured and maintained in Dulbecco's Modified Eagle Medium (DMEM) supplemented with 10% Fetal bovine serum (FBS). 5 × 103 cells per well were seeded into a 96-well plate for 24 h. These cells were treated with different concentrations of RGO nanopowder for two different time points 24 hrs and 74 hrs.

After 24 hrs of treatment of RGO, 100 µl MTT (3-(4,5-Dimethylthiazol-2-yl)-2,5-Diphenyltetrazolium Bromide) solution (5 mg/ml) in PBS was given in each well and keep the 96 well plate in the 5 % CO2 incubator at 37 °C for 4 hrs. Then the medium was taken from each well and dissolved in 100 µl of DMSO and kept in the incubator at 37 °C in shaking condition for 5-10 min to form violet coloured formazan crystals. The absorbance was measured by a microplate reader (*BIO-RAD, iMark^{TM}) at 595 nm wavelength.

% of cell proliferation was calculated by the following equation:

Cell viability = (O.D. of sample / Average O.D. of Control) *100

9.2.1.6. Live and Dead Assay:

Live and Dead assay was performed to analysis the cell viability after treatment with green synthesized RGO and compared with cell viability on tissue culture polystyrene (TCPs) as control. In this study, 10,000 L929 fibroblast cells per well were seeded into 24 well plates and incubated in incubator at 37℃ and 5 % CO_2 condition for 3 and 5 days. Cells were treated with different concentration of RGO (10,20,50,100,200 µg/ml). Different concentration of RGO solution was prepared by serial dilution method in complete DMEM media.

After, 3 days of incubation, media has discarded and carefully wash with tissue culture graded 1X PBS to remove extra RGO powder and dead cells also. Then, the cells were strained with calcein AM and ethidium bromide homodimer-1 (Molecular Probes) added DMEM media to visualize the population of live and dead cells after 3 days incubation. After, adding this calcein

and ethidium bromide strained solution added media incubated the cells at 37℃ for 20-30 mins to stain viable and non-viable cells, respectively. The images of strained viable and non-viable cells were taken by microscope.

9.2.1.7. FITC-DAPI Staining:

FITC-DAPI staining has done to for the phenotype study of green synthesized RGO treated cell. Here, $1*10^4$ L929 mouse fibroblast cells/ well in 24 well plate was treated with different concentrations of RGO in 2 ml of DMEM media and incubated for 72 hours at 37℃ and 5 % CO_2 condition. In one well cell was gown without RGO which is considered as control or tissue culture polystyrene (TCPs).

After 72 hours, aspirate the medium from the well and rinse with 1x cell culture graded PBS 3 times to remove present dead cells, RGO and other debris from the well and fixed with 3.7 % cell culture graded p- formaldehyde for 10 min. After fixation, remove the formaldehyde and wash with PBS for 3 times. For permializing the cells, the cells are immerged in 0.2 % triton X 100 and aspirate this tritonx100 after 5 mins. After washing 3 times (Wash for minimum 5 mins in each wash) with PBS.

After washing, fixed cells were incubated with 4′,6-diamidino-2-phenylindole (DAPI) (2 µl/ml DMEM media) concentrated staining solution for 5 min in room temperature. Then wash with PBS for 3 times and incubate with Phalloidin fluorescein isothiocyanate (FITC) dye (2 µl/ml DMEM media) for 10 min at room temperature and wash with PBS for 3 times.

Finally, the cells were observed under fluorescent confocal microscope (at 10X magnification) with help of KRUSS| ADVANCE (1.6.2.0) software. For, FITC staining, in green fluorescent cells were observed at ($\lambda_{excitation}$ 495 nm, $\lambda_{emission}$ 535 nm) and for DAPI staining, in blue fluorescent cells were observed at ($\lambda_{excitation}$ 359 nm, $\lambda_{emission}$, 461 nm).

9.2.2 Fabrication of Antibacterial Therapeutic Agents Doped Silk Fibroin PCL Based Nanofiber by Electrospun Method for Tissue Engineering

9.2.2.1 Extraction of Silk Fibroin (SF) from B. mori Silk cocoon

Regenerated silk fibroin extraction from B. mori silk cocoon is processed by previously established degumming method (Rnjak-Kovacina et al., 2015). In this method, gummy protein sericin which coated on the fibroin protein is removed.

Silk cocoons were cut into small pieces and boiled into 0.02 M sodium carbonate (Na_2CO_3) aqueous solution for 2-3 hrs at 90-100 ℃. In each 30 min, need to change this aqueous Na_2CO_3 solution and wash the silk worm cocoon's fiber with deionized water (DIW) and need to do it 5-6 times until total sericin will be removed and getting clear boiling solvent. After three hours when the texture of the cocoons had been changed, the fibrous material was washed several times with DIW and dried by keeping this fiber at room temperature overnight.

Then, this degummed fiber types material was again cut into small pieces and dissolved in 9.3 M LiBr solution in 1:4 (w/v) ratio and keep the SF- LiBr solution in incubator at 60 ℃ for 4 hrs. After 4 hrs of incubation, fibroin solution was transferred into dialysis tube and dialyzed against deionized water for 3-4 days until the water colour become transparent. The DIW was changed in every 6 hrs for 1st day and from 2nd day need to change this water once daily to remove the heavy salt of LiBr from the silk fibroin solution. After dialysis, this silk fibroin solution was centrifuged at 12000 rpm in cooling centrifuge at 4 ℃ and wash with DIW until getting the clear supernatant. Then lyophilized the precipitate for 48 hrs at -80 ℃ and stored this regenerated SF at 4℃ for further study.

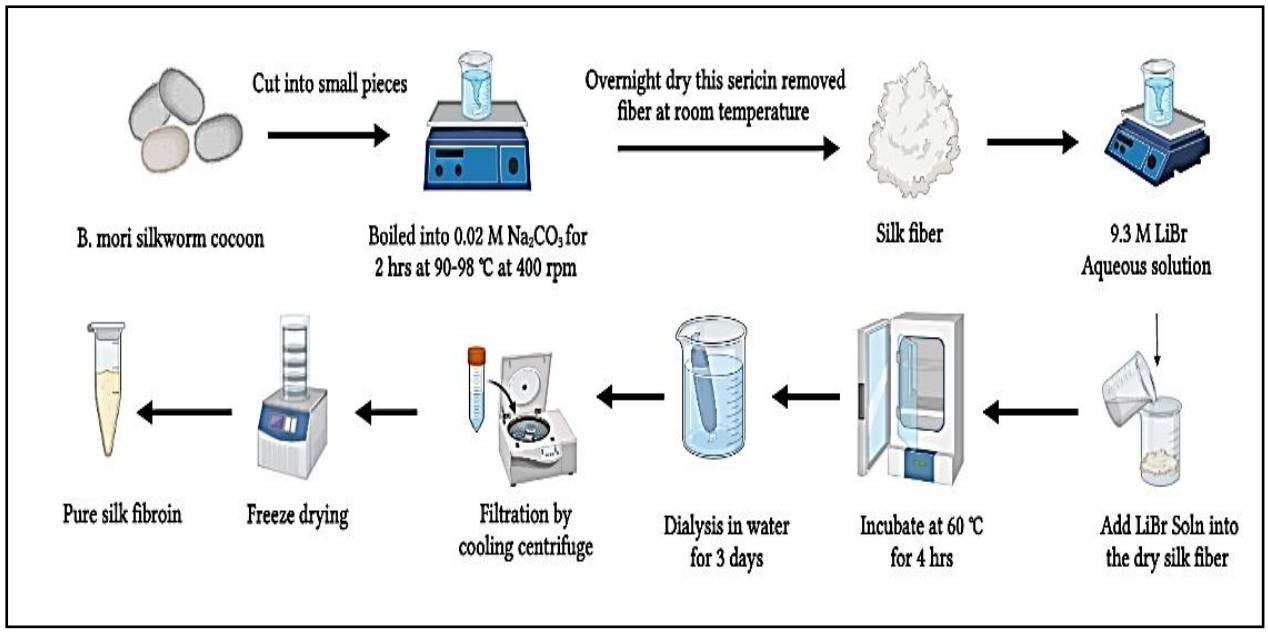

Fig 3: Schematic Representation of Degumming Method of Silk Fibroin from Bombyx mori silkworm cocoon.

9.2.2.2. Degumming loss:

Degumming weight loss calculation is a quantitative evaluation of the degumming efficiency which helps to analyse the weight loss in throughout the degumming process of B. mori silk fibroin cocoon to regenerated silk fibroin yield.

% of Degumming loss was calculated by the following equation:

= {(Initial weight of silk fibroin cocoon – weight of lyophilized silk fibroin)/ Initial weight of silk fibroin cocoon} *100

9.2.2.3. Measurement of protein concentration

Silk fibroin protein concentration was measured by Bradford protein assay (Oliveira Barud et al., 2015). 20 µl aqueous solution of SF was added with 200 µl Bradford reagent (HIMIDIA) in each well of 96 well plate and as control here, DIW was used. After adding, Bradford reagent with the sample and blank mix them properly and incubate at room temperature for 5 min. The absorbance was measured at 595 nm by Microplate reader (*BIO-RAD, iMark^{TM}).

Here, as standard protein BSA (bovine serum albumin) was used. (Bojedla et al., 2022)

9.2.2.4. Measurement of protein concentration

In Bradford assay, Coomassie blue G-250 dye have anionic groups which wants to bind with protein for its stability. The Coomassie blue G-250 dye when comes in contact with protein solution, the first electron of Coomassie blue G 250 is donated to the charged groups of protein which disrupt the structure of protein. Sulphonic acid groups of Coomassie brilliant blue bind to positive amine groups of protein and form hydrophobic pocket types protein-dye complex.

Here, this attraction is occurred due to Vander Waals forces. ("Bradford Assay | Bio-Rad," n.d.).

9.2.2.5. Analysis of Silk Molecular Weight:

Silk fibroin has broad range of molecular weight which depends on different parameters of degumming method such as boiling temperature, time, chemical and others methods of degumming process. M.W. was determined by sodium dodecyl sulphate polyacrylamide gel electrophoresis (SDS-PAGE) process. SDS-PAGE is a very basic and commonly used method to analyse the molecular weight of protein subunit which is based on electrophoresis mechanism.

Method:

8.2.2.5.1. Resolving Gel Preparation:

For preparing resolving gel, Acrylamide-bis acrylamide solution,1.5 M Tris-HCl (P^H 8.8), 10% SDS solution, 10% APS and TEMED mixed in a falcon and vortex for proper mixing. The gel casted upto ¾ th of total volume of casting chamber and wait until cross linking.

8.2.2.5.2. Stacking Gel Preparation:

For this SDS PAGE study, 12% of Stacking gel has prepared by mixing of Acrylamide-bis acrylamide solution, 1, .5 M Tris HCl (P^H 6.8), 10% SDS solution, 10% APS and TEMED in certain ratio ("SDS-PAGE for Silk Fibroin Protein," n.d.) and vortex in same way for proper mixing. This stacking gel cast of the rest port of casting chamber till the lower and of comb portion and put the comb. After crosslinking or solidify of both gel sample can be added for this test.

8.2.2.5.3. Sample Buffer Preparation:

Sample buffer or extraction buffer has prepared by mixing of 0.6M Tris-HCl (pH 6.8), 10% SDS, sucrose, BME and distilled water. Here, BME which acts as sample loading dye.

8.2.2.5.4. Sample Preparation:

To know the protein concentration of sample, Bradford assay was done. Protein sample was added with sample buffer in 1:1 (v/v) ratio. For, silk fibroin after adding sample with the sample buffer this mixture kept in heat bath at 95°C for 20 seconds only.

8.2.2.5.5. Sample Loading:

20 µl of heated sample was loaded inside the casting chamber through one teeth of comb. And through another teeth of comb standard Protein molecular weight markers was loaded for passing through the gel.

9.2.2.5.6. Running Buffer or Electrophoresis buffer Preparation:

Running buffer or Electrophoresis buffer was prepared by mixing of Tris base, glycine, SDS and water. The chamber of the SDS PAGE chamber was filled with this running buffer.

9.2.2.5.7. Staining Solution Preparation:

Staining solution has prepared by adding Briliant blue R-250, methanol and acetic acid.

9.2.2.5.8. Destaining Solution Preparation:

Destaining solution has prepared by adding methanol, glacial acetic acid and distilled water.

After sample loading, connect the minigel apparatus (Biorad) with the power pack and set constant voltage 80 V to pass through the gel. This voltage helps to pass the silk fibroin protein with help of the brilliant blue dye through the gel and helps to reaches the brilliant blue until the bottom end part of casting resolving gel. During this process, bubble formation has observed due to electrophoresis and redox reaction. It took around 2.5-3 hrs for completely pass the Briliant blue dye until the bottom end part of resolving gel.

After this, gel plates have opened after dismantle the gel apparatus and discard the stacking gel and place the separating gel in the staining solution for 2 hrs at room temperature in shaking condition.

After 2 hrs of staining, this gel has immersed into destaining solution and after 30 mins this solution has changed for proper destaining and again added fresh destaining solution and kept the gel for overnight at room temperature.

After proper destaining only visible band of tested protein sample and standard protein marker can be observed. The gel can now be used for immunoblotting with the help of Biorad gel electrophoresis instrument to determine the protein sample with the help of Bio-Rad's Image Lab software.

9.2.2.6. Fabrication of SF-PCL based Electrospun Nanofiber:

After several times of optimization, SF-PCL based nanofiber has fabricated.

Formic acid is a type of carboxylic acid that can be used to dissolve silk fibroin, though it is not the most commonly used method for doing so. Formic acid has the ability to break down the fibroin and make it more soluble in solvents. The process of dissolution is complex and requires the use of heat and agitation. The fiber must also be carefully monitored to ensure that the acid does not damage it. In this study, 10% (W/V) regenerated SF has dissolved in formic acid (FA) (85%) (SRL). For completely dissolve of SF, $CaCl_2$ (25% of SF weight) was mixed in the formic acid.

To dissolve PCL, binary solvent (Chloroform and acetic acid) has used. This binary solvent has prepared by mixing of chloroform and acetic acid in 4:1 ratio (v/v). 17 % PCL has dissolved in this mixture (W/V) by stirring at 600 rpm in room temperature for 3 hours.

For, pure PCL nanofiber has fabrication, 3 ml of 17% PCL solution has transferred into the 5 ml syringe and set in 12 cm distance from aluminium foil which has used as fabrication base at 1.5 ml/hrs flow rate and 18 kV voltage.

To prepare SF-PCL based nanofiber, 17% PCL has blend with 10% SF-FA solution in 4:1 volume ratio at 1000 rpm for overnight at room temperature which formed water in oil emulsion. This emulsion has transferred into 5 ml of disposable syringe and set at 12 cm distance from aluminium foil and set voltage 18 kV and 1.5 ml/hr flow rate.

In this study, here as dopant green synthesized RGO, silver nanoparticles (AgNPs) and calendula mother tincture have been used.

AgNPs doped with this SF-PCL emulsion in two different concentrations.

10 mg AgNPs has mixed with 10 ml SF-PCL emulsion by blending this mixture at 1000 rpm for overnight at room temperature to get stable emulsion. 3 ml of this emulsion has also transferred in same way into disposable plastic syringe and set 12 cm distance from aluminium foil and set voltage 18 kV with 1.5 ml/hour flow rate.

Another group of PCL-SF-Ag was prepared with adding 5 mg AgNPs in 10 ml of PCL-SF emulsion and fabricated in the same way (described for PCL-SF-1 Ag).

For, RGO doping here, 1 mg RGO has mixed with 10 ml of SF-PCL emulsion and blend it by stirring at 900-1000 rpm for overnight at room temperature. After proper blending 3 ml of this emulsion has transferred into disposable plastic syringe and set the syringe at 12 cm distance from aluminium foil at 1.5 ml/hr flow rate and 18 kV voltage.

The one more group of nanofibers has prepared by adding 1 mg of RGO and 10 mg of AgNPs into this PCL-SF based emulsion and blend in same manner by stirring at 1000 rpm for overnight. This group also fabricated in same way where parameters were same like above mentioned parameters.

The last group was PCL-SF-Calendula where, 0.5 ml of C. officinalis mother tincture has blended with 9.5 ml of PCL-SF emulsion by stirring at 1000 rpm for overnight at room temperature.

9.2.2.7 Characterization:

9.2.2.7.1. ATR- FTIR Analysis of SF-PCL based Nanofiber:

ATR- FTIR of PCL-SF based nanofiber have analysed by the characteristic spectral absorption peaks of ATR- FTIR spectrophotometer (IRAffinity-1S, SHIMADZU, Chicago, Illinois). All ATR-FTIR spectra of nanofiber were recorded between 4000 and 500 cm^{-1}.

9.2.2.7.2. X-Ray Diffraction (XRD) Analysis of SF-PCL based Nanofiber:

XRD of SF-PCL Based nanofiber were analysed by XRD (Ultima 4, Rigaku, Japan) which uses Ni- filtered Cukα radiation of wavelength 1.5418 Å. The selected range was between 0-60° along with step size of 0.02 and scan rate of 6 steps/ second.

9.2.2.7.3. Contact angle Measurement:

The samples underwent testing to evaluate the water contact angles and determine if the electrospun nanofibers were hydrophobic or hydrophilic. The sessile drop method was used to determine the contact angles between a 20 μL water droplet and flat nanofibers. With the use of the Krus programme, all of the photographs were taken 30 seconds after the water droplets were cast.

9.2.2.8. Swelling Index:

The swelling index (S.I) of the NFs was studied to check their water absorption capacity. For this study, 1*1 cm^2 piece of NF of each group were immersed into 50 ml phosphate buffer solution (PBS) and weighing them in different time intervals (0,1,2,3,4,5,6,20,21,22,23,24 hrs). Before taking the weight of the NFs at different time intervals, all NFs are soaked with filter paper to absorb the PBS droplets of NFs surface and keep over filter papers in room temperature for 10 mins to drying. The increased weight of NFs shows the swelling index property of the NFs. Here, the swelling index is calculated by determining the ratio of the increased weight of the NFs after immersing in PBS to the dry weight of the NFs before immerse in PBS.

% of Sweeling index was calculated by the following equation:

$$\% \text{ S.I} = \frac{(Wt - W0) * 100}{Wt}$$

W_t: Weight of the NFs at time t

W_0: Weight of the NFs before immerse in buffer solution

9.2.2.9. Invitro Biodegradation Study of PCL and PCL-SF based Electrospun Nanofiber:

In vitro biodegradation of PCL and PCL-SF electrospun nanofibers were estimated by incubating them in phosphate buffered solution (PBS), prepared by following the protocol developed by Kokubo et al.

To check the biodegradation property of SF-PCL based nanofiber, the mats were cut into small pieces (1*1cm^2) and weighed. The pieces of NFs then immersed in 10 ml freshly prepared 1x Phosphate buffered solution (PBS) and keep in incubator at 37℃ and 5 % CO_2 condition for certain time points (7,14,21 days).

In each time points the nanofibers were taken out from the PBS and soaked with tissue paper to remove excess droplets of PBS. Keep in room temperature and weighed again.

% of Weight loss was calculated by the following equation,

% of weight loss (W_L) = $\{(W_0-W_t)/W_0\}$ *100

Here,

W_L: % of weight loss,

W_0: the initial dry weight of sample when t=0,

W_t is dry weight of the sample after certain time points.

9.2.2.9. Mechanical Properties:

Tensile testing was performed on the 50 mm * 15 mm electrospun nanofibrous sheets after certain adjustments. (Elsayed et al., 2016) The samples, which had a gauge length of 20 mm, were pulled using a 100 N load cell in a Tinius Olsen UTM machine (Tinius Olsen) at a cross-head speed of 1 mm/min until the nanofiber was ruptured. Each sample has undergone a triplicate study.

9.2.2.10. Antimicrobial Test:

Here, antimicrobial assay of PCL, PCL-SF, PCL-SF-0.5% Ag, PCL-SF-1% Ag, PCL-SF-RGO, PCL-SF-RGO-Ag, PCL-SF-Calendula NFs was done by checking % of bacterial cell growth viability. Here, MTT assay was done to check the antimicrobial assay.(Balouiri et al., 2016) The Luria-Bertani (LB) broth containing a single colony of an Escherichia coli and *Bacillus subtilis* strain were cultured overnight at 37°C and was further diluted to obtain 0.1 O.D. bacterial cell suspension. Here, as positive control standard marketed antibiotic Streptomycin has been used.

All groups of nanofibers were cut into small pieces (1*1 cm^2) and sterilized by immersing them into 70% ethanol and washed with autoclaved water to remove ethanol and others debris. Then the pieces of nanofibers were taken into each well of 24 well plate and 100µl 0.1 O.D. bacterial suspension was seeded. Add 1 ml liquid Luria-Bertani (LB) broth media was poured into every well and keep them in the incubator at 37°C and 5 % CO_2 for overnight.

Next day, after changing the media, added 5 mg/ml concentrated MTT solution (in 1x PBS) into each well and keep the plates again in incubator for 4 hrs. After, 4 hrs add DMSO and incubate for 5 mins at 37 37°C and 5 % CO_2 condition to form formazan crystals and take O.D. From this O.D. by the following equation, bacterial cell viability was calculated by Microplate reader (*BIO-RAD, iMark^{TM}) at 595 nm.

9.2.2.11. Assessment of Cell viability and cytotoxicity:

In this study, MTT (3-(4,5-dimethyl-thiazol-2-yl)-2,5-diphenyltetrazolium bromide) assay was done to assay the cell cytotoxicity. L929, the mouse fibroblast cell line was taken for this assay. Nanofiber were cut into small pieces (1*1cm^2) and sterilized them by immersing them into 70% ethanol for 15-20 mins and then washed 3 times with autoclaved water to remove the ethanol from the fiber.

Now the fiber pieces are put into 24 well plate and in each well 1 x 10^4 L929 cells (approximately counted by haemocytometer) were seeded on per nanofiber and kept the plates in incubator at 37 ℃ and 5 % CO_2 for 1,3,7 days' time point. In this study cell proliferation has compared with tissue culture plates (TCPs).

5 mg/ml concentrated MTT solution was prepared by dissolving the MTT reagent in Dulbecco's phosphate-buffered saline (DPBS). For this assay after the respective time points plate was taken out from the incubator and removed the media and washed with 1X cell culture graded PBS to remove the dead cells. Add 500 µl MTT solution in each well of 24 well plate and again kept the plate in incubator for 4 hrs. After, 4hrs of incubation aspirated the MTT solution added 500 ml of DMSO in each well. Mix it properly and incubate again 5-10 mins at 37 ℃ and 5 % CO_2 condition to form formazan crystals. Then it transferred into 96 well plate the absorbance was measured by a microplate reader (*BIO-RAD, iMark^{TM}) at 595 nm wavelength.

10. Results and Discussion:

10.1 One Pot Green Synthesis of RGO from GO by Using C. officinalis mother tincture

10.1.1 FTIR Study of Green Synthesized RGO:

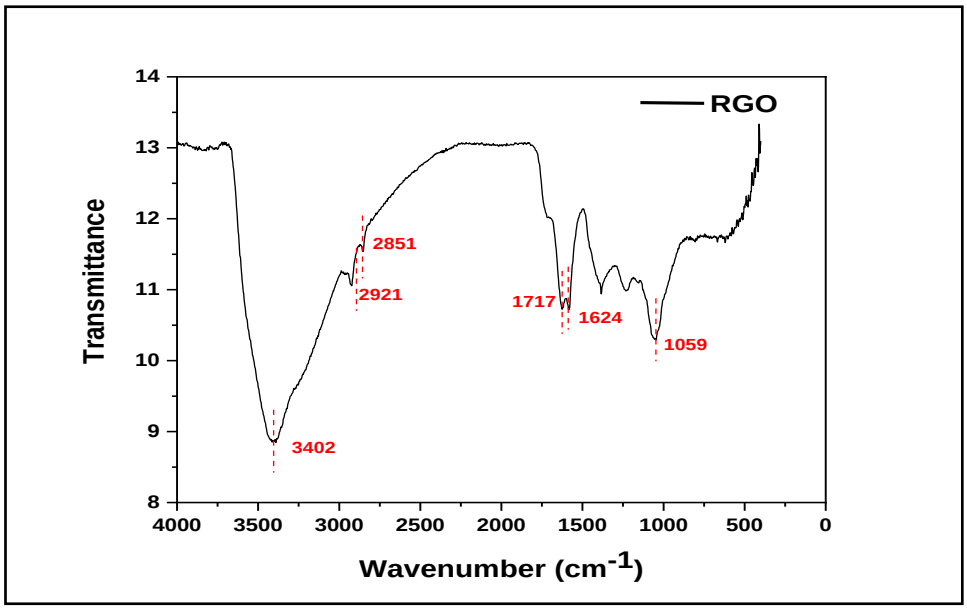

Fig 4: FTIR spectra of prepared Green synthesized RGO

The presence of wide band at 3402 cm^{-1} correspond to stretching vibrations of the -OH bond in C-OH group, with possible contribution from water and presence of calendula mother tincture (Feipeng et al., 2018). The small peaks at 2921 cm^{-1} and 2851 cm^{-1} are attributed the stretching vibrations of CH_2. The peak at 1624 cm^{-1} indicates the stretching in the sp^2 vibration plane of C=C bond (Aragaw, 2020). The peak at 1717 cm^{-1} corresponds to the stretching of carboxyl group. The peak at 1059 cm^{-1} corresponds to the C-O stretching vibration of epoxy group (Lee et al., 2017) (Olfati et al., 2021).

Table 1: FTIR Peak analysis of RGO prepared by using Calendula officinalis mother tincture

Absorption Frequency Range (cm^{-1})	Bond present in RGO	Functional Groups
1059	Stretch C-O	Alkoxy, epoxy
1624	C=C stretch	Aromatic C=C
1717	C=O stretch	Carbonyls

2851	-CH2-	methylene
2921	-CH2-	methylene
3402	O-H stretch, H bond	Alcohols, phenols, hydroxyl

10.1.2. XRD Study of prepared Green synthesized RGO:

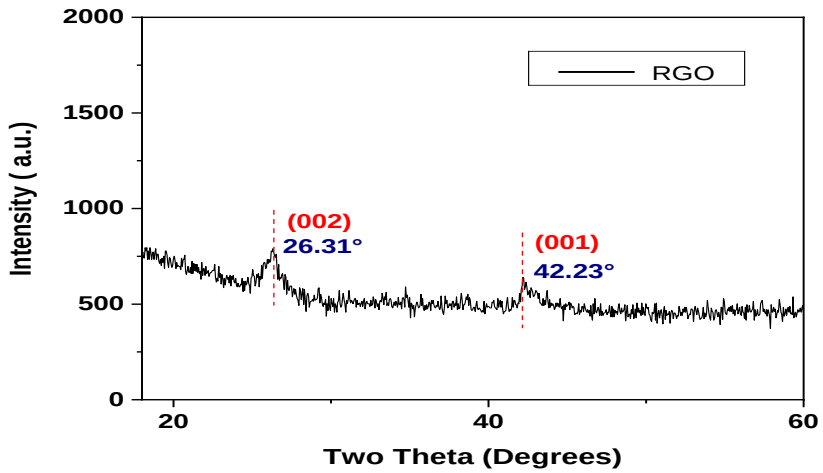

Fig 5: XRD spectrum of prepared RGO by using Calendula officinalis mother tincture

For green synthesized, XRD has been employed to look into the crystal phase and determine the interlayer spacing. At 2 = 26.31°, a wider peak of green synthesised RGO can be seen, indicating that the -conjugated structure of graphene has been significantly restored at the generated RGO (Soomro et al., 2018). For this prepared RGO, the broad peak (002) indicated the crystal phase. The decrease of RGO from GO can result in the formation of single or several layers of RGO. RGO nanosheet were attracted to one another as a result of the strong Vander Waals forces present. The turbostratic band of disordered carbon mate is responsible for another, less intense peak that can be detected at 2=42.23° with (001) orientation (Gualdrón-Reyes et al., 2015).

10.1.3 Raman Spectroscopy Study of prepared Green synthesized RGO:

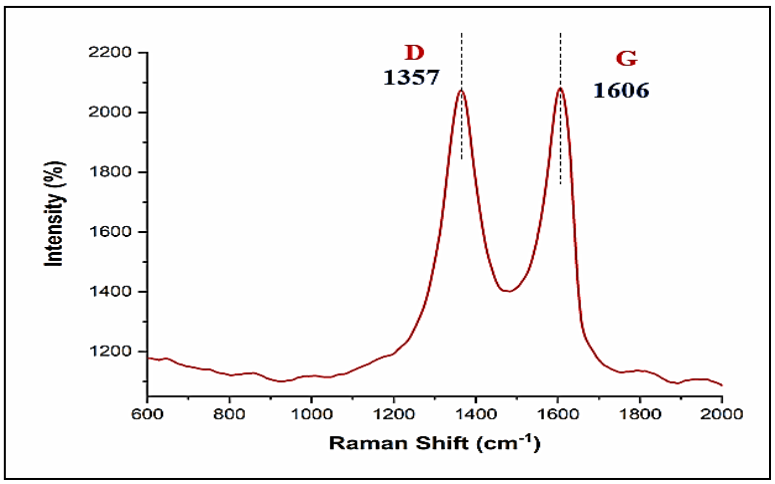

Fig 6: RAMAN Spectra of prepared RGO by using Calendula officinalis mother tincture

An effective and non-destructive instrumentation technique for identifying the electrical and structural characteristics of carbon materials is Raman spectroscopy. Instead of using a laser, it gives information based on the inelastic (Raman) scattering of a molecule exposed to monochromatic light. In this case, RGO exhibits two fundamental vibrations between 600 and 2000 cm-1.

At 1357 cm-1 for RGO, the D vibration band, which is made up of a breathing mode of j-point photons with A1g symmetry, may be seen. On the other hand, the G vibration band for RGO developed around 1606 cm-1 as a result of the first-order scattering of E2g phonons by sp2 carbon. (Thakur and Karak, 2012) Furthermore, the stretching C-C bond, which is present in all sp2 carbon systems, also contributed to the G vibration band. The disorder bands and tangential bands, respectively, are represented by the Raman spectrum's D band and G band in Fig. 5. (Ding et al., 2014)

The intensity ratio of this RGO-Calendula nanocomposite is 0.84.

10.1.4 Scanning Electron Microscopy Image Analysis of Green Synthesized RGO:

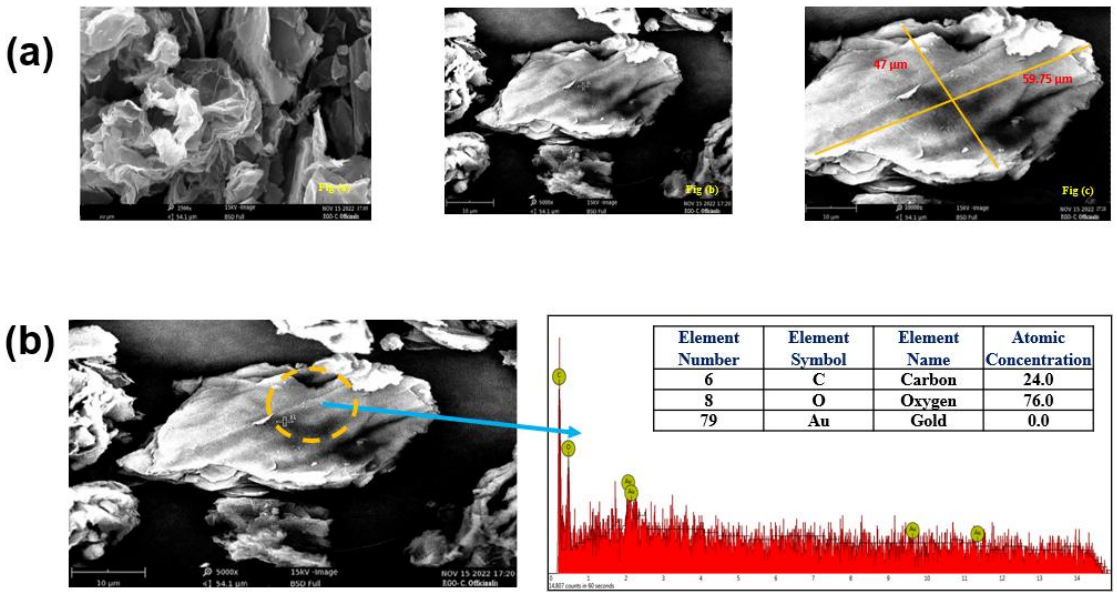

Fig 7. (a) Scanning Electron Microscopy Image Analysis of RGO by using Calendula officinalis mother tincture (a) 2500x, (b) 5000x and (c) 10000x; 7. (b) EDX Analysis of prepared RGO by using Calendula officinalis mother tincture

Morphological study is needed to characterize the topography image, morphological structure, shape and size of the nanoparticle. To check on the morphological structure of RGO here, SEM has used. The micro graphical image obtained from SEM gave a highly magnified image on the surface of a material. Figure (6) shows the micrographs for RGO sample at different magnification of 2500x, 5000x and 10000x.

The morphological images of RGO prepared by green synthesis method which surface contained crumpled thin flex like sheets which accumulated to form disordered structure material (Aunkor et al., 2016).

10.1.5 Energy-dispersive X-ray spectroscopy (EDX or EDS analysis) with SEM

From EDS spectrum analysis, here it is confirmed about the presence of carbon (24%) and oxygen (76%) molecule in this prepared RGO sample (Low et al., 2015) (Aragaw, 2020).

10.1.6 Transmission Electron Microscopy Image Analysis of Green Synthesized RGO

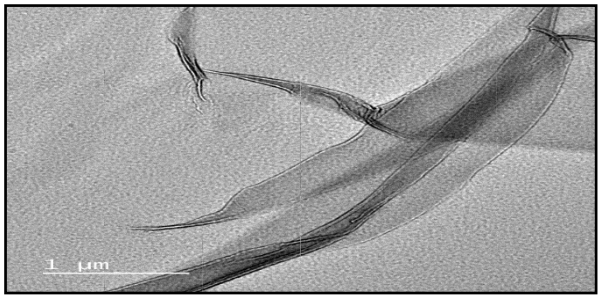

Fig 8: TEM Image of Green Synthesized RGO

Transmission electron microscopy (TEM) is used to see the morphological characterization of particle formation, size, structure, shell formation or elements distribution in material of materials. RGO looks like silk like nanosheet structure (Santha kumar et al., 2015).

10.2 Hemocompatibility analysis of Green Synthesized:

To evaluate the haemolytic activity of green synthesized RGO, hemolysis assay of different concentrations of RGO solution has measured by calculating their haemolytic activity on human blood sample. It was studied in dose dependent manner which form conjugates with RBC (Red blood cell) membrane. (Joshi et al., 2020)

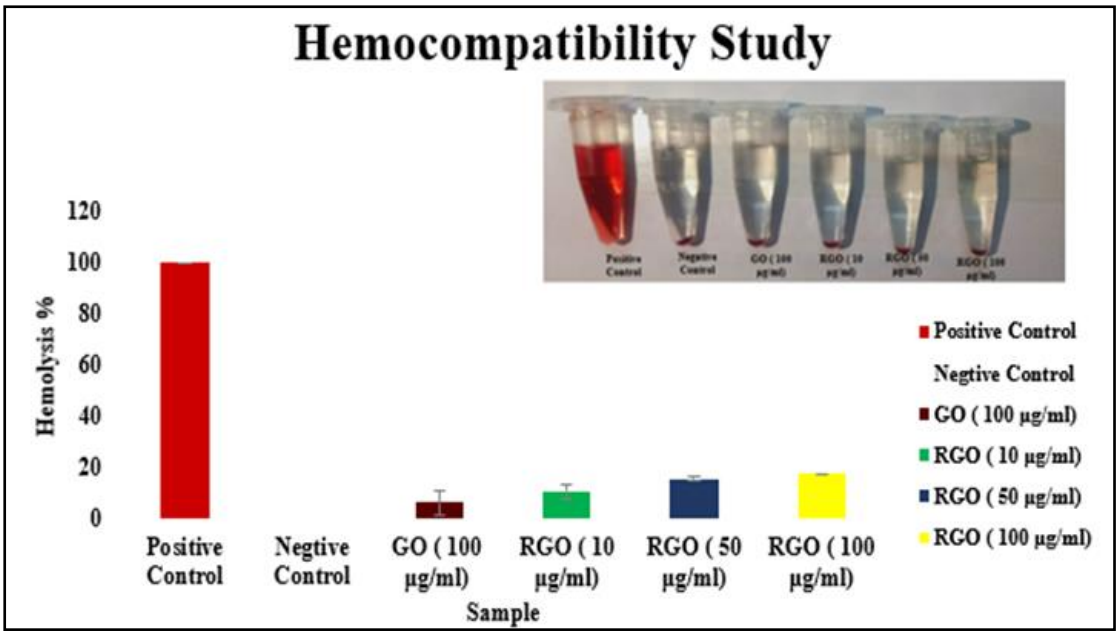

Fig 9: Hemocompatibility Study of GO and Prepared RGO

Table 2: Hemocompatibility Study of GO and Prepared RGO

Sample	% of Hemolysis
Positive Control	100
Negtive Control	0
GO (100 microgram/ml)	0.925895062
RGO (10 microgram/ml)	4.320987654
RGO (50 microgram/ml)	7.716049691
RGO (100 microgram/ml)	9.567901543

The result of hemolysis assay of green synthesized RGO has shown in table 2 which indicates the release of haemoglobin due to the RBC membrane lysis. In table 2, only 0.93 % of hemolysis occurred due to effect of 100 µg/ml GO concentration. Here, RGO shows a dose dependent hemolysis effect where at 10 µg/ml RGO concentration shows only 4.32 % of hemolysis with increasing the RGO concentration % of hemolysis has also increased such as

for 50 µg/ml, it shows 7.71% hemolysis and for 100 µg/ml it shows 9.56 % of hemolysis. From this discussion it can be said that up to 100 µg/ml RGO is hemocompatible therapeutic agent.

10.3 Antibacterial Study of GO and Green Synthesized RGO:

From this bacterial viability minimum inhibitory concentration of GO and RGO has been measured for both E. coli and B. substilis. The bacterial cell viability has gradually decreased along with increasing the sample concentration for both GO and RGO.

In this study, MIC values of GO and RGO on E. coli 125 µg/ml, 63 µg/ml (Fig 10) respectively and for B. substilis (Fig 11) 63 µg/ml and 125 µg/ml respectively

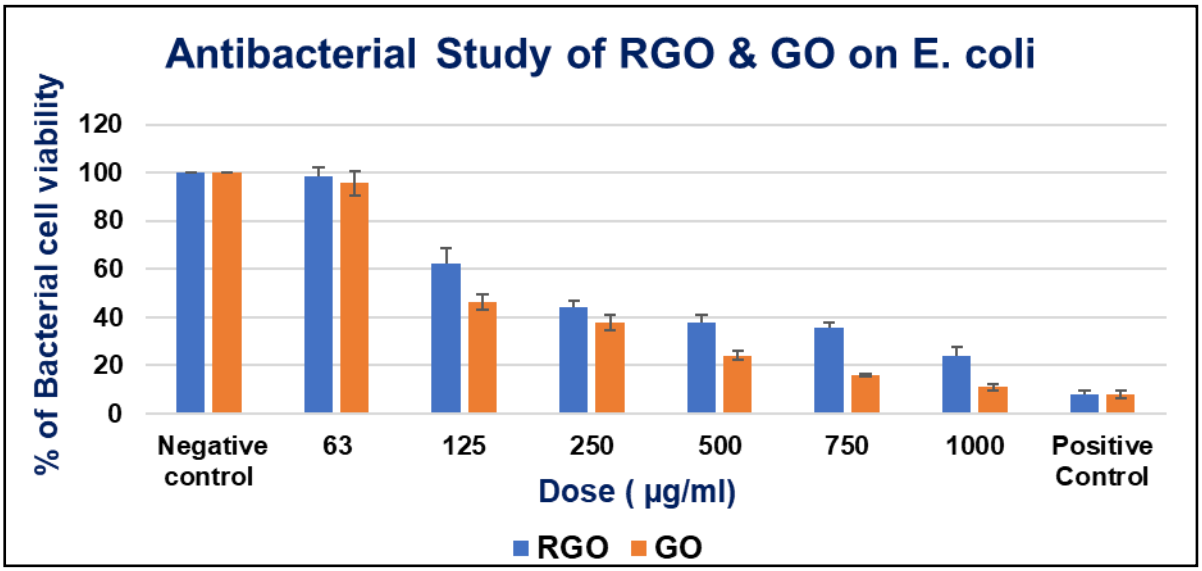

Fig 10: Antibacterial Study of GO and RGO on E. coli

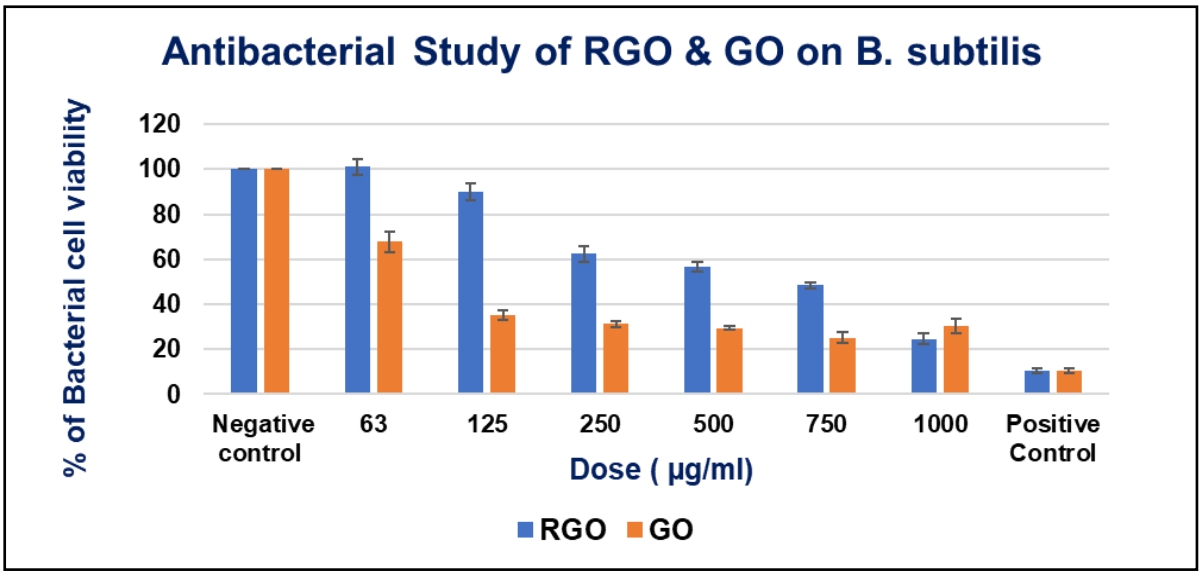

Fig 11: Antibacterial Study of GO and RGO on B. subtilis

From this OD value, bacterial cell viability has been calculated with respect of negative control. Microsoft Excel 11 was used to obtain the MIC 50 values through a linear regression between the % of bacterial cell viable and different concentrations of GO and RGO powder.

Table 3: Antibacterial Effect of GO and RGO

Bacteria Species	MIC Value (µg/ml)		MIC 50 (µg/ml)	
	GO	RGO	GO	RGO
E. coli	63	125	372.51	492.34
Bacillus subtilis	125	63	1095.44	644.45

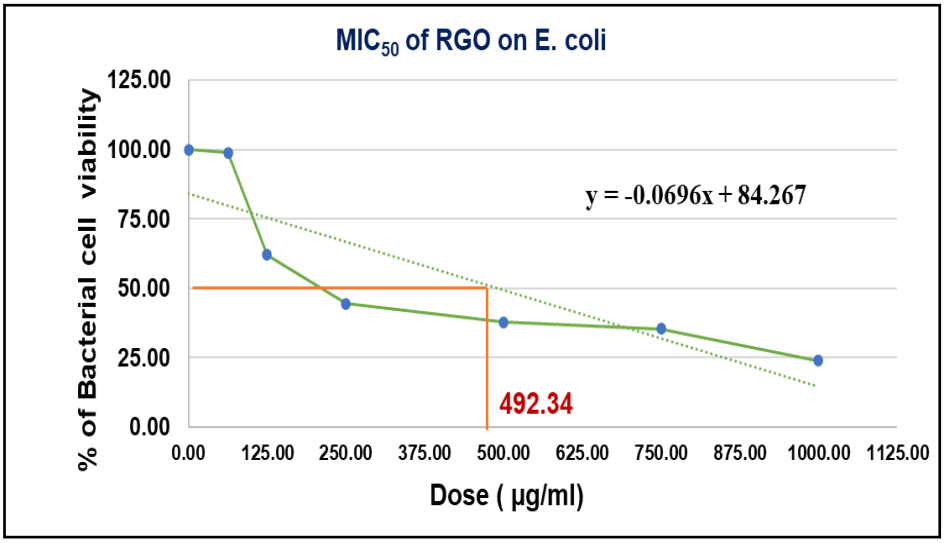

Fig 12: MIC_{50} of RGO on E. coli

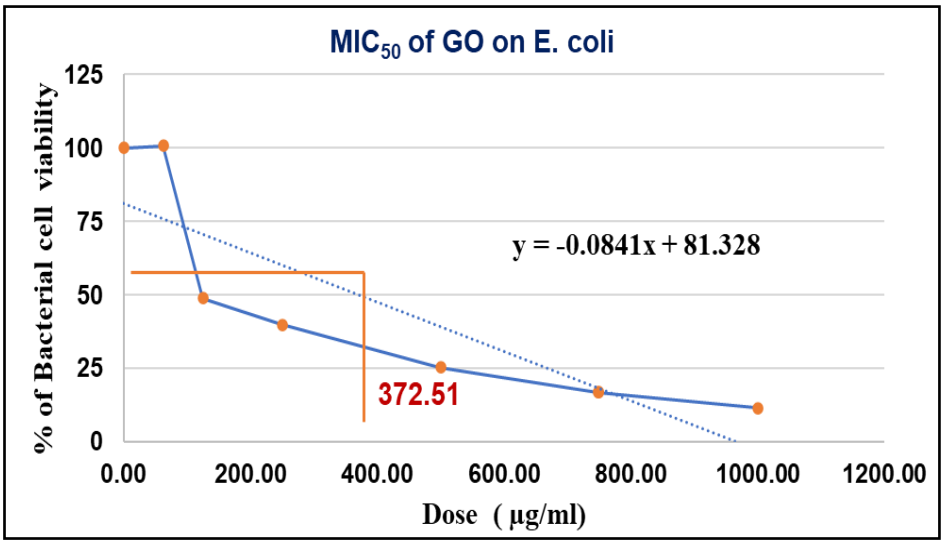

Fig 13: MIC_{50} of GO on E. coli

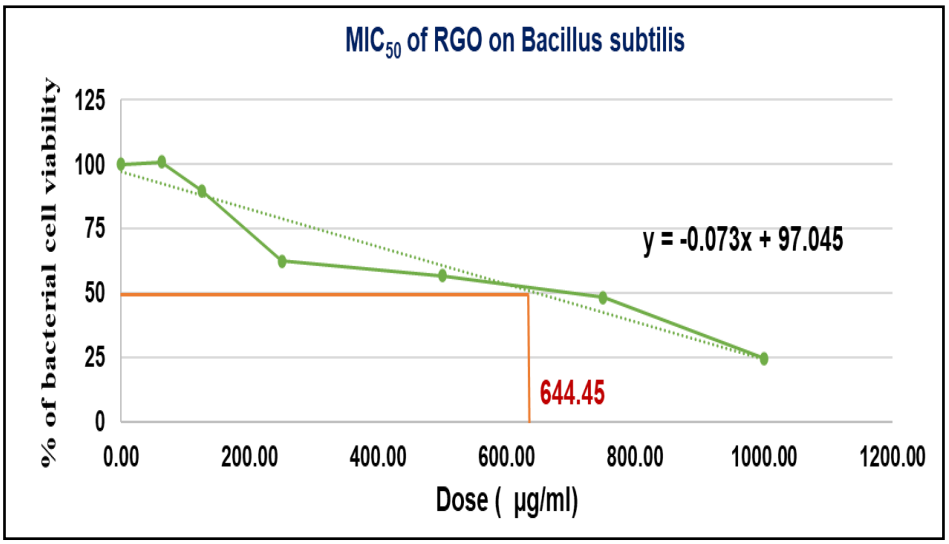

Fig 14: MIC_{50} of RGO on B. subtilis

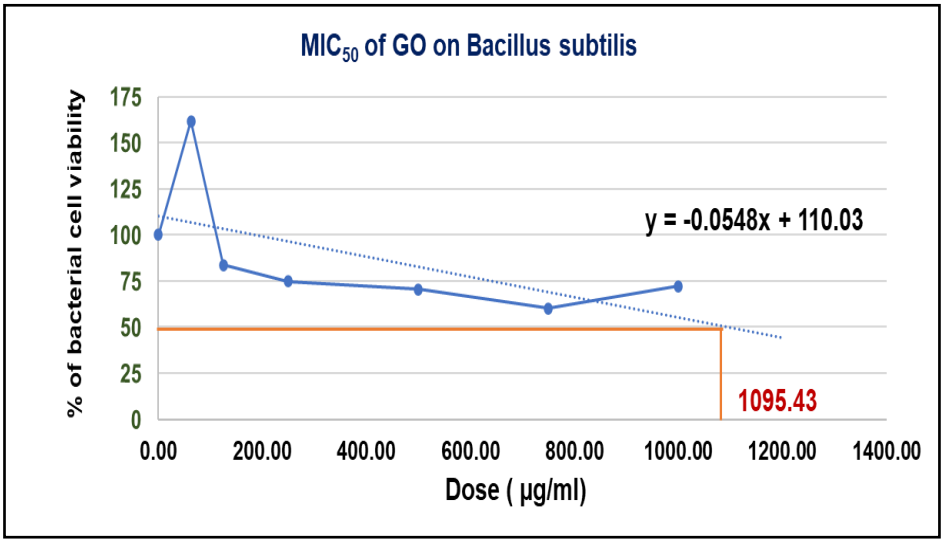

Fig 15: MIC_{50} of GO on B. subtilis

10.4 Cytotoxicity Assay and Cell Proliferation Assay of Green Synthesized RGO:

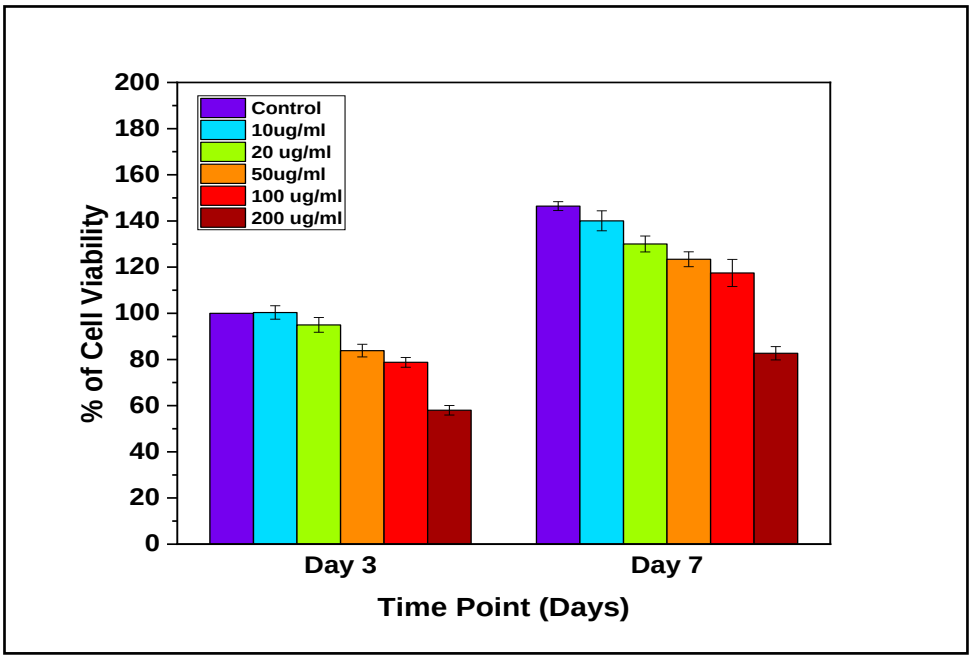

Fig 16: Cytotoxicity studies of Green Synthesized RGO on L929 cell lines for 3 and 7 Days

In this study, cytotoxicity study has been done through MTT assay on L929 cell for 3 and 7 days with different concentration of green synthesized RGO solution which showed a dos dependent result. The results are indicated in fig … cells without RGO solution were marked as control with 100 % cell viability.

From these results, it is clear that in day 3 time point, at lower concentration of RGO (10 µg/ml, 20 µg/ml and 50 µg/ml, 100 µg/ml) shows no toxicity as the cell viability is more than 75 %. For, 200 µg/ml the cell viability is considerably lower than control which is approximately 58 % that indicates about minor toxicity.

For, day 7 cell viability has increased than day 3 cell viability of each concentration of RGO solution.

10.5 Physical Interaction of Green Synthesized RGO and Cellular Phenotype Study by Live and Dead Assay:

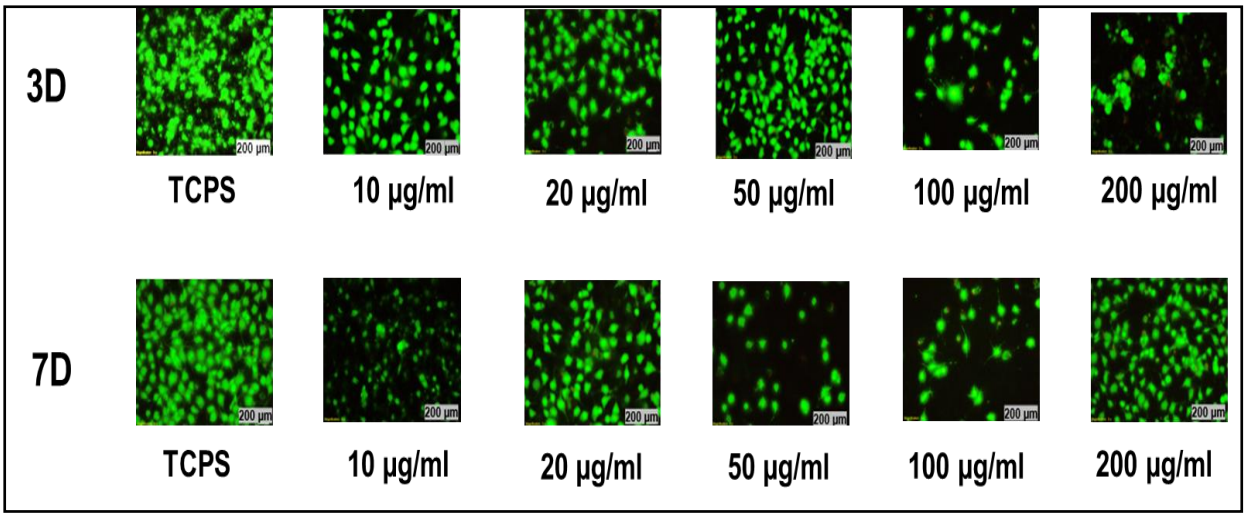

Fig 17: Live and Dead assay on L929 mouse fibroblast cells at Day 3 and Day 7 timepoints after treatment with different concentration of Green Synthesized RGO

In this experiment, Live/Dead assay was done on L929 cell which were treated with different concentration of RGO for day 3 and day 7 time point.

After 3 days of incubation, it is seen in fig 17 that at lower concentrations such as 10 µg/ml, 20 µg/ml and 50 µg/ml there is no presence of dead cells. At, 100 µg/ml and 200 µg/ml concentrations presence of dead cells (red stained) are visible. At day 7, presence of dead cells is viable at higher concentrations (100 µg/ml and 200 µg/ml) but their amount is very less. So, it can be said that green synthesized RGO is non cytotoxic in 100 µg/ml.

10.6. Physical Interaction of Green Synthesized RGO and Cellular Phenotype Study by FITC-DAPI Staining

In this study, MTT assay has done to evaluate its cytotoxicity and cell proliferation properties. (Thorat et al., 2014) Phenotype study increase the assurance of MTT assay that also helps to determine the morphological change of treated cell. Here, different concentration of green synthesized RGO treated L929 cells mouse fibroblast cell was stained with FITC and DAPI dyes to evaluate the cell toxicity. (Shao et al., 2017) This type of multiple staining coupled with microscopy observations helpful for live and dead cells more qualitatively and accurately.

FITC dye enters into the live cells and emits green fluorescence by generating fluorescein due to enzymatic hydrolysis of FITC in live cells. DAPI binds strongly with the nucleus of the live cells and emits blue fluorescence. From fig 18, it is observed that after 3 days of green synthesized RGO treatment and comparison with untreated cells cellular characteristics such

as cell death, including cell shrinkage, presence of floating cells was not observed in observed in L929 cells exposed to green synthesized RGO. However, from this image, it can be said that a loss of membrane integrity has been observed at higher concentrations 200 µg/ml.

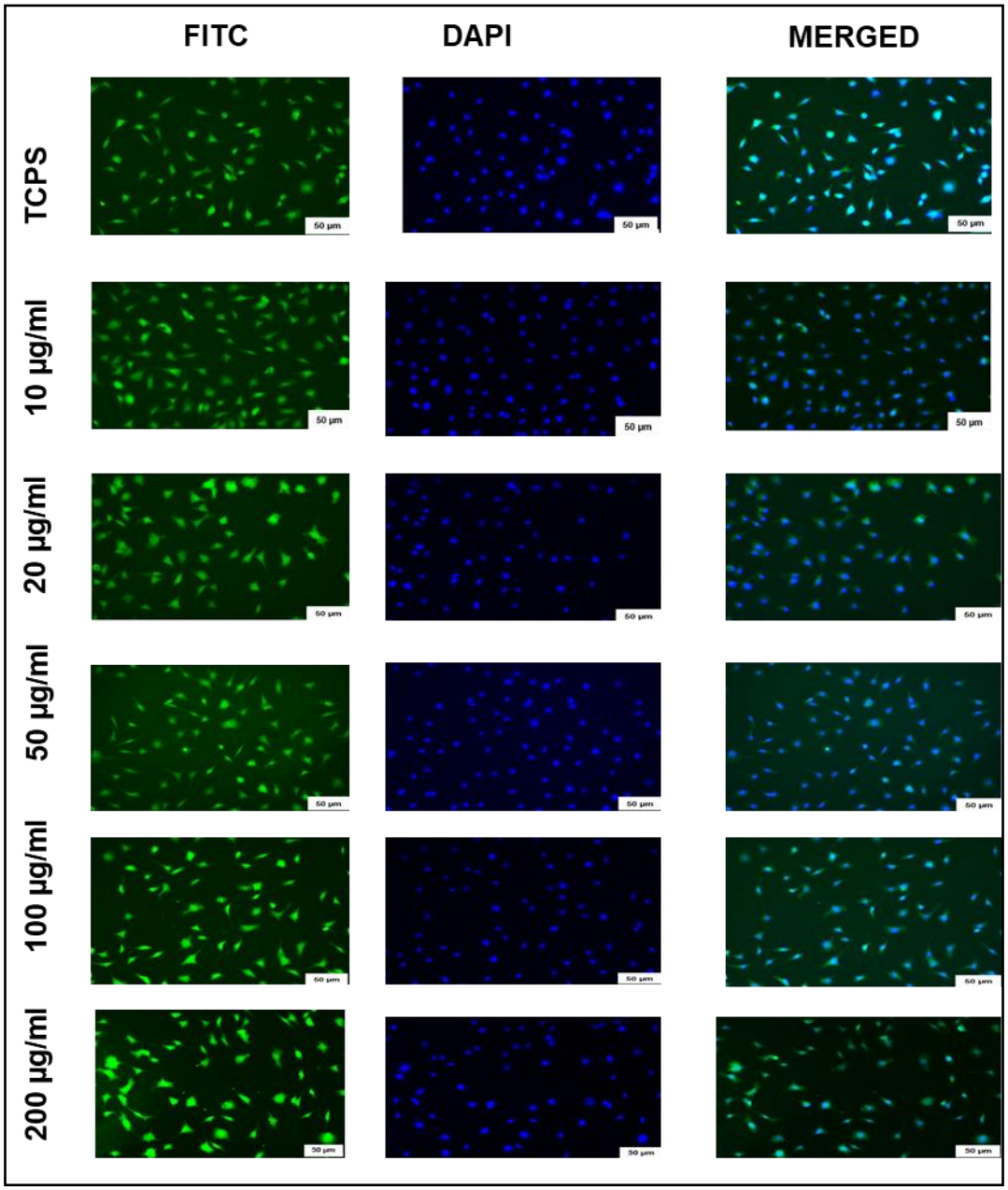

Fig 18: The fluorescence images of FITC-DAPI stained L929 cells cultured with Different concentration of Green Synthesized RGO for Day 3

10.2 Fabrication of Antibacterial Therapeutic Agents Doped Silk Fibroin PCL Based Nanofiber by Electrospun Method for Tissue Engineering

10.2.1. Degumming loss:

Degumming loss of Silk fibroin has calculated by this following equation.

% of Degumming loss was calculated by the following equation:

= {(Initial weight of silk fibroin cocoon – weight of lyophilized silk fibroin)/ Initial weight of silk fibroin cocoon} *100

= {(300-16.34)/300} *100 % = 94.55 %

In this study, total cocoon was taken 300 gm and after degumming the weight of lyophilized regenerated silk fibroin is 16.34 gm.

Hence, the % yield of degummed silk is = (100-94.55) = 5.45%

10.2.2 Analysis of Silk Molecular Weight

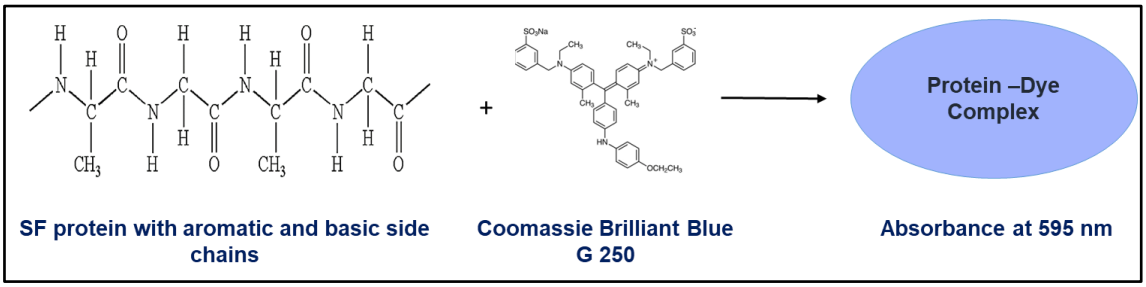

Fig 19: Mechanism of action Coomassie Blue G250 dye with SF protein

Proteins can be separated from other bio-macromolecules using the sodium dodecyl sulphate polyacrylamide gel electrophoresis (SDS-PAGE) method according to their mass, size, and charge. It is the approach that is most frequently used to research proteins and their interactions. Degummed silk fibroin must first be solubilized in a denaturing buffer containing SDS before being exposed to electrophoresis in a polyacrylamide gel in order to perform SDS-PAGE. Following electrophoresis, the separated proteins will be stained with colours like Coomassie Brilliant Blue or silver nitrite to make them visible. This technique can be used to examine the dimensions, composition, and number of silk fibroin proteins.

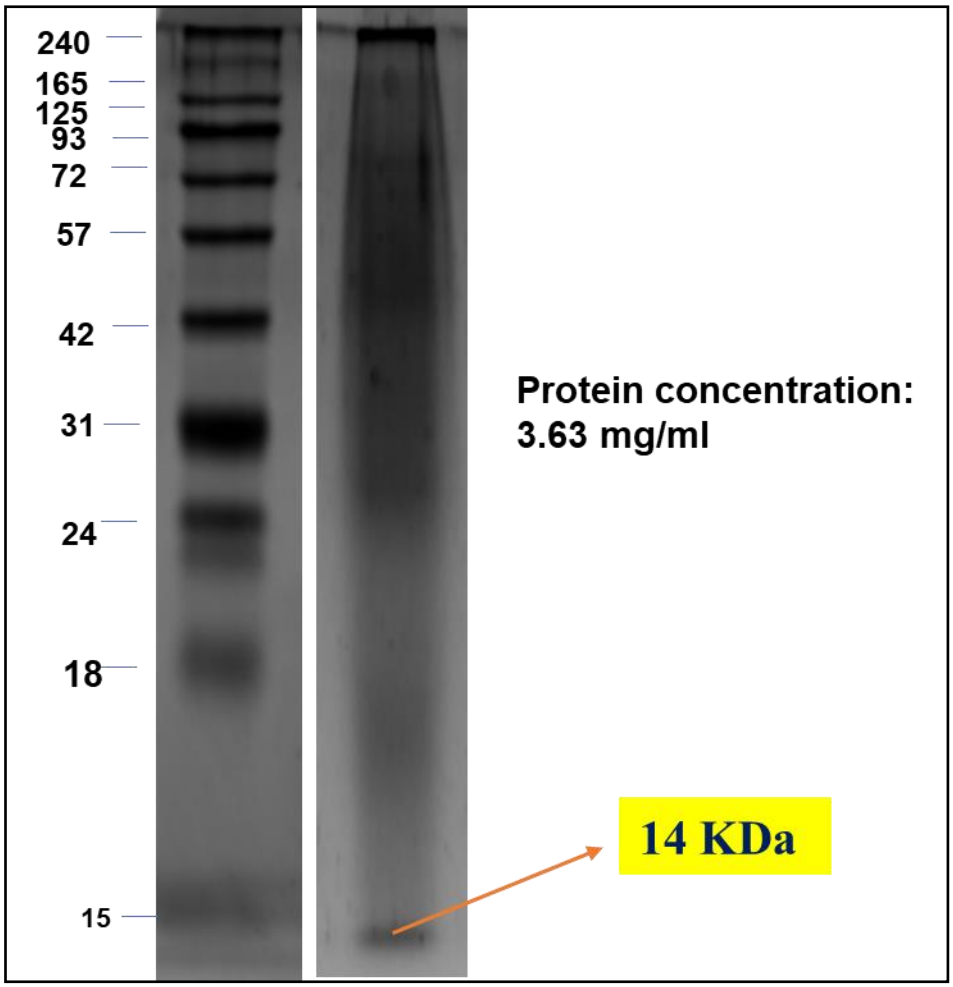

Fig 20: Molecular weight of Na_2CO_3 Treated Degumming Silk Fibroin Protein after comparing with standard protein marker

According to previous published work, it was concluded that silk fibroin has broad molecular weight range due to presence of high molecular weight chain and low molecular weight chain. During this degumming process, due to the effects of used chemicals such as degumming agent and temperature, some parts of silk fibroin protein is degraded so it gives different molecular weight. Molarity of Na_2CO_3 and LiBr and using temperature also are responsible for the molecular weight. (Wang and Zhang, 2013)

In this experiment, obtained molecular weight from fig 20, image of gel after SDS-PAGE experiment of tested SF is around 14 KDa.

10.2.3 Fabrication of SF-PCL based Electrospun Nanofiber:

The fabrication procedure of all groups of nanofibers have described in tabular form in table 4.

Table 4: Details Parameters of Fabricated Nanofiber with Obtained Diameters

Groups of NF	Solvent for PCL	Solvent for SF	Volume (ml)	Flow Rate (ml/hrs)	Distance (cm)	Voltage (kV)	Average Diameter (nm)
PCL	17% PCL in the mixture of CHCL3 and CH3COOH (80:20)	------	3 ml	1.5	12	18	226.84
PCL- SF	17% PCL in the mixture of CHCL3 and CH3COOH (80:20)	10% SF in 85% HCOOH	3 ml emulsion of PCL:SF (4:1)	1.5	12	18	368.52
PCL- SF-0.5 % Ag	17% PCL in the mixture of CHCL3 and CH3COOH (80:20)	10% SF in 85% HCOOH	3 ml emulsion of PCL:SF (4:1)	1.5	12	18	374.82
PCL- SF-1 % Ag	17% PCL in the mixture of CHCL3 and CH3COOH (80:20)	10% SF in 85% HCOOH	3 ml emulsion of PCL:SF (4:1)	1.5	12	18	304.47
PCL- SF-RGO	17% PCL in the mixture of CHCL3 and CH3COOH (80:20)	10% SF in 85% HCOOH	3 ml emulsion of PCL:SF (4:1) & RGO	1.5	12	18	430.25
PCL- SF-RGO-Ag	17% PCL in the mixture of CHCL3 and CH3COOH (80:20)	10% SF in 85% HCOOH	3 ml emulsion of PCL:SF (4:1) & RGO	1.5	12	18	406.23
PCL- SF-Calendula	17% PCL in the mixture of CHCL3 and CH3COOH (80:20)	10% SF in 85% HCOOH	3 ml emulsion of PCL:SF (4:1) & RGO	1.5	12	18	378.74

Discussion:

From the discussion of table 4, the diameters of all groups of fabricated nanofibers are in range all are under 1000 nm. The diameter and the histogram analysed by the help of SEM images in 10X magnification by using Origin 2018 software and Image J software. It is seen that use of silk fibroin with PCL increase its average diameter.

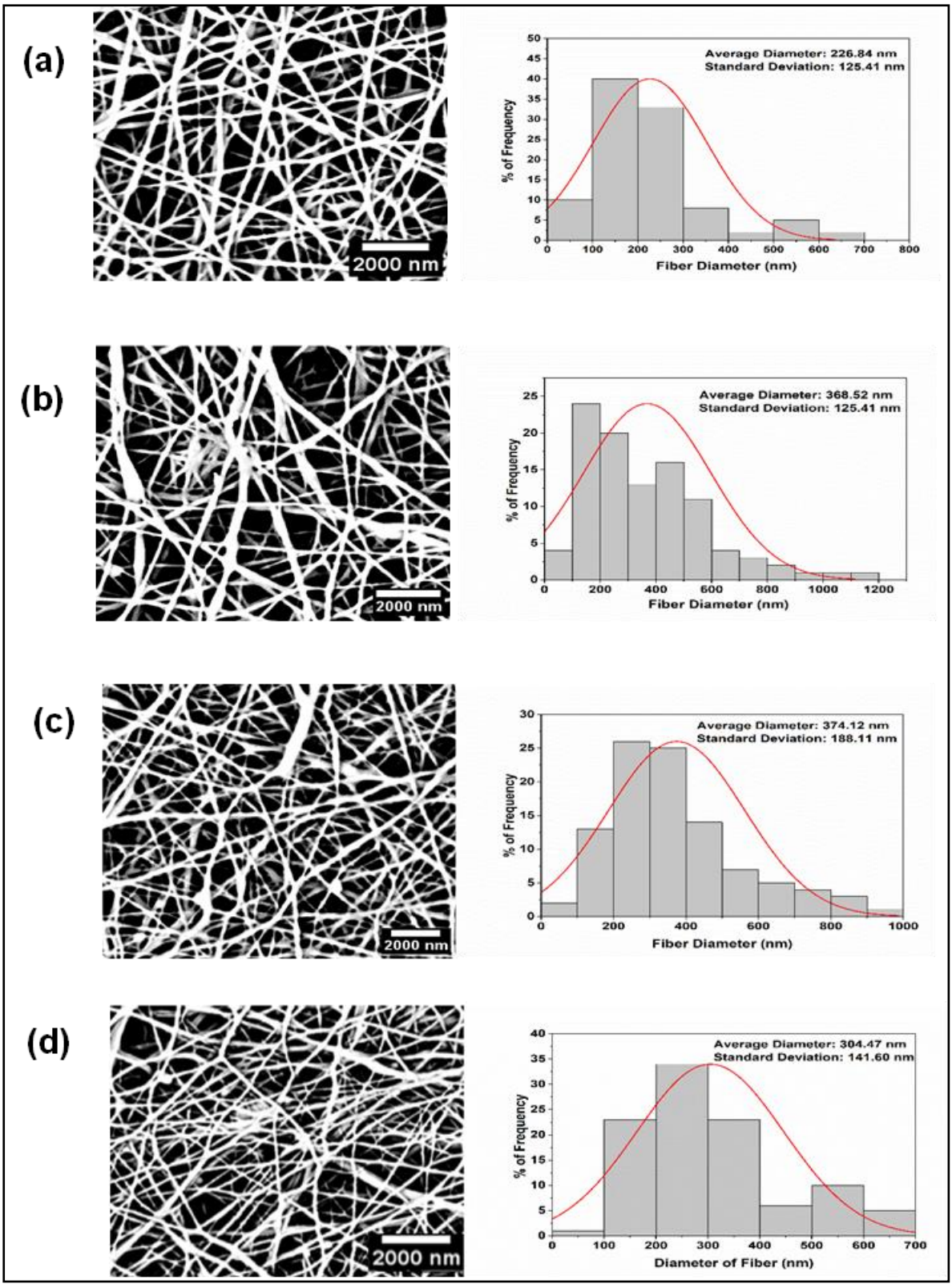
(a)
2000 nm
Average Diameter: 226.84 nm
Standard Deviation: 125.41 nm
% of Frequency
Fiber Diameter (nm)
(b)
2000 nm
Average Diameter: 368.52 nm
Standard Deviation: 125.41 nm
% of Frequency
Fiber Diameter (nm)
(c)
2000 nm
Average Diameter: 374.12 nm
Standard Deviation: 188.11 nm
% of Frequency
Fiber Diameter (nm)
(d)
2000 nm
Average Diameter: 304.47 nm
Standard Deviation: 141.60 nm
% of Frequency
Diameter of Fiber (nm)

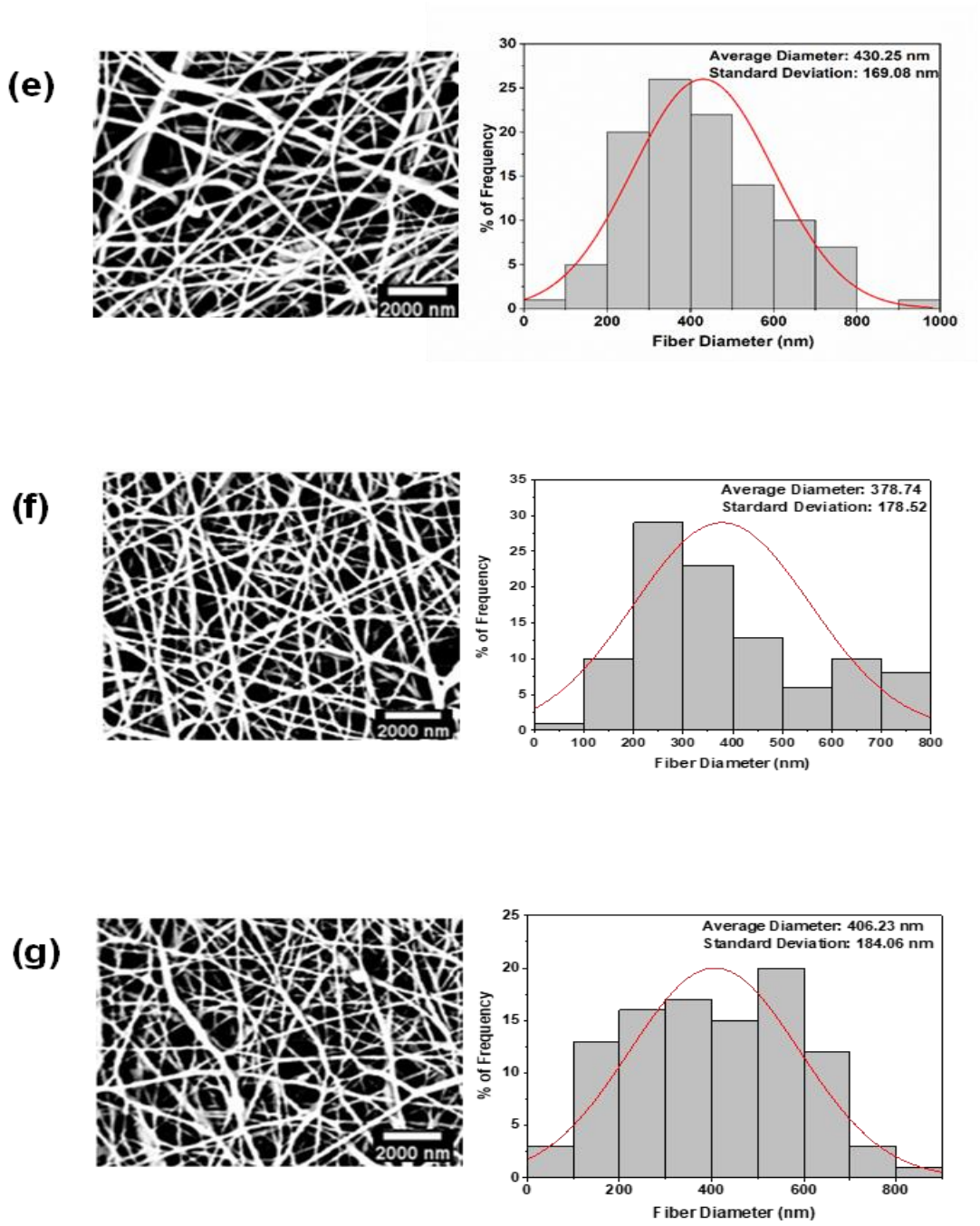

FIG 21: SEM images and diameter measurement of (a) Pure PCL, (b) PCL SF, (c) PCL SF 0.5% Ag (d) PCL SF 1% Ag (e) PCL-SF-1%RGO, (e) PCL-SF- RGO (f) PCL-SF-Calendula, (g) PCL-SF-RGO-Ag Nanofiber (For data analysis Origin software and Image J software have used)

10.2.4 ATR-FTIR Study of SF-PCL Based Nanofibers:

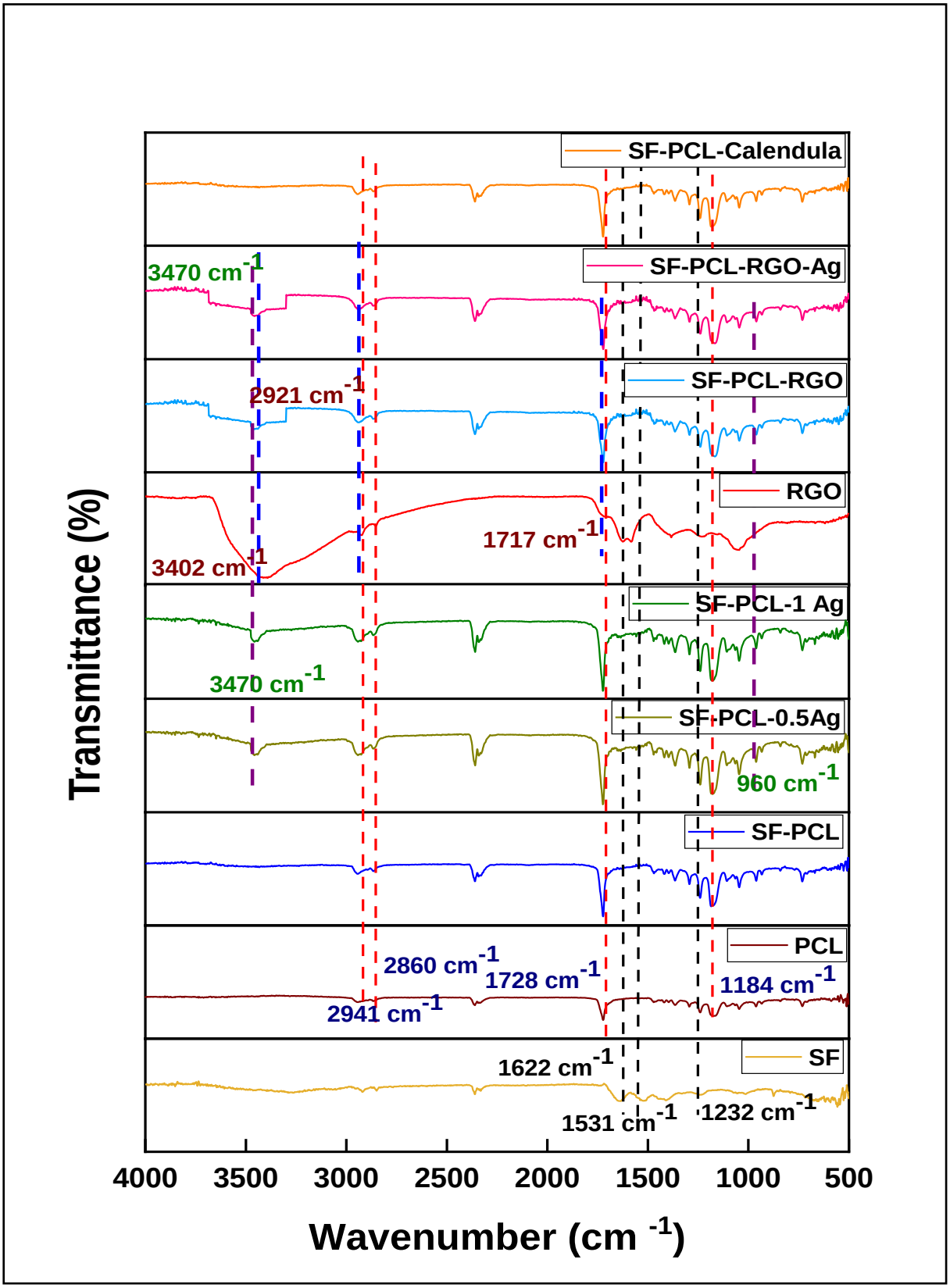

Fig 22: ATR FTIR analysis of SF-PCL Based electrospun Nanofiber

ATR- FTIR of PCL-SF based nanofiber have analysed by the characteristic spectral absorption peaks of ATR- FTIR spectrophotometer (IRAffinity-1S, SHIMADZU, Chicago, Illinois). All ATR-FTIR spectra of nanofiber were recorded between 4000 and 500 cm^{-1}.

One of the most effective sampling techniques for Fourier transform infrared (FTIR) spectroscopy is attenuated total reflectance. In order to offer both qualitative and quantitative information on the chemical composition of examined samples, FTIR is a potent analytical technique used in both research and industry. The degree of secondary structural modifications as well as the existence of functional groups like amides, alkynes, trace gases, and other functionalities can all be determined using FTIR.

In this study, Spectroscopic techniques such as ATR-FTIR used to study the structure of silk fibroin. FTIR spectra of silk fibroin provide information about its molecular structure, which can then be used to characterize the physical properties of the material. FTIR spectra of silk fibroins usually show strong absorbances at 1622 cm-1 and 1531 cm-1, corresponding to C=O stretching vibrations, and at 1031 cm-1 and 921 cm-1, corresponding to C–N stretching vibrations, which are indicative of the two different polypeptide chains that make up the silk fibroin molecule. The strong peaks at 1231 cm-1, which correspond to the stretching vibrations of the amide group. The stretching vibrations of the amide I band are mainly attributed to N-H stretching and C-N stretching, and can be further divided into three sub-bands: the strong peak around 1650 cm-1 corresponds to N-H bending; the weak peak at 1530 cm-1 is due to C-H symmetric deformation; and the broad peak at 1228 cm^{-1} is due to the a-helix conformation of the protein chain. The amide II band appears as a wide peak from 1000 to 1300 cm^{-1}, and is mainly attributed to C-N stretching and C-C stretching.

The obtained ATR FTIR peak of PCL nanofiber is typically observed at 2941 cm^{-1} (attributed to the C–H stretching vibrations of methyl and methylene groups), 2860 cm^{-1} C-H stretching vibration), 1728 cm^{-1} (associated with the C=O stretching vibration as well as the C-H bending mode.), and 1184 cm^{-1} (C-O stretching modes).

In SF-PCL nanofiber, peaks of both SF and PCL are present which confirm about the presence of SF and PCL.

The Obtained ATR FTIR peak for silver nanoparticles incorporated SF-PCL-0.5 Ag and SF-PCL-0Ag electrospun nanofiber are at 3470 cm-1 (stretching vibration of the surface-active

species such as hydroxyls-OH and related adsorbed species) and peak at 960 cm-1 in the spectrum of silver nanoparticles is associated with a deformation mode of the silver lattice along with presence of SF and PCL peak.

For, ATR-FTIR spectrum of RGO the presence of wide band at 3402 cm^{-1} correspond to stretching vibrations of the -OH bond in C-OH group, with possible contribution from water and presence of calendula mother tincture (Feipeng et al., 2018). The small peaks at 2921 cm^{-1} and 2851 cm^{-1} are attributed the stretching vibrations of CH_2. The peak at 1624 cm^{-1} indicates the stretching in the sp^2 vibration plane of C=C bond (Aragaw, 2020). The peak at 1717 cm^{-1} corresponds to the stretching of carboxyl group. The peak at 1059 cm^{-1} corresponds to the C-O stretching vibration of epoxy group (Lee et al., 2017) (Olfati et al., 2021).
In the spectrum of SF-PCL-RGO nanofiber the present peaks are 3402 cm^{-1}, 2921 cm^{-1}, 1624 cm^{-1}, 1717 cm^{-1} along with peaks of SF and PCL nanofiber.

In the spectrum of SF-PCL-RGO-Ag all peaks of SF, PCL, Ag and RGO are present which gives the conformation about presence of SF, PCL, green synthesized RGO and Ag.

In the spectrum of SF-PCL-Calendula nanofiber, the peaks are also seen.

10.2.5 X-ray diffraction (XRD) Study of SF-PCL Based Nanofibers:

By bombarding it with X-rays and seeing how the beams are diffracted, this is accomplished. The diffraction pattern that is produced can reveal details about the sample's atoms' dimensions, shapes, and locations. This enables scientists to examine and comprehend the makeup of silk fibroin molecules. A highly effective approach for determining the structure and orientations of nanofibers produced from polycaprolactone (PCL) and silk fibroin is the use of X-ray diffraction (XRD). The molecular structure of the nanofiber can change depending on the processing conditions, and this can be determined by using XRD for identifying crystallinity. The nanofibers' dimensions and shapes, as well as any potential interactions between the individual components, can also be revealed by XRD. In order to understand how the processing circumstances, such as the degree of mechanical stretching and solvent casting, influence the physical and chemical properties of these materials, it is of the utmost importance to understand the XRD data on silk fibroin/PCL nanofibers.

In this study, PCL -SF polymers were used which are semicrystalline polymer. In fig… XRD peak of silk fibroin has seen at 2θ = 20.6° which is represented by deep navy-blue line which given confirmation about regeneration of silk fibroin from B. mori silkworm cocoon.

In PCL structure represented by bottle green coloured line, broad peaks are observed at 21.3° and 23.6° which represents crystal plane (110) and (200) respectively. (Wu, 2010)

For SF-PCL nanofiber which represented by sky blue coloured line, peaks are observed at 20.6°, 21.3° and 23.6° which ensured about the presence of SF (for 2θ = 20.6°) and presence of PCL (respectively 21.3° and 23.6°).

SF-PCL-0.5Ag nanofiber is represented in fig… by purple coloured line where, 37.46° and 44.5° are obtained due to presence of AgNPs which are responsible for crystalline plane (111) and (200). Peaks of PCL and SF are also present in this XRD graph. All peaks are also present in SF-PCL-1Ag nanofiber which is represented in this figure by deep brown coloured line.

Here, a broader peak of green synthesized RGO can be seen at 2θ = 26.31° (Soomro et al., 2018) which indicates about the π-conjugated structure of graphene has been restored considerably at the produced RGO. The presence of broad peak (002) for this RGO-Calendula composite implied the crystal phase. Single or multiple layers of RGO can be formed during the reduction of RGO from GO. Due to presence of strong Vander Waals forces RGO nanosheet were stalked to each other. Another less intense peak can be seen at 2θ=42.23° with (001) orientation which attributed by the turbostratic band of disordered carbon mate (Gualdrón-Reyes et al., 2015). In this figure RGO is represented by red coloured line.

SF-PCL-RGO nanofiber is represented by black coloured line where, peaks are observed at 26.31°, 42.23° for the presence of RGO; 20.6° for SF and 21.3° and 23.6°.

XRD peak of SF-PCL-RGO-Ag nanofiber shows peaks at 20.6° due to presence of SF, 21.3°,23.6° for the presence of PCL, 26.31°, 42.23° for presence of RGO and 37.46° and 44.5° for the presence of silver nanoparticles.

In the XRD peak of SF-PCL-Calendula which is represented in fig 23, by orange coloured line there are only peaks of SF and PCL are present. There is no any significant peak for calendula mother tincture.

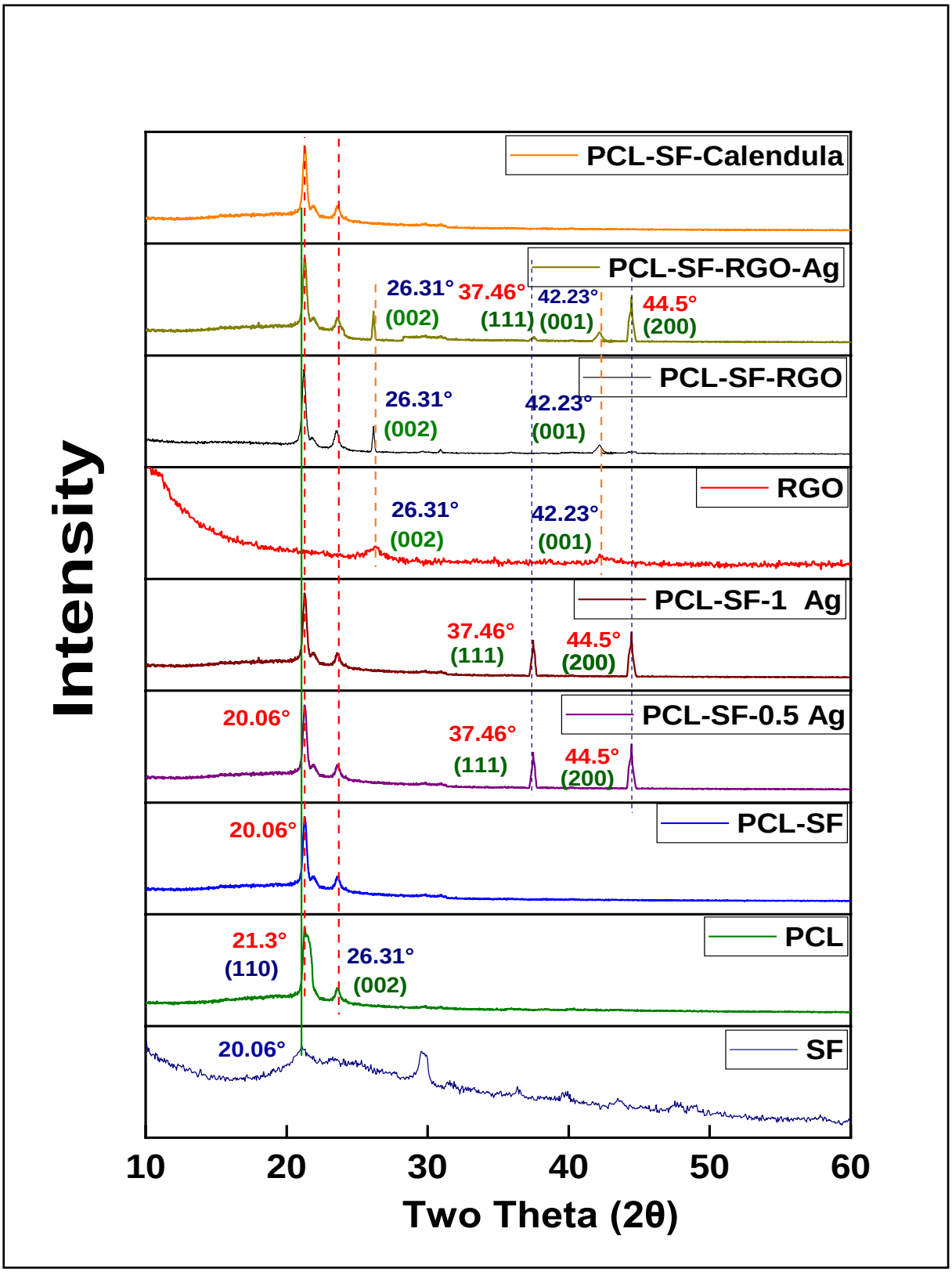

Fig 23: XRD Study of SF-PCL based Nanofiber

10.2.6 Contact angle Measurement of Nanofibers:

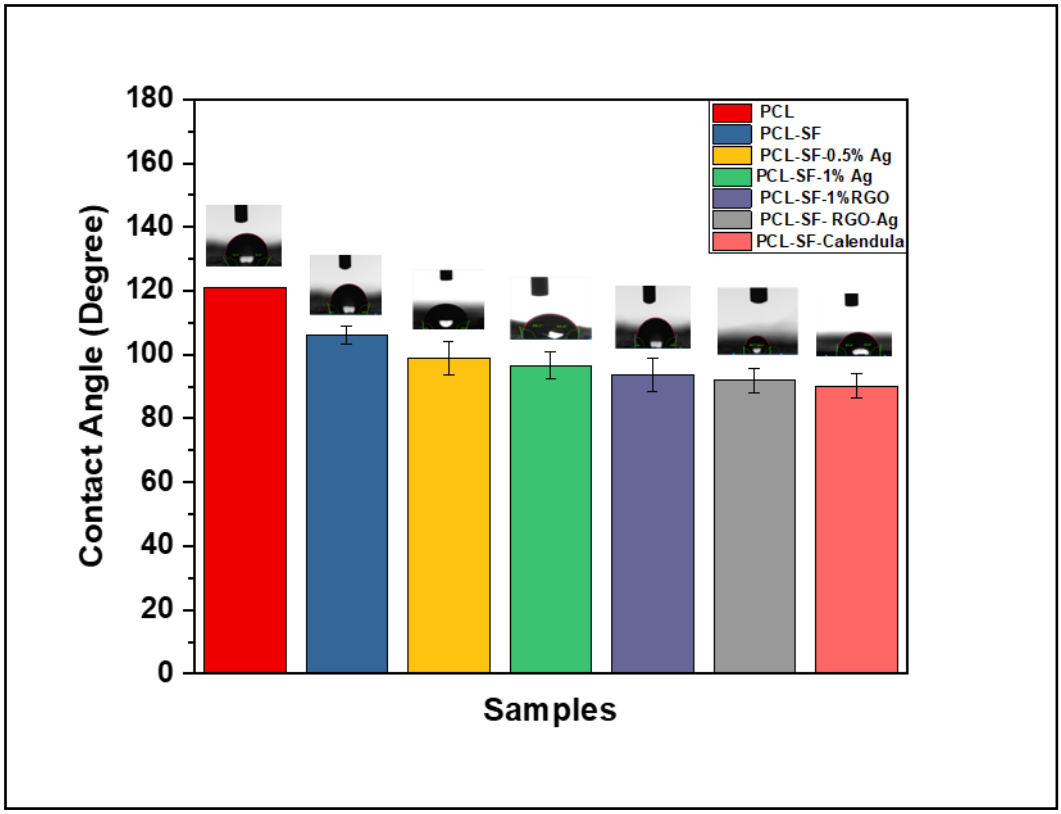

Fig 24: Graphical representation of contact angle of SF-PCL based nanofiber

The purpose of this study is to determine the water contact angle of nanofibers made of polycaprolactone (PCL) and silk fibroin. The sample's contact angle will be determined using the sessile drop method, and the findings will be recorded for comparison. Additionally, the study is going to look at how environmental variables including temperature, pH, and relative humidity affect the water contact angle of silk fibroin/PCL nanofibers. For the purpose of trying to understand their function in the interfacial interactions between water and silk fibroin/PCL nanofibers, it will also be examined the way various surface modifiers affect the hydrophilic property of the nanofiber. Finally, the implications of the study's findings will be examined to determine how the results may be used in a variety of scenarios, including tissue engineering and medical devices. (Chaiarwut et al., 2021)

Water contact angle of pure PCL nanofibers where binary solvent was the mixture of chloroform and acetic acid in 4:1 (v/v). Sessile drop technique was used to measure the contact angle of the nanofibers, analysing the contact angle as a function of surface chemistry. Results showed that the contact angle of the PCL na0nofibers increased with increasing surface hydrophobicity. It can be said that PCL nanofibers exhibit greater hydrophobicity when produced with chloroform and acetic acid mixture, and can be used in applications where higher hydrophobicity is desired.

The hydrophobic surface of nanofibers can be a disadvantage for cell adhesion due to the difficulty of proteins and cells binding to the surface. (Zhang et al., 2022) To increase cell adhesion, the hydrophobicity of the surface must be reduced or eliminated altogether. This can be accomplished through various methods, such as chemical modifications, surface modifications, and introducing functional groups onto the nanofiber surface. Additionally, bioactive molecules such as peptides, carbohydrates, or polymers can be grafted onto the nanofiber surface to create an environment conducive for cell adhesion. In previous study, it was reported that water contact angle (WCA) of PCL nanofiber lies between 150° and 158° (Megaraj and Keppannan, 2018) In this study, WCA of 17% pure PCL nanofiber is 121± 0.07°.

The next nanofiber group is PCL-SF which provide WCA is decreased than pure PCL 106±2.83° which is also hydrophobic. 1% and 0.5% AgNPs doped SF-PCL nanofiber WCA are 96.65±5.20° and 93.75±4.31° respectively. These are also slightly hydrophobic in nature.

Green synthesized RGO doped PCL-SF based nanofiber shows its WCA 92±5.30° and RGO- and AgNPs both doped PCL-SF-RGO-Ag shows WCA around 92±3.82°.

Calendula officinalis mother tincture containing PCL-SF-Calendula nanofiber shown WCA is 90.20±3.96°.

From the above discussion, it can be concluded that, incorporation of SF in PCL (PCL: SF = 4:1 (v/v)) decrease the hydrophobicity.

Table 5: WCA of SF-PCL Based Nanofiber

Groups of Nanofibers	Contact Angle
PCL	121± 0.07
PCL-SF	106±2.83
PCL-SF-0.5% Ag	96.65±5.20
PCL-SF-1% Ag	93.75±4.31
PCL-SF-1%RGO	92±5.30
PCL-SF- RGO-Ag	92±3.82
PCL-SF-Calendula	90.20±3.96

10.2.7 Mechanical Properties Measurement of Silk Fibroin-PCL Based Nanofiber:

Mechanical properties such as young modulus, ultimate strain %, Ultimate tensile Strength (MPa) are the important parameters related with crystal orientation and crystallization when Nanofibers are used as scaffold of biological tissue engineering or as implant.

Tensile testing is a method for determining the mechanical characteristics of PCL-Silk fibroin-based nanofibers, such as tensile strength. This method evaluates a material's capacity to withstand tension or elongation when a force is applied to it. The specimen is stretched during the test until it breaks, at which point the peak tensile stress (ultimate tensile strength) and total elongation at break are calculated. Utilising a Universal Testing Machine (UTM), PCL-Silk fibroin-based nanofibers' tensile strength is routinely evaluated. These nanofibers typically have tensile strengths between 12 and 14 MPa. (Khan et al., 2022)

Mechanical properties can be described by the obtained stress strain curve for tensile testing of the SF-PCL based nanofibers by measuring with UTM machine (Tinius Olsen). From the obtained result in table 6 It is seen that the elastic modulus of SF-PCL based nanofibers were increased than pure PCL nanofiber.

Table 6: Mechanical Properties of Fabricated SF-PCL Based Nanofiber

Sample	Elastic Modulus (Mpa)	Ultimate Tensile Stength (Mpa)	Maximum Strain (%)
Pure PCL	9.68	1.82	24.2
PCL-SF	91.9	6.34	11.9
PCL-SF-RGO	10.5	0.614	11.3
PCL-SF-1Ag	2.37	0.152	7.48
PCL-SF-RGO-Ag	34.7	2.16	6.71
PCL-SF-Calendula	13.4	0.292	5.11

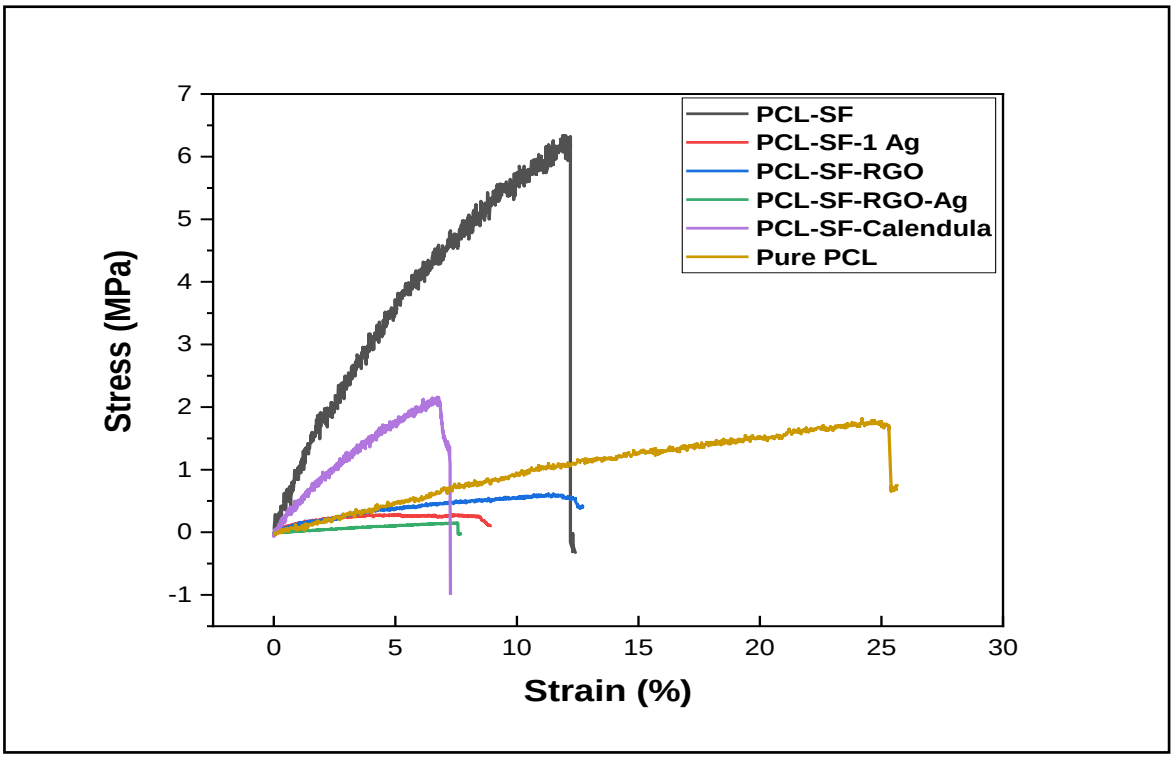

Fig 25: Tensile Strength Test of Nanofibers by UTM

The maximum breaking stress of pure PCL, PCL-SF, PCL-SF-RGO, PCL-SF-Ag, PCL-SF-RGO-Ag, PCL-SF-Calendula are 1.82,6.34,0.614,0.152,2.16,0.292 where it is seen after adding SF, tensile strength has increased than pure PCL. (Kim et al., 2017) From fig 25 it can be said that highest % of strain is 24.2 which is shown by pure PCL where PCL-SF nanofiber has shown less % of strain around 11.9%. PCL-SF-RGO, PCL-SF-1Ag and PCL-SF-RGO-Ag nanofiber given maximum strain 11.3%, 7.48 and 6.71% respectively. PCL-SF-Calendula nanofiber shown least % of strain 5.111%.

10.2.8 Swelling Index Study of Nanofiber:

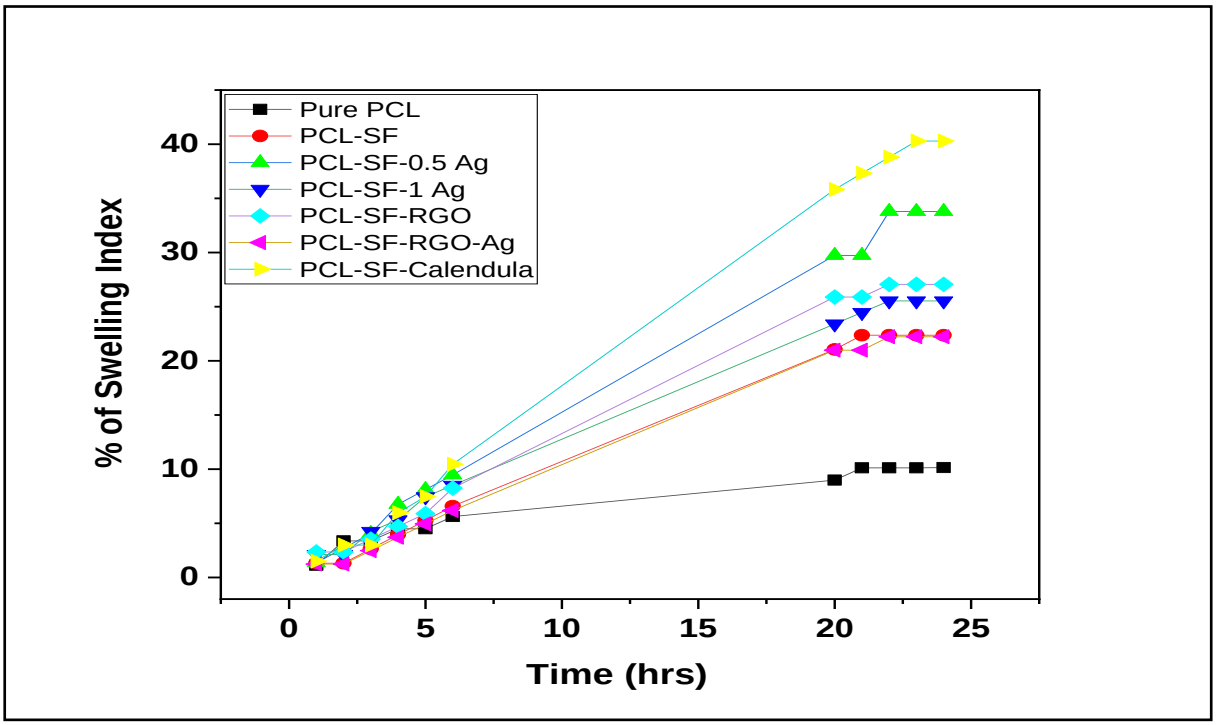

Fig 26: Swelling Index Study of SF-PCL Based Electrospun Nanofibers

The graphical representation from figure 26, Present a study on the swelling index of silk fibroin and polycaprolactone (PCL) based nanofibers. The samples were prepared using electrospinning and evaluated the in vitro swelling behaviour. The results showed that silk fibroin nanofibers demonstrated the highest swelling index when compared to PCL nanofibers due to their lesser hydrophobicity. The water uptake ability of silk fibroin nanofibers was also higher than that of PCL nanofibers. The swelling properties of the nanofibers were found to be dependent on the nature of the polymer, as well as the pH of the solution. (Ertas et al., 2023) This study can be useful for developing components of medical devices that require high swelling properties.

Here, swelling behaviour of electrospun nanofibers have measured at equilibrium condition by keeping small piece (1*1 cm^2) of fiber in PBS (p^H) at 37°C and measured its swelling index which is similar to physiological environment of human body. Others parameters such as gaseous exchange, nutrient transport, tissue regeneration capability of the nanofiber play an important role. From fig 26 it can be said that after 20 hrs swelling index have increased in same way for all nanofibers. Here, pure PCL has shown lowest % of swelling index which

indicates more hydrophobicity PCL-SF-Calendula has shown highest % of swelling index which indicates more hydrophilicity among all groups of nanofibers.

10.2.9 Invitro Biodegradation Study of PCL and PCL-SF based Electrospun Nanofiber:

This study aims to investigate the biodegradation of silk fibroin and polycaprolactone (PCL) based nanofibers in vitro. The efficacy of biodegradation will be assessed by examining the weight loss of the samples over a given period of time. Different parameters such as pH, temperature, and medium composition are also responsible for this biodegradation process. This study is one of the most important studies for the use of any scaffold in in vivo use or use in preclinical as well as clinical study. By understanding the biodegradation mechanisms of these types of polymers, future applications can be developed to make them more sustainable and longer lasting.

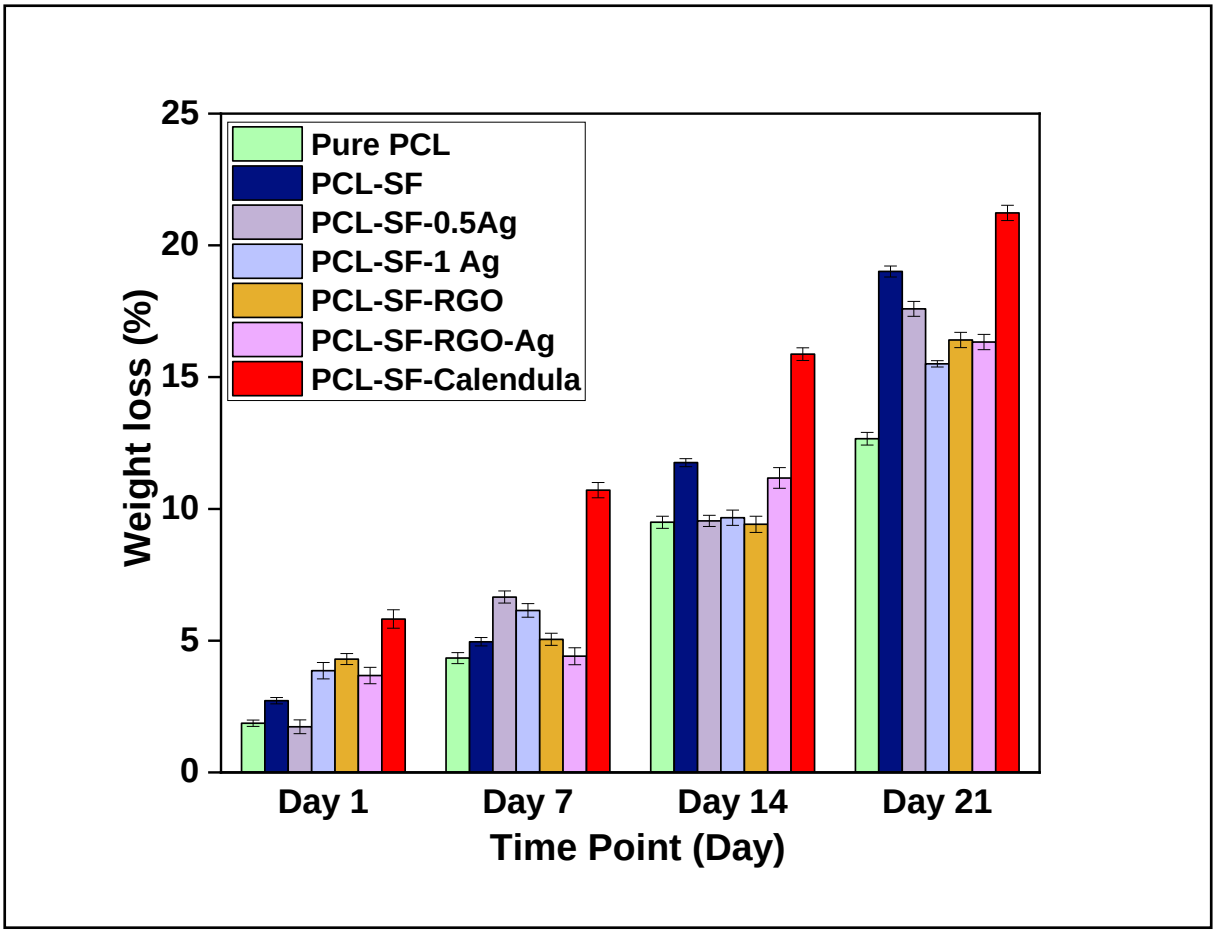

Fig 27: Invitro Biodegradation Study of Silk fibroin PCL based Nanofibers in PBS

In fig 27, it is shown that, weight loss is lowest for pure PCL nanofiber in all time point; at day 1 time point % of mass only 1.87% and at day 21 % of weight loss is 12.66% which indicates its hydrophobicity nature.

After incorporating 20% SF-FA with 80% of PCL, % of weight loss has increased in SF-PCL nanofiber which is at day 1 is 2.72% and at day 21 is 19%. The highest % of weight loss is observed in SF-PCL-Calendula electrospun nanofiber which is at day 1 is 5.82% and at day 21 is 22.24 %. It can be attributed that incorporation of SF increased % of weight loss as well as less hydrophobicity nature. In, SF-PCL-Calendula nanofiber presence of 10% of Calendula officinalis mother tincture of total volume indicates more water base of that emulsion which shows highest % of weight loss in biodegradation study.

10.2.10 Antimicrobial Assay of Nanofibers:

Silk fibroin and PCL based nanofibers have been extensively studied for their potential as antibacterial agents due to their structural characteristics. Silk Fibroin nanofibers possess a permanent antimicrobial activity due to their lipophilic/hydrophobic membrane in addition to being a source of a mixed cationic/anionic peptides, while PCL nanofibers show an amphiphilic surface, enabling them to interact with bacterial membrane molecules, leading to antimicrobial activity. Studies have shown that both silk fibroin and PCL-based nanofibers can effectively inhibit the growth of various pathogenic bacteria such as *Escherichia coli, Bacillus subtilis, Staphylococcus aureus and Pseudomonas aeruginosa.*

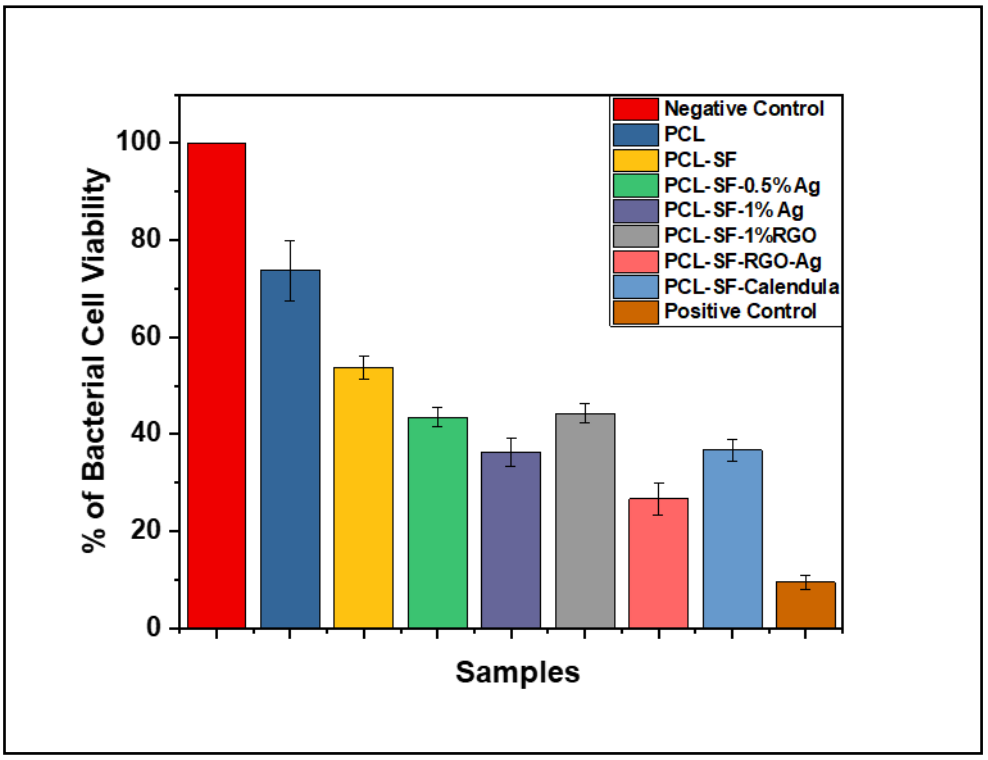

Fig 28: Graphical Representation of Antibacterial Effects of SF-PCL Based Nanofiber on E. coli

Here, in this study antimicrobial properties of fabricated SF-PCL based nanofiber has evaluated by checking inhibition of % of bacterial cell growth viability. In the graph of antibacterial effect on E. coli bacteria of fig…(a) it is seen that the total bacterial cell viability on negative control (bacterial growth without any antibiotic effect) is 100% and E. coli growth due to effect of Streptomycin is very less only 9.41% with respect of negative control.

PCL nanofiber has antibacterial effect (Lyu et al., 2019) as here bacterial growth has reduced in 73% where bacterial growth in negative control is 100%. SF-PCL based nanofiber shown more antibacterial effect from that can be said that SF has self-antibacterial effect. Silver doped SF-PCL has shown more antibacterial effect due to presence of AgNPs and SF. (Shao et al., 2021)

Green synthesized RGO doped SF-PCL-RGO nanofiber shown a promising result against E. coli growth (Mann et al., 2021) by showing 44% of bacterial growth only.

When green synthesized RGO and Ag both are doped in SF-PCL that also shown a good antibacterial effect (26%) Calendula officinalis also shown a good antibacterial effect on E. coli (36%).

Among all groups of nanofibers, SF-PL-RGO-Ag has shown highest antibacterial effect on E. coli.

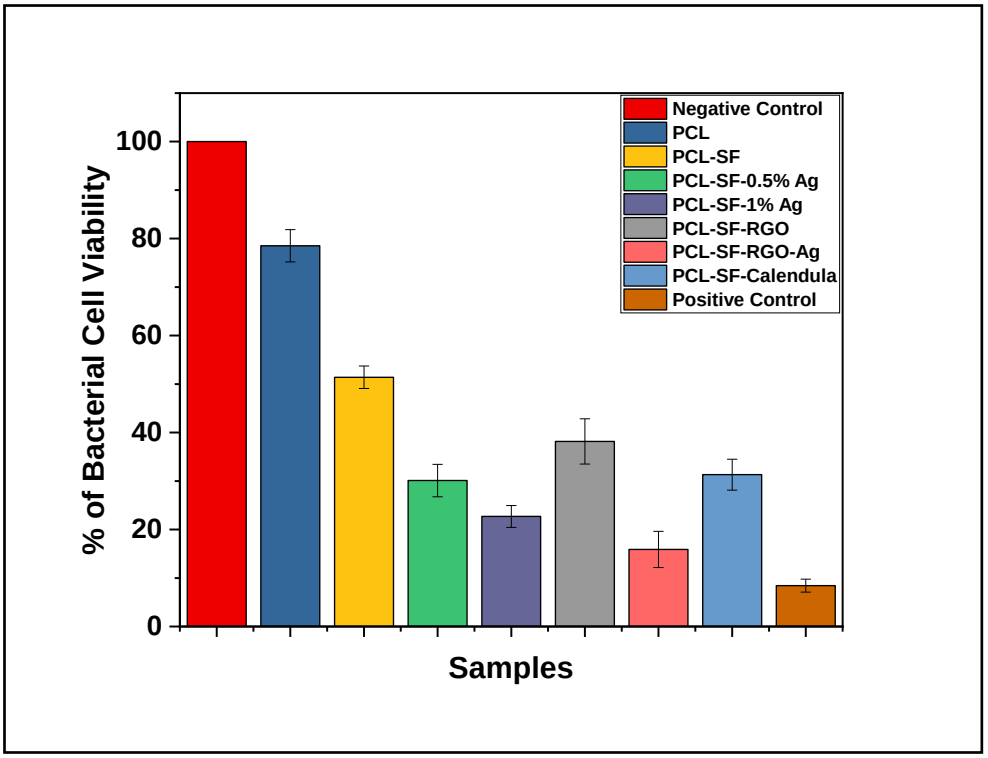

Fig 29: Graphical Representation of Antibacterial Effects of SF-PCL Based Nanofiber on B. subtilis

Recent research has revealed that nanofibers composed of silk fibroin and polycaprolactone (PCL) possess antibacterial properties against the Gram-positive bacterium Bacillus subtilis. In particular, it has been shown that these nanofibers have a strong inhibitory effect on the growth of B. subtilis, with minimal inhibitory concentrations (MICs) lower than those of other commonly used antibiotics such as ciprofloxacin and erythromycin. (Ghalei and Handa, 2022) Furthermore, it has been observed that the antibacterial activity of the silk fibroin/PCL nanofibers against B. subtilis is highly effective even at low concentrations and does not result in any significant cytotoxicity. These findings suggest that the silk fibroin/PCL nanofibers may be a promising alternative to traditional antibiotics for the treatment of bacterial infections caused by B. subtilis.

Here in Fig 29, It is seen that after incorporating SF into PCL it shows better antibacterial result. In this study, negative control is untreated B. subtilis growth was which growth was considered as 100%. As a positive control in this study, 100 µg/ml concentrated streptomycin was used that allows only 8.42% of B. subtilis growth with respect of negative control. (Liu et al., 2010)

Pure PCL nanofiber given 78% bacterial growth where PCL-SF nanofiber shown 51% of bacterial growth which proved self-antibacterial property of regenerated silk fibroin.

AgNPs doped PCL-SF has shown a great antibacterial effect. PCL-SF-0.5 Ag shown 30% bacterial growth where PCL-SF-1Ag shown only 22% of B. subtilis growth. (Hu et al., 2020).

Green synthesized RGO doped PCL-SF-RGO nanofiber also given a good antibacterial effect as here B. subtilis growth was only 38 %. SF-PCL-RGO-Ag doped SF-PCL Based nanofiber shown an excellent antibacterial result against B. subtilis (15.9%). SF-PCL-Calendula nanofiber also shown.

10.2.11. Cell Proliferation and Cytotoxicity Assay:

The growth and division of L929 mouse fibroblast cells has used for in vitro cell proliferation. Many aspects, like as the availability of nutrients, cell-cell contact, and the presence of growth factors, are necessary for this process to occur. The quantity of cells can be quantified to determine the rate of cell proliferation, or it can be determined indirectly using additional sophisticated methods, such as detecting the quantity of DNA present in the cell culture. Understanding the impact of various treatments, such as medications or chemicals, on cell growth and development requires studies of cell proliferation. (Karakecili et al., 2007) To determine the impact on cell growth, the proliferation of L929 cells on PCL-Silk fibroin-based nanofibers was investigated. The research results demonstrated that PCL-Silk nanofibers might encourage cell division, with a PCL-SF-Ag 1 nanofiber group achieving the highest cell division rate. The study also discovered that PCL-Silk nanofibers promoted cell differentiation and had an advantageous effect on cell adhesion and survival. These results suggest that PCL-Silk nanofibers may have applications in the field of biomedical sciences. (Singh et al., 2020)

Fig 30, shown the cell proliferation result of SF-PCL based nanofiber on L929 mouse fibroblast cell on day 1,3 and 7 time point. The OD of control or TCPS considered as 100% cell viability. From day 1 result, it is shown that cell proliferation was increased in SF-PCL (120%) based nanofiber than pure PCL (96%). Among all groups of nanofibers, SF-PCL-1Ag (116%) shows better cell proliferation that sf-pcl-0.5 Ag (111%). Green synthesize RGO incorporated SF-PCL-RGO shows good cell proliferation (121%) and SF-PCL-Ag-RGO shows approximately 97% cell viability where SF-PCL-Calendula shows 97% cell viability, From. This result it can

be said that at day 1 time point SF-PCL-RGO electrospun nanofiber shows best result in cell proliferation and there is no cytotoxicity effect among these nanofibers.

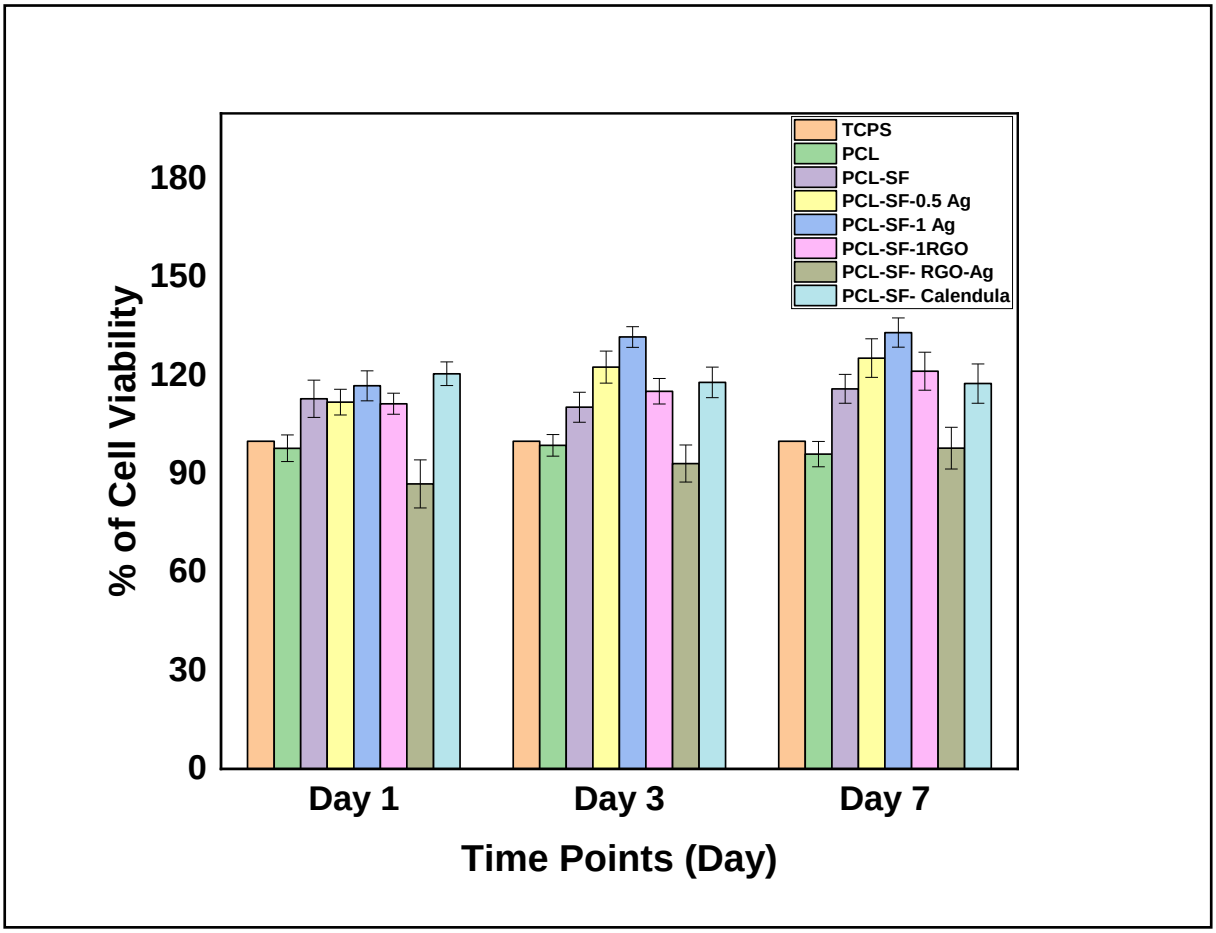

Fig 30: Cell proliferation and Cytotoxicity Study through MTT Assay of Silk fibroin- PCL based Nanofiber

At day 3 and 7 time point, SF-PCL-1 Ag (122%) has shown highest cell proliferation property than SF-PCL-RGO (115% and 121 % respectively day 3 and day 7). From the data of table… it is seen that when green synthesized RGO and Ag both dopants were used in SF-PCL nanofiber, the cell proliferation has decreased than TCPS which indicates slightly cell cytotoxicity than other dopants and control also. When Calendula officinalis mother tincture doped in SF-PCL nanofiber, it also shown a good cell proliferation data without cytotoxicity effect.

11. Conclusion:

The present work focuses on the green synthesis of RGO from GO with *Calendula officinalis* mother tincture. The green synthesized RGO was characterized by FTIR, XRD and RAMAN Spectroscopy peak formation. SEM images showed about the formation of flex like RGO nanosheet. TEM images also shown about its fold like nanosheet formation. This green synthesized RGO also exhibited a good dose dependent antibacterial activity when compared with standard antibacterial drug Streptomycin Sulphate for both gram positive (B. subtilis) and gram negative (E. coli) bacteria. *Calendula officinalis* green synthesized RGO also shown in vitro hemocompatible and non-cytotoxic properties (MTT assay). Dose dependent different concentration of RGO treated phenotype study of L929 mouse fibroblast cells shows non cytotoxic property of green synthesized RGO. In live and dead assay, it is shown that at lower concentrations (10,20 and 50 μg/ml) there are no presence of dead cells and at 100 μg/ml the number of present dead cells was very low and at 200 μg/ml concentrated RGO there are few numbers of dead cells. For, FITC-DAPI staining it is shown that there is no any significant difference of cell phenotype with control or without RGO treated cells. From the above discussion, it can be said that as a green reducing agent C. officinalis mother tincture is able to synthesis RGO from GO which can be used as hemocompatible antibacterial, non-cytotoxic therapeutic agent in tissue engineering. This preliminary study could help in further preparation of antibacterial, tissue regenerative formulations in future. Fabricated Silk fibroin-PCL based nanofibers can be used in a variety of applications due to their excellent mechanical, biocompatibility, and cell proliferation properties. Addition of silk fibroin with PCL increased its cell proliferation on L929 mouse fibroblast cell and antibacterial properties on both E. coli and B. subtilis bacteria. They also have good swelling index, in vitro biodegradability and excellent adhesion, making them ideal for wound healing and tissue engineering. As a dopant among silver nanoparticle, green synthesized RGO and C. officinalis mother tincture best result was given by SF-PCL-1Ag nanofiber.

12. Future Aspects:

- In vitro wound healing study (scratch assay) of green synthesized RGO
- Further pharmaceutical and biomedical devices preparation of antibacterial, tissue regenerative formulations in future.
- Silver ion release (ICP), XPS, EDX-SEM and invitro cell assessment study of Nanofibers.

13. REFERENCE

1. Ahmadi, Y., Popalzai, N.R., Furmuly, M., Azizi, N., 2022. Chapter 11 - Fiber-reinforced nanocomposites, in: Song, H., Nguyen, T.A., Yasin, G., Singh, N.B., Gupta, R.K. (Eds.), Nanotechnology in the Automotive Industry, Micro and Nano Technologies. Elsevier, pp. 215–227. https://doi.org/10.1016/B978-0-323-90524-4.00011-6
2. Albertsson, A.-C., Varma, I.K., 2003. Recent Developments in Ring Opening Polymerization of Lactones for Biomedical Applications. Biomacromolecules 4, 1466–1486. https://doi.org/10.1021/bm034247a
3. Armeda, T., 2018. FABRICATION OF PCL-COLLAGEN NANOFIBER USING CHLOROFORM-FORMIC ACID SOLUTION AND ITS APPLICATION AS WOUND DRESSING CANDIDATE. J. Stem Cell Res. Tissue Eng. 1. https://doi.org/10.20473/jscrte.v1i1.7567
4. Balouiri, M., Sadiki, M., Ibnsouda, S.K., 2016. Methods for in vitro evaluating antimicrobial activity: A review. J. Pharm. Anal. 6, 71–79. https://doi.org/10.1016/j.jpha.2015.11.005
5. Behravan, M., Hossein Panahi, A., Naghizadeh, A., Ziaee, M., Mahdavi, R., Mirzapour, A., 2019. Facile green synthesis of silver nanoparticles using Berberis vulgaris leaf and root aqueous extract and its antibacterial activity. Int. J. Biol. Macromol. 124, 148–154. https://doi.org/10.1016/j.ijbiomac.2018.11.101
6. Belhaj Khalifa, I., Ladhari, N., Touay, M., 2012. Application of sericin to modify textile supports. J. Text. Inst. 103, 370–377. https://doi.org/10.1080/00405000.2011.580539
7. Biswal, B., Dan, A.K., Sengupta, A., Das, M., Bindhani, B.K., Das, D., Parhi, P.K., 2022. Extraction of Silk Fibroin with Several Sericin Removal Processes and its Importance in Tissue Engineering: A Review. J. Polym. Environ. 30, 2222–2253. https://doi.org/10.1007/s10924-022-02381-w
8. Bojedla, S.S.R., Chameettachal, S., Yeleswarapu, S., Nikzad, M., Masood, S.H., Pati, F., 2022. Silk fibroin microfiber-reinforced polycaprolactone composites with enhanced biodegradation and biological characteristics. J. Biomed. Mater. Res. A 110, 1386–1400. https://doi.org/10.1002/jbm.a.37380
9. Bradford Assay | Bio-Rad [WWW Document], n.d. URL https://www.bio-rad.com/en-in/feature/bradford-assay.html (accessed 5.14.23).
10. Brown, J.E., Gulka, C.P., Giordano, J.E.M., Montero, M.P., Hoang, A., Carroll, T.L., 2019. Injectable Silk Protein Microparticle-based Fillers: A Novel Material for Potential Use in Glottic Insufficiency. J. Voice 33, 773–780. https://doi.org/10.1016/j.jvoice.2018.01.017
11. Cai, K., Yao, K., Cui, Y., Yang, Z., Li, X., Xie, H., Qing, T., Gao, L., 2002. Influence of different surface modification treatments on poly(d,l-lactic acid) with silk fibroin and

their effects on the culture of osteoblast in vitro. Biomaterials 23, 1603–1611. https://doi.org/10.1016/S0142-9612(01)00287-3

12. Chaiarwut, S., Ekabutr, P., Chuysinuan, P., Chanamuangkon, T., Supaphol, P., 2021. Surface immobilization of PCL electrospun nanofibers with pexiganan for wound dressing. J. Polym. Res. 28, 344. https://doi.org/10.1007/s10965-021-02669-w

13. Chen, H.-W., Lin, M.-F., 2020. Characterization, Biocompatibility, and Optimization of Electrospun SF/PCL/CS Composite Nanofibers. Polymers 12, 1439. https://doi.org/10.3390/polym12071439

14. Chen, K., Hu, H., Zeng, Y., Pan, H., Wang, S., Zhang, Y., Shi, L., Tan, G., Pan, W., Liu, H., 2022. Recent advances in electrospun nanofibers for wound dressing. Eur. Polym. J. 178, 111490. https://doi.org/10.1016/j.eurpolymj.2022.111490

15. Chouhan, D., Chakraborty, B., Nandi, S.K., Mandal, B.B., 2017a. Role of non-mulberry silk fibroin in deposition and regulation of extracellular matrix towards accelerated wound healing. Acta Biomater. 48, 157–174. https://doi.org/10.1016/j.actbio.2016.10.019

16. Chouhan, D., Chakraborty, B., Nandi, S.K., Mandal, B.B., 2017b. Role of non-mulberry silk fibroin in deposition and regulation of extracellular matrix towards accelerated wound healing. Acta Biomater. 48, 157–174. https://doi.org/10.1016/j.actbio.2016.10.019

17. Chutipakdeevong, J., Ruktanonchai, U., Supaphol, P., 2015. Hybrid biomimetic electrospun fibrous mats derived from poly(ε-caprolactone) and silk fibroin protein for wound dressing application. J. Appl. Polym. Sci. 132. https://doi.org/10.1002/app.41653

18. Clark, R.A.F., Ghosh, K., Tonnesen, M.G., 2007. Tissue engineering for cutaneous wounds. J. Invest. Dermatol. 127, 1018–1029. https://doi.org/10.1038/sj.jid.5700715

19. Craig, C.L., Riekel, C., 2002. Comparative architecture of silks, fibrous proteins and their encoding genes in insects and spiders. Comp. Biochem. Physiol. B Biochem. Mol. Biol. 133, 493–507. https://doi.org/10.1016/s1096-4959(02)00095-7

20. Das, G., Shin, H.-S., Campos, E.V.R., Fraceto, L.F., del Pilar Rodriguez-Torres, M., Mariano, K.C.F., de Araujo, D.R., Fernández-Luqueño, F., Grillo, R., Patra, J.K., 2021. Sericin based nanoformulations: a comprehensive review on molecular mechanisms of interaction with organisms to biological applications. J. Nanobiotechnology 19, 30. https://doi.org/10.1186/s12951-021-00774-y

21. Doustar, Y., Mohajeri, D., Fathiazad, F., Namvaran Abbas Abad, A., 2010. Study of apoptosis induced by Calendula officinalis extract on experimental colon carcinoma in rats. Med. Sci. J. Islam. Azad Univesity - Tehran Med. Branch 20, 1–4.

22. Elsayed, Y., Lekakou, C., Labeed, F., Tomlins, P., 2016. Fabrication and characterisation of biomimetic, electrospun gelatin fibre scaffolds for tunica media-equivalent, tissue engineered vascular grafts. Mater. Sci. Eng. C Mater. Biol. Appl. 61, 473–483. https://doi.org/10.1016/j.msec.2015.12.081

23. Ertas, I.F., Uzun, M., Altan, E., Kabir, M.H., Gurboga, M., Ozakpinar, O.B., Tinaz, G., Gunduz, O., 2023. Investigation of silk fibroin-lanolin blended nanofibrous structures. Mater. Lett. 330, 133263. https://doi.org/10.1016/j.matlet.2022.133263

24. Farokhi, M., Mottaghitalab, F., Reis, R.L., Ramakrishna, S., Kundu, S.C., 2020. Functionalized silk fibroin nanofibers as drug carriers: Advantages and challenges. J. Controlled Release 321, 324–347. https://doi.org/10.1016/j.jconrel.2020.02.022

25. Gh, A., F, D., C, J., T, C., Rl, H., J, C., H, L., J, R., Dl, K., 2003. Silk-based biomaterials. Biomaterials 24. https://doi.org/10.1016/s0142-9612(02)00353-8

26. Ghalei, S., Handa, H., 2022. A review on antibacterial silk fibroin-based biomaterials: current state and prospects. Mater. Today Chem. 23, 100673. https://doi.org/10.1016/j.mtchem.2021.100673

27. Gupta, S., Alrabaiah, H., Christophe, M., Rahimi-Gorji, M., Nadeem, S., Bit, A., 2021. Evaluation of silk-based bioink during pre and post 3D bioprinting: A review. J. Biomed. Mater. Res. B Appl. Biomater. 109, 279–293. https://doi.org/10.1002/jbm.b.34699

28. Gurtner, G.C., Werner, S., Barrandon, Y., Longaker, M.T., 2008. Wound repair and regeneration. Nature 453, 314–321. https://doi.org/10.1038/nature07039

29. He, P., Sahoo, S., Ng, K.S., Chen, K., Toh, S.L., Goh, J.C.H., 2013. Enhanced osteoinductivity and osteoconductivity through hydroxyapatite coating of silk-based tissue-engineered ligament scaffold. J. Biomed. Mater. Res. A 101A, 555–566. https://doi.org/10.1002/jbm.a.34333

30. Hu, W., Wang, Z., Zha, Y., Gu, X., You, W., Xiao, Y., Wang, X., Zhang, S., Wang, J., 2020. High Flexible and Broad Antibacterial Nanodressing Induces Complete Skin Repair with Angiogenic and Follicle Regeneration. Adv. Healthc. Mater. 9, 2000035. https://doi.org/10.1002/adhm.202000035

31. Jiménez-Medina, E., Garcia-Lora, A., Paco, L., Algarra, I., Collado, A., Garrido, F., 2006. A new extract of the plant calendula officinalis produces a dual in vitroeffect: cytotoxic anti-tumor activity and lymphocyte activation. BMC Cancer 6, 119. https://doi.org/10.1186/1471-2407-6-119

32. Joshi, S., Siddiqui, R., Sharma, P., Kumar, R., Verma, G., Saini, A., 2020. Green synthesis of peptide functionalized reduced graphene oxide (rGO) nano bioconjugate with enhanced antibacterial activity. Sci. Rep. 10. https://doi.org/10.1038/s41598-020-66230-3

33. Jyotisree, G., Sruthi, R., Biju, C.R., Menon, A.S., 2020. Calendula officinalis and Echinacae purpurae as antimicrobial agent 8.

34. Kang, M.S., Park, R., Jo, H.J., Shin, Y.C., Kim, C.-S., Hyon, S.-H., Hong, S.W., Oh, J., Han, D.-W., 2023. Spontaneous Osteogenic Differentiation of Human Mesenchymal Stem Cells by Tuna-Bone-Derived Hydroxyapatite Composites with Green Tea Polyphenol-Reduced Graphene Oxide. Cells 12, 1448. https://doi.org/10.3390/cells12111448

35. Karakecili, A.G., Demirtas, T.T., Satriano, C., Gümüsderelioglu, M., Marletta, G., 2007. Evaluation of L929 fibroblast attachment and proliferation on Arg-Gly-Asp-Ser (RGDS)-immobilized chitosan in serum-containing/serum-free cultures. J. Biosci. Bioeng. 104, 69–77. https://doi.org/10.1263/jbb.104.69

36. Khan, R.S., Rather, A.H., Wani, T.U., Rather, S. ullah, Abdal-hay, A., Sheikh, F.A., 2022. A comparative review on silk fibroin nanofibers encasing the silver nanoparticles as antimicrobial agents for wound healing applications. Mater. Today Commun. 32, 103914. https://doi.org/10.1016/j.mtcomm.2022.103914

37. Kijanska, M., Marmaras, A., Hegglin, A., Kurtcuoglu, V., Giovanoli, P., Lindenblatt, N., 2016. In vivo characterization of the integration and vascularization of a silk-derived surgical scaffold. J. Plast. Reconstr. Aesthet. Surg. 69, 1141–1150. https://doi.org/10.1016/j.bjps.2016.01.017

38. Kim, E., Lee, J., Kim, D., Lee, K.E., Han, S.S., Lim, N., Kang, J., Park, C.G., Kim, K., 2009. Solvent-responsive polymernanocapsules with controlled permeability: encapsulation and release of a fluorescent dye by swelling and deswelling. Chem. Commun. 1472–1474. https://doi.org/10.1039/B823110A

39. Kim, H., Kim, D.J., Seo, D.-H., Yeom, M.S., Kang, K., Kim, D.K., Jung, Y., 2012. Ab Initio Study of the Sodium Intercalation and Intermediate Phases in Na0.44MnO2 for Sodium-Ion Battery. Chem. Mater. 24, 1205–1211. https://doi.org/10.1021/cm300065y

40. Kim, H.J., Kim, M.K., Lee, K.H., Nho, S.K., Han, M.S., Um, I.C., 2017. Effect of degumming methods on structural characteristics and properties of regenerated silk. Int. J. Biol. Macromol. 104, 294–302. https://doi.org/10.1016/j.ijbiomac.2017.06.019

41. Kundu, B., Rajkhowa, R., Kundu, S.C., Wang, X., 2013. Silk fibroin biomaterials for tissue regenerations. Adv. Drug Deliv. Rev., Bionics - Biologically inspired smart materials 65, 457–470. https://doi.org/10.1016/j.addr.2012.09.043

42. Kundu, S.C., Kundu, B., Talukdar, S., Bano, S., Nayak, S., Kundu, J., Mandal, B.B., Bhardwaj, N., Botlagunta, M., Dash, B.C., Acharya, C., Ghosh, A.K., 2012. Invited review nonmulberry silk biopolymers. Biopolymers 97, 455–467. https://doi.org/10.1002/bip.22024

43. Kunz, R.I., Brancalhão, R.M.C., Ribeiro, L. de F.C., Natali, M.R.M., 2016. Silkworm Sericin: Properties and Biomedical Applications. BioMed Res. Int. 2016, 8175701. https://doi.org/10.1155/2016/8175701

44. Kwak, H.W., Ju, J.E., Shin, M., Holland, C., Lee, K.H., 2017. Sericin Promotes Fibroin Silk I Stabilization Across a Phase-Separation. Biomacromolecules 18, 2343–2349. https://doi.org/10.1021/acs.biomac.7b00549

45. Lanzalaco, S., Armelin, E., 2017. Poly(N-isopropylacrylamide) and Copolymers: A Review on Recent Progresses in Biomedical Applications. Gels 3, 36. https://doi.org/10.3390/gels3040036

46. Li, X., Cui, R., Liu, W., Sun, L., Yu, B., Fan, Y., Feng, Q., Cui, F., Watari, F., 2013. The Use of Nanoscaled Fibers or Tubes to Improve Biocompatibility and Bioactivity of

Biomedical Materials. J. Nanomater. 2013, e728130. https://doi.org/10.1155/2013/728130

47. Liu, T., Miao, J., Sheng, W., Xie, Y., Huang, Q., Shan, Y., Yang, J., 2010. Cytocompatibility of regenerated silk fibroin film: a medical biomaterial applicable to wound healing*. J. Zhejiang Univ. Sci. B 11, 10–16. https://doi.org/10.1631/jzus.B0900163

48. Luo, D., Zhang, R., Wang, S., Iqbal, M.Z., Zhao, R., Kong, X., 2022. Regulation effect of osteoblasts towards osteocytes by silk fibroin encapsulation. Front. Mater. Sci. 16, 220617. https://doi.org/10.1007/s11706-022-0617-5

49. Lutolf, M.P., Hubbell, J.A., 2005. Synthetic biomaterials as instructive extracellular microenvironments for morphogenesis in tissue engineering. Nat. Biotechnol. 23, 47–55. https://doi.org/10.1038/nbt1055

50. Lyu, J.S., Lee, J.-S., Han, J., 2019. Development of a biodegradable polycaprolactone film incorporated with an antimicrobial agent via an extrusion process. Sci. Rep. 9, 20236. https://doi.org/10.1038/s41598-019-56757-5

51. Mahdieh, Z., Mitra, S., Holian, A., 2020. Core–Shell Electrospun Fibers with an Improved Open Pore Structure for Size-Controlled Delivery of Nanoparticles. ACS Appl. Polym. Mater. 2, 4004–4015. https://doi.org/10.1021/acsapm.0c00643

52. Mann, R., Mitsidis, D., Xie, Z., McNeilly, O., Ng, Y.H., Amal, R., Gunawan, C., 2021. Antibacterial Activity of Reduced Graphene Oxide. J. Nanomater. 2021, e9941577. https://doi.org/10.1155/2021/9941577

53. Megaraj, M., Keppannan, M., 2018. Fabrication of a Superhydrophobic Nanofibers by Electrospinning, in: Electrospinning Method Used to Create Functional Nanocomposites Films. IntechOpen. https://doi.org/10.5772/intechopen.75357

54. Midwood, K.S., Williams, L.V., Schwarzbauer, J.E., 2004. Tissue repair and the dynamics of the extracellular matrix. Int. J. Biochem. Cell Biol., Modulatory Adhesion Molecules in Tissue Homeostasis 36, 1031–1037. https://doi.org/10.1016/j.biocel.2003.12.003

55. Ming, J., Liu, Z., Bie, S., Zhang, F., Zuo, B., 2014. Novel silk fibroin films prepared by formic acid/hydroxyapatite dissolution method. Mater. Sci. Eng. C 37, 48–53. https://doi.org/10.1016/j.msec.2013.12.041

56. Mo, X.M., Xu, C.Y., Kotaki, M., Ramakrishna, S., 2004. Electrospun P(LLA-CL) nanofiber: a biomimetic extracellular matrix for smooth muscle cell and endothelial cell proliferation. Biomaterials 25, 1883–1890. https://doi.org/10.1016/j.biomaterials.2003.08.042

57. Mollaghadimi, B., 2022. Preparation and characterisation of polycaprolactone–fibroin nanofibrous scaffolds containing allicin. IET Nanobiotechnol. 16, 239–249. https://doi.org/10.1049/nbt2.12092

58. Mostafavi, P., Naeimi, M., 2022. Investigation of vitamin D-loaded silk fibroin electrospun scaffolds for bone tissue engineering applications. Mater. Technol. 37, 1329–1337. https://doi.org/10.1080/10667857.2021.1940426

59. Narayanan, G., Gupta, B.S., Tonelli, A.E., 2015. Enhanced mechanical properties of poly (ε-caprolactone) nanofibers produced by the addition of non-stoichiometric inclusion complexes of poly (ε-caprolactone) and α-cyclodextrin. Polymer 76, 321–330. https://doi.org/10.1016/j.polymer.2015.08.045

60. Naskar, D., Barua, R.R., Ghosh, A.K., Kundu, S.C., 2014. 1 - Introduction to silk biomaterials, in: Kundu, S.C. (Ed.), Silk Biomaterials for Tissue Engineering and Regenerative Medicine. Woodhead Publishing, pp. 3–40. https://doi.org/10.1533/9780857097064.1.3

61. Oliveira Barud, H.G., Barud, H. da S., Cavicchioli, M., do Amaral, T.S., Junior, O.B. de O., Santos, D.M., Petersen, A.L. de O.A., Celes, F., Borges, V.M., de Oliveira, C.I., de Oliveira, P.F., Furtado, R.A., Tavares, D.C., Ribeiro, S.J.L., 2015. Preparation and characterization of a bacterial cellulose/silk fibroin sponge scaffold for tissue regeneration. Carbohydr. Polym. 128, 41–51. https://doi.org/10.1016/j.carbpol.2015.04.007

62. Pan, P., Li, J., Liu, X., Hu, C., Wang, M., Zhang, W., Li, M., Liu, Y., 2023. Plasmid containing VEGF-165 and ANG-1 dual genes packaged with fibroin-modified PEI to promote the regeneration of vascular network and dermal tissue. Colloids Surf. B Biointerfaces 224, 113210. https://doi.org/10.1016/j.colsurfb.2023.113210

63. Park, W., Shin, H., Choi, B., Rhim, W.-K., Na, K., Keun Han, D., 2020. Advanced hybrid nanomaterials for biomedical applications. Prog. Mater. Sci. 114, 100686. https://doi.org/10.1016/j.pmatsci.2020.100686

64. Park, Y.R., Sultan, Md.T., Park, H.J., Lee, J.M., Ju, H.W., Lee, O.J., Lee, D.J., Kaplan, D.L., Park, C.H., 2018. NF-κB signaling is key in the wound healing processes of silk fibroin. Acta Biomater. 67, 183–195. https://doi.org/10.1016/j.actbio.2017.12.006

65. Qi, Y., Wang, H., Wei, K., Yang, Y., Zheng, R.-Y., Kim, I.S., Zhang, K.-Q., 2017a. A Review of Structure Construction of Silk Fibroin Biomaterials from Single Structures to Multi-Level Structures. Int. J. Mol. Sci. 18, 237. https://doi.org/10.3390/ijms18030237

66. Qi, Y., Wang, H., Wei, K., Yang, Y., Zheng, R.-Y., Kim, I.S., Zhang, K.-Q., 2017b. A Review of Structure Construction of Silk Fibroin Biomaterials from Single Structures to Multi-Level Structures. Int. J. Mol. Sci. 18, 237. https://doi.org/10.3390/ijms18030237

67. Rastogi, S., Kandasubramanian, B., 2020. Processing trends of silk fibers: Silk degumming, regeneration and physical functionalization. J. Text. Inst. 111, 1794–1810. https://doi.org/10.1080/00405000.2020.1727269

68. Rnjak-Kovacina, J., Wray, L.S., Burke, K.A., Torregrosa, T., Golinski, J.M., Huang, W., Kaplan, D.L., 2015. Lyophilized Silk Sponges: A Versatile Biomaterial Platform for

Soft Tissue Engineering. ACS Biomater. Sci. Eng. 1, 260–270. https://doi.org/10.1021/ab500149p

69. Rockwood, D.N., Preda, R.C., Yücel, T., Wang, X., Lovett, M.L., Kaplan, D.L., 2011a. Materials fabrication from Bombyx mori silk fibroin. Nat. Protoc. 6, 1612–1631. https://doi.org/10.1038/nprot.2011.379

70. Rockwood, D.N., Preda, R.C., Yücel, T., Wang, X., Lovett, M.L., Kaplan, D.L., 2011b. Materials fabrication from Bombyx mori silk fibroin. Nat. Protoc. 6, 1612–1631. https://doi.org/10.1038/nprot.2011.379

71. Sakai, S., Yoshii, A., Sakurai, S., Horii, K., Nagasuna, O., 2020. Silk fibroin nanofibers: a promising ink additive for extrusion three-dimensional bioprinting. Mater. Today Bio 8, 100078. https://doi.org/10.1016/j.mtbio.2020.100078

72. Scheibel, T., 2005. Protein fibers as performance proteins: new technologies and applications. Curr. Opin. Biotechnol., Protein technologies and commercial enzymes 16, 427–433. https://doi.org/10.1016/j.copbio.2005.05.005

73. SDS-PAGE for Silk Fibroin Protein [WWW Document], n.d. URL https://bio-protocol.org/exchange/protocoldetail?id=3054&type=1 (accessed 5.28.23).

74. Shao, D., Lu, M., Zhao, Y., Zhang, F., Tan, Y., Zheng, X., Pan, Y., Xiao, X., Wang, Z., Dong, W., Li, J., Chen, L., 2017. The shape effect of magnetic mesoporous silica nanoparticles on endocytosis, biocompatibility and biodistribution. Acta Biomater. 49, 531–540. https://doi.org/10.1016/j.actbio.2016.11.007

75. Shao, J., Cui, Y., Liang, Y., Liu, H., Ma, B., Ge, S., 2021. Unilateral Silver-Loaded Silk Fibroin Difunctional Membranes as Antibacterial Wound Dressings. ACS Omega 6, 17555–17565. https://doi.org/10.1021/acsomega.1c02035

76. Shimura, K., 1983. Chemical composition and biosynthesis of silk proteins. Experientia 39, 455–461. https://doi.org/10.1007/BF01965160

77. Shiroud Heidari, B., Ruan, R., Vahabli, E., Chen, P., De-Juan-Pardo, E.M., Zheng, M., Doyle, B., 2023. Natural, synthetic and commercially-available biopolymers used to regenerate tendons and ligaments. Bioact. Mater. 19, 179–197. https://doi.org/10.1016/j.bioactmat.2022.04.003

78. Singh, M., Becker, M., Godwin, A.R.F., Baldock, C., 2021. Structural studies of elastic fibre and microfibrillar proteins. Matrix Biol. Plus 12, 100078. https://doi.org/10.1016/j.mbplus.2021.100078

79. Singh, R., Eitler, D., Morelle, R., Friedrich, R.P., Dietel, B., Alexiou, C., Boccaccini, A.R., Liverani, L., Cicha, I., 2020. Optimization of cell seeding on electrospun PCL-silk fibroin scaffolds. Eur. Polym. J. 134, 109838. https://doi.org/10.1016/j.eurpolymj.2020.109838

80. Sofregen Receives 510(k) Clearance for Silk Voice® - The First and Only Natural Silk Protein Injectable Product for Tissue Bulking [WWW Document], 2019. . Sofregen. URL https://www.sofregen.com/press-release-3/press-release-3 (accessed 4.6.23).

81. Song, W.-T., Zhu, F.-F., Chen, K.-P., 2021. The molecular mechanisms and factors affecting the feeding habits of silkworm (Lepidoptera: Bombyxidae). J. Asia-Pac. Entomol. 24, 955–962. https://doi.org/10.1016/j.aspen.2021.08.010

82. Stadelmann, W.K., Digenis, A.G., Tobin, G.R., 1998. Physiology and healing dynamics of chronic cutaneous wounds. Am. J. Surg. 176, 26S-38S. https://doi.org/10.1016/s0002-9610(98)00183-4

83. Sultan, M.T., Lee, O.J., Kim, S.H., Ju, H.W., Park, C.H., 2018. Silk Fibroin in Wound Healing Process. Adv. Exp. Med. Biol. 1077, 115–126. https://doi.org/10.1007/978-981-13-0947-2_7

84. Sun, W., Gregory, D.A., Tomeh, M.A., Zhao, X., 2021. Silk Fibroin as a Functional Biomaterial for Tissue Engineering. Int. J. Mol. Sci. 22, 1499. https://doi.org/10.3390/ijms22031499

85. Sung, H.-J., Meredith, C., Johnson, C., Galis, Z.S., 2004. The effect of scaffold degradation rate on three-dimensional cell growth and angiogenesis. Biomaterials 25, 5735–5742. https://doi.org/10.1016/j.biomaterials.2004.01.066

86. Thorat, N., Otari, S., Patil, R., Bohara, R., Yadav, H., Koli, b, Chaurasia, A., Ningthoujam, F.N.A.S., Raghumani, 2014. Synthesis, Characterization and Biocompatibility of Chitosan functionalized superparamagnetic nanoparticles for heat activated curing of cancer cells. Dalton Trans. 43, 17343–17351. https://doi.org/10.1039/c4dt02293a

87. Vepari, C., Kaplan, D.L., 2007. Silk as a biomaterial. Prog. Polym. Sci., Polymers in Biomedical Applications 32, 991–1007. https://doi.org/10.1016/j.progpolymsci.2007.05.013

88. Volkov, V., Ferreira, A.V., Cavaco-Paulo, A., 2015. On the Routines of Wild-Type Silk Fibroin Processing Toward Silk-Inspired Materials: A Review. Macromol. Mater. Eng. 300, 1199–1216. https://doi.org/10.1002/mame.201500179

89. Vidya, M., Rajagopal, S., 2021a. Silk Fibroin: A Promising Tool for Wound Healing and Skin Regeneration. Int. J. Polym. Sci. 2021, e9069924. https://doi.org/10.1155/2021/9069924

90. Vidya, M., Rajagopal, S., 2021b. Silk Fibroin: A Promising Tool for Wound Healing and Skin Regeneration. Int. J. Polym. Sci. 2021, e9069924. https://doi.org/10.1155/2021/9069924

91. Wang, H.-Y., Zhang, Y.-Q., 2013. Effect of regeneration of liquid silk fibroin on its structure and characterization. Soft Matter 9, 138–145. https://doi.org/10.1039/C2SM26945G

92. Wang, K., Ma, Q., Zhou, H.-T., Zhao, J.-M., Cao, M., Wang, S.-D., 2022. Review on Fabrication and Application of Regenerated Silk Fibroin Materials. Autex Res. J. {"content-type":"ahead-of-print","content":0}. https://doi.org/10.2478/aut-2021-0059

93. Wu, C.-S., 2010. Preparation and characterizations of polycaprolactone/green coconut fiber composites. J. Appl. Polym. Sci. 115, 948–956. https://doi.org/10.1002/app.30955

94. Yan, B., Liu, W., Duan, G., Ni, P., Jiang, Y., Zhang, C., Wang, B., Lu, Y., Chen, C., 2021. Colorimetric detection of acetylcholinesterase and its inhibitor based on thiol-regulated oxidase-like activity of 2D palladium square nanoplates on reduced graphene oxide. Microchim. Acta 188, 162. https://doi.org/10.1007/s00604-021-04817-x

95. Yin, I.X., Zhang, J., Zhao, I.S., Mei, M.L., Li, Q., Chu, C.H., 2020. The Antibacterial Mechanism of Silver Nanoparticles and Its Application in Dentistry. Int. J. Nanomedicine 15, 2555–2562. https://doi.org/10.2147/IJN.S246764

96. Zarei, M., Seyedi, N., Maghsoudi, S., Nejad, M.S., Sheibani, H., 2021. Green synthesis of Ag nanoparticles on the modified graphene oxide using Capparis spinosa fruit extract for catalytic reduction of organic dyes. Inorg. Chem. Commun. 123, 108327. https://doi.org/10.1016/j.inoche.2020.108327

97. Zhang, Jiali, Yang, H., Shen, G., Cheng, P., Zhang, Jingyan, Guo, S., 2010. Reduction of graphene oxide via L-ascorbic acid. Chem. Commun. Camb. Engl. 46, 1112–1114. https://doi.org/10.1039/b917705a

98. Zhang, M., Song, W., Tang, Y., Xu, X., Huang, Y., Yu, D., 2022. Polymer-Based Nanofiber–Nanoparticle Hybrids and Their Medical Applications. Polymers 14, 351. https://doi.org/10.3390/polym14020351

99. Zuluaga-Vélez, A., Quintero-Martinez, A., Orozco, L.M., Sepúlveda-Arias, J.C., 2021. Silk fibroin nanocomposites as tissue engineering scaffolds – A systematic review. Biomed. Pharmacother. 141, 111924. https://doi.org/10.1016/j.biopha.2021.111924

MTech draft 3

ORIGINALITY REPORT

7%
SIMILARITY INDEX

PRIMARY SOURCES

1	Anustup Chakraborty, Sakthi Prasad, Shashi Kant, Rathina Vel et al. "Thermally stable bioactive borosilicate glasses: Composition–structure–property correlations", Journal of Materials Research, 2023 Crossref	173 words — 1%
2	www.researchgate.net Internet	69 words — < 1%
3	docksci.com Internet	57 words — < 1%
4	etheses.whiterose.ac.uk Internet	43 words — < 1%
5	N.M.S Hidayah, W.W. Liu, C.S. Khe, C.W. Lai, N.Z. Noriman, U. Hashim. "Synthesis and Characterization of Alkylated Graphene Oxide (AGO) and Reduced Graphene Oxide (ARGO)", Materials Today: Proceedings, 2019 Crossref	42 words — < 1%
6	Siddiqua, Ayesha. "Electrospun Silkworm Silk Fibroin-Indocyanine Green Biocomposite Fibers: Fabrication, Characterization and Application towards Hemorrhage Control", Illinois Institute of Technology, 2022 ProQuest	35 words — < 1%

7	mdpi-res.com Internet	35 words — < 1%
8	worldwidescience.org Internet	35 words — < 1%
9	Guru Janani, Manishekhar Kumar, Dimple Chouhan, Joseph Christakiran Moses et al. "Insight into Silk-Based Biomaterials: From Physicochemical Attributes to Recent Biomedical Applications", ACS Applied Bio Materials, 2019 Crossref	29 words — < 1%
10	Riti Mann, Dimitrios Mitsidis, Zhirun Xie, Oliver McNeilly, Yun Hau Ng, Rose Amal, Cindy Gunawan. "Antibacterial Activity of Reduced Graphene Oxide", Journal of Nanomaterials, 2021 Crossref	29 words — < 1%
11	Soongee Hong. "Electrospun Polycaprolactone/Silk Fibroin/Small Intestine Submucosa Composites for Biomedical Applications", Macromolecular Materials and Engineering, 06/15/2010 Crossref	29 words — < 1%
12	Mehdi Farokhi, Fatemeh Mottaghitalab, Rui L. Reis, Seeram Ramakrishna, Subhas C. Kundu. "Functionalized silk fibroin nanofibers as drug carriers: Advantages and challenges", Journal of Controlled Release, 2020 Crossref	27 words — < 1%
13	www.ncbi.nlm.nih.gov Internet	27 words — < 1%
14	cyberleninka.org Internet	26 words — < 1%

15	Chengbin Yang, Haoqiang Huang, Nishtha Manish Singh, Cheng Zhou et al. "Synthetic Conjugated Oligoelectrolytes Are Effective siRNA Transfection Carriers: Relevance to Pancreatic Cancer Gene Therapy", Biomacromolecules, 2022 Crossref	23 words — < 1%
16	link.springer.com Internet	22 words — < 1%
17	Julian Chesterman, Zheng Zhang, Ophir Ortiz, Ritu Goyal, Joachim Kohn. "Biodegradable polymers", Elsevier BV, 2020 Crossref	21 words — < 1%
18	kb.psu.ac.th:8080 Internet	18 words — < 1%
19	mdpi.com Internet	18 words — < 1%
20	www.mdpi.com Internet	18 words — < 1%
21	www.spandidos-publications.com Internet	18 words — < 1%
22	Williams, G.M.. "Cell density alters matrix accumulation in two distinct fractions and the mechanical integrity of alginate-chondrocyte constructs", Acta Biomaterialia, 200511 Crossref	17 words — < 1%
23	shodhganga.inflibnet.ac.in Internet	17 words — < 1%

24	Huajie Shen, Liangzhou Dong, Xinyuan Zheng, Donghai Huang. "Construction of organic-inorganic hybrid coating polymer with in situ SiO2/PDMS on the surface of wood", Research Square Platform LLC, 2023 Crossref Posted Content	16 words — < 1%
25	iopscience.iop.org Internet	16 words — < 1%
26	journals.plos.org Internet	16 words — < 1%
27	www.frontiersin.org Internet	15 words — < 1%
28	www.jocpr.com Internet	15 words — < 1%
29	Mohammadreza Tahriri, Fathollah Moztarzadeh. "Preparation, Characterization, and In Vitro Biological Evaluation of PLGA/Nano-Fluorohydroxyapatite (FHA) Microsphere-Sintered Scaffolds for Biomedical Applications", Applied Biochemistry and Biotechnology, 2014 Crossref	14 words — < 1%
30	Xi-Feng Zhang, Sangiliyandi Gurunathan. "Biofabrication of a novel biomolecule-assisted reduced graphene oxide: an excellent biocompatible nanomaterial", International Journal of Nanomedicine, 2016 Crossref	14 words — < 1%
31	Yi, E.. "Noradrenergic innervation of rabbit pancreatic ganglia", Autonomic Neuroscience: Basic and Clinical, 20050207 Crossref	14 words — < 1%
32	www.bsmiab.org	

Internet

14 words — < 1%

33 Aguilar, C.A.. "Direct micro-patterning of biodegradable polymers using ultraviolet and femtosecond lasers", Biomaterials, 200512
Crossref

13 words — < 1%

34 G. Sabarees, G.P. Tamilarasi, V. Velmurugan, V. Alagarsamy et al. "Emerging trends in silk fibroin based nanofibers for impaired wound healing", Journal of Drug Delivery Science and Technology, 2022
Crossref

13 words — < 1%

35 www.woah.org
Internet

13 words — < 1%

36 repository-tnmgrmu.ac.in
Internet

12 words — < 1%

37 Ahmed, Salahuddin. "Fabrication and Characterization of Force Spun Polymeric Nanofiber for Drug Delivery and Tissue Engineering Applications", The University of Texas Rio Grande Valley, 2023
ProQuest

11 words — < 1%

38 Bergey's Manual® of Systematic Bacteriology, 2012.
Crossref

11 words — < 1%

39 Dias, A.G.. "In vitro degradation studies of calcium phosphate glass ceramics prepared by controlled crystallization", Journal of Non-Crystalline Solids, 20031115
Crossref

11 words — < 1%

40 onlinelibrary.wiley.com
Internet

11 words — < 1%

41	bioresources.cnr.ncsu.edu Internet	10 words — < 1%
42	eprints.usq.edu.au Internet	10 words — < 1%
43	file.scirp.org Internet	10 words — < 1%
44	rusjphysiol.org Internet	10 words — < 1%
45	ubm.opus.hbz-nrw.de Internet	10 words — < 1%
46	www.ifrj.upm.edu.my Internet	10 words — < 1%
47	Amir Bahoor, Reza Ahmadi, Mojgan Heydari, Mozhgan Bagheri, Aliasghar Behnamghader. "Synthesis and Evaluation of Cross-linked Gelatin Nanoparticles for Controlled Release of an Anti-diabetic Drug: Gliclazide", Inorganic Chemistry Communications, 2023 Crossref	9 words — < 1%
48	Jha, Deepak Kumar. "Phytochemical and Antidiabetic Evaluation of Fruits of Momordica Dioica Roxb", Rajiv Gandhi University of Health Sciences (India), 2023 ProQuest	9 words — < 1%
49	Kocak, Fatma Zehra. "Smart pH and Thermosensitive Injectable Hydrogels:Chitosan – Hydroxyapatite – Heparin Based Functionalised Biomaterials for Bone Regeneration", Lancaster University (United Kingdom), 2021 ProQuest	9 words — < 1%

50	Lu Wang, Yimin Zhou. " Stable visible light photocatalyst based on the graphene protected Ag PO nanocomposite ", Fullerenes, Nanotubes and Carbon Nanostructures, 2016 Crossref	9 words — < 1%
51	S.C. Reshma, S. Syama, P.V. Mohanan. "Nano-biointeractions of PEGylated and bare reduced graphene oxide on lung alveolar epithelial cells: A comparative in vitro study", Colloids and Surfaces B: Biointerfaces, 2016 Crossref	9 words — < 1%
52	archive.org Internet	9 words — < 1%
53	jurnal.fp.unila.ac.id Internet	9 words — < 1%
54	msbmb.org Internet	9 words — < 1%
55	oro.open.ac.uk Internet	9 words — < 1%
56	www.medical-xprt.com Internet	9 words — < 1%
57	www.science.gov Internet	9 words — < 1%
58	www.tandfonline.com Internet	9 words — < 1%
59	Ahamed, Mohammed Elbushra Hassan. "Development and Application of Molecularly Imprinted Polymers for Selective Separation and Recovery of	8 words — < 1%

Gold and Silver from Industrial Wastewaters", University of Johannesburg (South Africa), 2023
ProQuest

60 Chang Lu, Po-Jung Jimmy Huang, Biwu Liu, Yibin Ying, Juewen Liu. "Comparison of Graphene Oxide and Reduced Graphene Oxide for DNA Adsorption and Sensing", Langmuir, 2016 — 8 words — < 1%
Crossref

61 Gowri, R.. "Pharmacognostical, Phytochemical and Pharmacological Studies on the Botanical Sources of the Ayurvedic Drug, Munditika", Rajiv Gandhi University of Health Sciences (India), 2023 — 8 words — < 1%
ProQuest

62 H.G. Becker. "Einführung cyclischer Amidinein nitrilhaltige Polymere in der Schmelze", Chemie Ingenieur Technik, 02/06/2003 — 8 words — < 1%
Crossref

63 Hojati Najafabadi, Zohreh. "Genetic Manipulation of the Biosynthetic Pathway for Production of the Calcium-Dependent Antibotic in Streptomyces coelicolor A3(2)", The University of Manchester (United Kingdom), 2023 — 8 words — < 1%
ProQuest

64 Keman, Deniz. "Outer Membrane Protein Profiling of Escherichia Coli O157:H7 in Response to Phenolic Acid Stress", Izmir Institute of Technology (Turkey), 2021 — 8 words — < 1%
ProQuest

65 Kenjiro Yazawa, Kana Ishida, Hiroyasu Masunaga, Takaaki Hikima, Keiji Numata. "Influence of Water Content on the β-Sheet Formation, Thermal Stability, Water Removal, and Mechanical Properties of Silk Materials", Biomacromolecules, 2016 — 8 words — < 1%

Crossref

66 Konstantina Iliou, Stefanos Kikionis, Efstathia Ioannou, Vassilios Roussis. "Marine Biopolymers as Bioactive Functional Ingredients of Electrospun Nanofibrous Scaffolds for Biomedical Applications", Marine Drugs, 2022 — 8 words — < 1%
Crossref

67 Ruvimbo Mautsa, Stanley Mukanganyama. " Leaf Extracts Cause Cellular Membrane Disruption and Nucleic Acid Leakage in ", Journal of Biologically Active Products from Nature, 2017 — 8 words — < 1%
Crossref

68 Shihui Liu, Thomas H. Bugge, Arthur E. Frankel, Stephen H. Leppla. "Chapter 10 Dissecting the Urokinase Activation Pathway Using Urokinase-Activated Anthrax Toxin", Springer Science and Business Media LLC, 2009 — 8 words — < 1%
Crossref

69 X.D. Kong, F.Z. Cui, X.M. Wang, M. Zhang, W. Zhang. "Silk fibroin regulated mineralization of hydroxyapatite nanocrystals", Journal of Crystal Growth, 2004 — 8 words — < 1%
Crossref

70 Xin Chen, Zhengzhong Shao, David P. Knight, Fritz Vollrath. "Conformation transition kinetics of Bombyx mori silk protein", Proteins: Structure, Function, and Bioinformatics, 2007 — 8 words — < 1%
Crossref

71 acikbilim.yok.gov.tr — 8 words — < 1%
Internet

72 discovery.ucl.ac.uk — 8 words — < 1%
Internet

73 jkamprs.springeropen.com

	Internet	8 words — < 1%
74	mobt3ath.com Internet	8 words — < 1%
75	orca.cardiff.ac.uk Internet	8 words — < 1%
76	pdfs.semanticscholar.org Internet	8 words — < 1%
77	scholarship.rice.edu Internet	8 words — < 1%
78	theses.gla.ac.uk Internet	8 words — < 1%
79	uvadoc.uva.es Internet	8 words — < 1%
80	www.freepatentsonline.com Internet	8 words — < 1%
81	www.waset.org Internet	8 words — < 1%
82	Jiangbin Wu, Kadiam C Venkata Subbaiah, Omar Hedaya, Si Chen, Joshua Munger, Wai Hong Wilson Tang, Chen Yan, Peng Yao. "FAM210A Regulates Mitochondrial Translation and Maintains Cardiac Mitochondrial Homeostasis", Cold Spring Harbor Laboratory, 2023 Crossref Posted Content	7 words — < 1%
83	R., Sadashivaiah. "Development and Evaluation of Transdermal Drug Delivery Systems for Anti	7 words — < 1%

Parkinsons and Antipsychotic Drugs", Rajiv Gandhi University of Health Sciences (India), 2023
ProQuest

84 Saliu, Oluwaseyi Damilare. "Design of Conductive Biopolymer-Based Nano-Architectural Electrodes for Energy Storage Applications in Supercapacitors", University of Johannesburg (South Africa), 2023 — 7 words — < 1%
ProQuest

85 Hlobsile Kgomo, Somandla Ncube, Vimbai Mhuka, Temesgen Girma Kebede, Simiso Dube, Mathew M. Nindi. "A Comparative Study on the Dissolution of Argema mimosae Silk Fibroin and Fabrication of Films and Nanofibers", Polymers, 2021 — 6 words — < 1%
Crossref

86 Methods in Molecular Biology, 2014. — 6 words — < 1%
Crossref

87 Sangiliyandi Gurunathan, Jae Woong Han, Jung-Hyun Park, Eun Su Kim, Yun-Jung Choi, Deug-Nam Kwon, Jin-Hoi Kim. "Reduced graphene oxide–silver nanoparticle nanocomposite: a potential anticancer nanotherapy", International Journal of Nanomedicine, 2015 — 6 words — < 1%
Crossref

88 Theanmalar Masilamani, Thavamanithevi Subramaniam, Norshariza Nordin, Rozita Rosli. "Neuroprotective effects of Peltophorum pterocarpum leaf extract against hydrogen peroxide induced oxidative stress and cytotoxicity", Clinical Phytoscience, 2017 — 6 words — < 1%
Crossref

EXCLUDE QUOTES OFF EXCLUDE SOURCES OFF

EXCLUDE BIBLIOGRAPHY OFF

EXCLUDE MATCHES OFF